KINETICS OF SULPHUR TRANSFER FROM CARBON SATURATED IRON TO SLAGS

by

YUNG HONG KIM

Thesis submitted to the Department of Metallurgy,
University of Strathclyde for the
Degree of Doctor of Philosopy.

October, 1978

SUMMARY

The kinetics of sulphur transfer from carbon saturated iron to CaO - MgO - SiO_2 slag was investigated at 1460° C under CO gas atmospheres. To elucidate the reaction mechanism the present experiments were carried out varying the following reaction conditions: sulphur content of metal, slag composition, melt geometry, Si addition, MnO and FeO addition, and ambient pressure.

The observed experimental results indicate that the desulphurization reaction is not controlled by either diffusion of sulphur in the metal or the slag but by an electrochemical reaction.

Desulphurization takes place in three reaction stages controlled by different reaction mechanisms; the initial fastest stage is dependent on anodic reactions of iron transfer and CO evolution, the second medium rate stage is controlled by CO evolution, and the final slowest stage controlled by silica reduction from the silicate slag. The reaction mechanism during the initial stage is dependent on the properties of slag; for acid slag with high viscosity and low oxygen ion activity, the anodic reaction of iron transfer seems to be predominant whilst for basic slag with low viscosity and high activity of oxygen ion carbon monoxide plays a significant role.

The effects of silicon additions to metal, and MnO and FeO additions to slag, and decreasing the ambient pressure result in increased desulphurization rates and confirm the proposed mechanisms.

CONTENTS

INTRODUCTION

INTRODUCTION

Of all the slag-metal reactions in iron and steel making the thermodynamics and kinetics of sulphur transfer have been studied most intensively. This shows the importance of the desulphurization reaction in iron and steel making processes. The operation of a blast furnace has become nowadays largely dependent upon the sulphur content of materials charged and the desired limit of sulphur in the product. It is well known that of the two major steps in steel making the blast furnace removes the larger amount of sulphur in its waste product, the slag, most effectively. However most of the sulphur which appears in finished steel is also introduced in the blast furnace primarily from the coke used for reduction and smelting of the ores. As the sulphur content of raw materials increases with depletion of higher grade ores and coal and lower sulphur specifications continue to be set for many grades of steel, an understanding of the desulphurization process has become increasingly important.

The thermodynamics of steel making reactions have been studied more intensively than the kinetics over the past several decades. Equilibrium data from the thermodynamics are essential to the understanding of any process and such knowlege has the practical utility of placing a limit beyond which control measures can not succeed. Industrial processes, however, seldom proceed to equilibrium and information on the factors which control the rates of reactions are therefore often of greater importance than equilibrium data in order to establish full control of the process.

The desulphurization of molten pig iron by slag within the blast furnace is one such process in which the actual degree of desulphurization by slag does not approach the equilibrium distribution ratio obtained for similar slag-metal systems in the laboratory (1). This is amply demonstrated by the experiments in which actual blast furnace metals and slag were remelted together in graphite crucibles and further desulphurization was obtained (2).

Most of the kinetic studies have been performed on sulphur transfer from carbon saturated iron to slag under reducing conditions, which has contributed a good deal of information for a better understanding of desulphurization in the blast furnace.

Even though there have been abundant experimental observations since the first kinetic studies by Chang and Goldman (3) the mechanism of desulphurization has not yet been perfectly understood. Some workers (4)(5)(6)(7) have suggested that sulphur transfer is controlled by an interfacial chemical reaction whilst others have suggested that it is controlled by diffusion in the slag (8) or in the metal (9). There have been two different suggestions for the chemical reaction control step; the rate controlling reaction for the desulphurization is the sluggish CO gas evolution by a heterogeneous interfacial reaction between slag, metal and gas phase as one step of consecutive reactions (4); or the deleterious silica reduction which occurs concurrently during the desulphurization reaction (5).

These different explanations have arisen mainly because of the complexity of side reactions during sulphur transfer.

Review of the previous significant experimental observations suggest that a more detailed observation of the side reactions, such as silica reduction and CO gas evolution, is still necessary.

It was hoped, therefore, that this investigation would provide a clue to solve the long standing arguments on the mechanism which controls the desulphurization.

CHAPTER 1

LITERATURE REVIEW

CHAPTER 1

LITERATURE REVIEW

1.1 INTRODUCTION

In order to understand which problems remain to be solved in the kinetics of the sulphur transfer reaction, and how the previous investigators tried to suggest successful explanations for the reaction mechanism, it is necessary to review the abundant experimental observations piled up over the past three decades.

It is well known from kinetic studies on desulphurization that the transfer of sulphur alone can not be considered but that behaviour of the accompanying elements must also be studied. The whole transfer process of sulphur can be considered to involve the following steps;

(1) Transfer of sulphur and other reactants to the slag-metal interface, e.g. [S], [Fe] (O^{2-})

(2) Reaction at the interface

(3) Transfer of products to respective phases, e.g. (S^{2-}), (Fe^{2+}), [O]

If one of these steps is significantly slower than the other two, then the rate of this step will control the rate of the whole process and identification of this step would be of considerable value in understanding the factors governing the sulphur transfer rate. Steps(1) and (3) are dependent upon the diffusion of reactants and products in slag and metal. An investigation of the diffusion profile of sulphur in slag and metal, or of the effect of mechanical stirring on desulphurization will provide some evidence with which one can say whether sulphur transfer is controlled by diffusion or not.

The slag-metal sulphur reaction can be represented by the following equation. (6) (10)

$$[S] + (O^{2-}) = [O] + (S^{2-}) \qquad (1)$$

[ ] denotes metal phase and ( ) slag phase.

In the case of the presence of C in metal it follows that the above [O] reacts with C in metal producing CO gas;

$$[C] + [O] = \{CO\} \qquad (2)$$

where { } denotes gas phase.

It is expected from studies of reaction kinetics that the overall rate of reaction 1 increases as the activity of [S] and (O^{2-}) increases, or if the activities of the reaction products are decreased. Therefore it follows that the removal of oxygen dissolved in iron by a suitable deoxidizer should increase the rate of desulphurization, whereas oxidizing by an oxide addition to slag, or by the reduction of an oxide component of slag, decreases the transfer rate. Increasing the activity of free oxygen ion in slag, (O^{2-}), by an increase of the slag basicity should be favourable for the desulphurization reaction.
It is also worth noting that CO gas evolution according to equation 2 will affect the desulphurization rate because of the difficulty of heterogeneous reaction between metal, slag, and gas phases.

Most kinetic studies of sulphur transfer have been carried out by noting the effect of changing reaction conditions, such as change of slag composition, addition of deoxidants to the metal, addition of reducible oxide to the slag and applying a current, on the rate of sulphur transfer and on the rates of transfer of other elements.

Studies into diffusion control and chemical reaction control are reviewed seperately.

1.2. INVESTIGATIONS INTO DIFFUSION CONTROL

Several investigations were carried out to examine whether the diffusion processes of steps 1 and 3 are rate controlling for sulphur transfer.

G.Derge et al. (4) measured the rate of diffusion of sulphur in slag in their study of the kinetics of sulphur transfer from metal to slag and found a diffusion coefficient of 6×10^{-6} cm^2 sec^{-1} at 1600° C which is around ten times less than the diffusion coefficient of sulphur in liquid carbon saturated iron (the order of $10^{-4} cm^2$ sec^{-1}, observed by Holbrook et al. (11). Later Saito and Kawai (12) reported a value of $D = 0.8 \times 10^{-6}$ cm^2 sec^{-1} for diffusion of sulphur in a 42.5 % CaO, 9.6 % Al_2O_3, 47.9 % SiO_2 slag at 1440 C, and Kawai (13) measured the diffusion coefficient of sulphur in carbon saturated iron as $D = 2 \times 10^{-5}$ cm^2 sec^{-1}.

Derge et al. thought in their study (4) that the rates of diffusion of sulphur in both iron and slag are much slower than the observed sulphur transfer rate from metal to slag, therefore it is necessary to assume that convection, by CO gas evolution accompanying the sulphur transfer, provides the mechanism of carrying sulphur to and from the slag-metal interface.

However in one of the earliest studies made into sulphur transfer, by O.V. Travin et al. (9), with radioactive S^{35}, it was concluded that this reaction is controlled by the transport of sulphur from metal to the slag-metal interface. Against this observation Hatano (8) investigated more recently the slow movement of sulphur in slag by autoradiography. He examined the concentration profile of sulphur in the vicinity of the interface by using the same radioisotope S^{35} and found the presence of the thick boundary layer for diffusion in slag

phase as shown in Fig. 1.1.

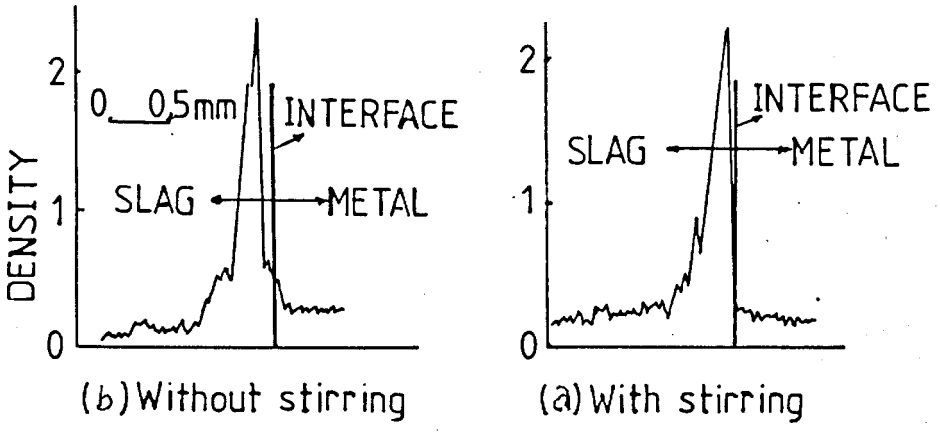

FIG.1.1. SULPHUR CONCENTRATION CURVES AT THE INTERFACE OBTAINED BY MICROPHOTOMETRY

(a) WITH VISCOUS BASIC SLAG (CaO/SiO_2= 1.50)

(b) WITH LOW VISCOUS SLAG WITH Na_2O (CaO/SiO_2= 1.22)

FROM M.HATANO et al.(8)

In view of the contradictory results, from these direct experiments it is very difficult to come to a firm conclusion about the role of diffusion during sulphur transfer.

Apart from these investigations directly into diffusion control, indirect evidence can be obtained from other studies. Ward et al.(14) examined diffusion of sulphur in slag as a possible rate controlling step in the desulphurization by comparing the activation energy value for sulphur transfer obtained from their experiments,with the activation energy for diffusion of sulphur in slag, which was calculated from data given by Saito et al.(12). If sulphur transfer is diffusion controlled, both activation energies should be identical. They found

that the activation energy for sulphur transfer lies within the wide error band for diffusion, but the diffusion values used for comparison were so indefinite that the apparent agreement could not be regarded as a conclusive evidence for the diffusion control of sulphur transfer.

They also tried to compare the rate of sulphur flow calculated by assuming a diffusion process with that obtained by transfer experiments. The flux of sulphur by diffusion from the interface into the slag can be represented by Fick's first law;

$$Js = Ds/x \cdot [\% S] \cdot Ls \quad g\ min^{-1} \qquad (3)$$

where Ds : diffusion coefficient of sulphur in slag,

x : thickness of the slag boundary layer,

Ls : the slag/metal sulphur distribution ratio.

If the diffusion of sulphur in slag is rate controlling, this flow should be equal to the flow of sulphur across the interface from the sulphur transfer experiments;

$$Js = Km \cdot [\% S] \quad g\ min^{-1} \qquad (4)$$

where Km : rate coefficient of sulphur transfer from metal to slag.

The equivalence between these two equations could not be checked as the thickness of the boundary layer x was unknown, but when the equality was assumed for 50 % CaO, 40 % SiO_2, 10 % Al_2O_3 slag for which Ls was taken as equal to 100, a value of 0.03 cm was obtained for the slag boundary thickness which was of the same order as that quoted by Darken(15). Ward et al.(14) thought that this value seemed entirely reasonable and although this did not constitute proof of diffusion control, it indicated again that diffusion control could account for the observed results.

N.J.Grant et al.(5) reported that a large increase in stirring efficiency did not materially increase desulphurization rates in the

slower more easily observable acid slag experiment. However,later, Fulton and Chipman (16) observed that the sulphur transfer rate was increased by a drastic increase of mechanical stirring up to 500 r.p.m., using metal containing 6 % Si to maintain equilibrium with SiO_2 in the slag as shown in Fig. 1.2.

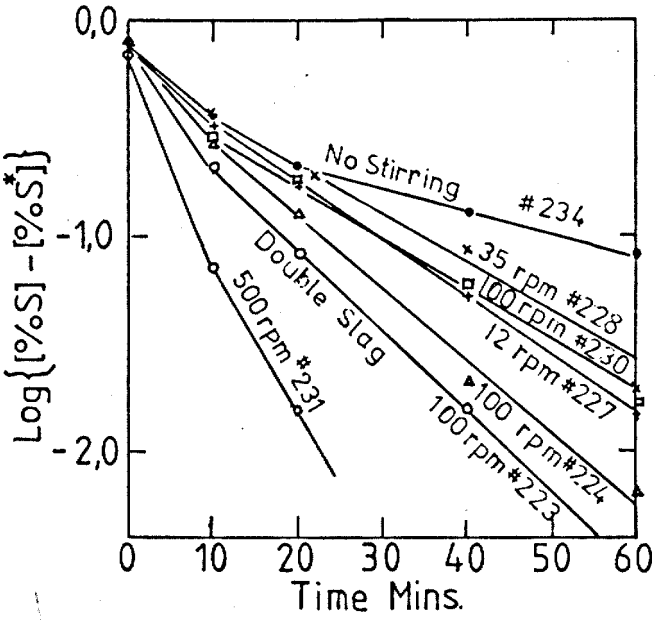

FIG.1.2. INFLUENCE OF STIRRING RATE ON THE RATE OF DESULPHURIZATION AT 1500°C FROM FULTON AND CHIPMAN (16)

Criticising the report of Fulton et al., Nilas and Froberg(17) considered that as the hydrodynamic profile of the metal-slag interface may change by mechanical stirring and also at stirring rates of 500 r.p.m. parts of the slag are entrained into the metal, the increase in the sulphur transfer appears primarily to be based on the increase in the interfacial area and therefore in this way diffusion control of sulphur transfer can not be demonstrated.

More recently K.Ogino et al.(18) and M.Hatano (8) also observed a significant mechanical stirring effect and took this fact as indicating that diffusion of sulphur in slag is the rate determining step.

The major drawback of all these diffusion control arguments is that they can not explain the observation that the addition of deoxidizers to metal increases the rate of desulphurization.(6)(7)(17)(19)

1.3. INVESTIGATIONS INTO CHEMICAL REACTION CONTROL

It can be considered that among the early experimental observations the experiments reported in a series of three papers (3)(4)(19) by Chang, Goldman, Derge, and Philbrook provided us for the first time with a good approach for understanding the mechanism of sulphur transfer. In their first study Chang and Goldman demonstrated that the reaction is first order with respect to the sulphur content of the metal. This was later confirmed by other workers.(7)(14)(21). Chang et al.(3) interpreted their transfer data in the following way; Assuming that the rate of transfer of sulphur from metal to slag is proportional to the concentration of sulphur in the metal,and that from slag to metal is proportional to the concentration of sulphur in the slag; the net transfer of sulphur from metal to slag may be given by the following equation:

$$\frac{Ws}{100A} \cdot \frac{d(\%\,S)}{dt} = Km\ [\%\,S]^{m} - Ks\ (\%\,S)^{n} \qquad (5)$$

where Ws : weight of slag,

A : interfacial area between slag and metal,

$[\%\,S]$, $(\%\,S)$: concentration of sulphur in metal and slag respectively in weight percent,

Km , Ks : coefficient of transfer of sulphur from metal to slag and from slag to metal respectively,

m , n : order of reaction of the forward and reverse transfer reaction respectively.

If the reaction is first order, i.e. m,n = 1, and the sulphur concentration in metal is assumed to be constant at the beginning of run, then it follows that a plot of d(% S)/dt vs. (% S) should be a straight line with a slope proportional to Ks and an intercept on the ordinate proportional to Km. Their experiment points fit straight line relationship as predicted. Fig 1.3. shows some of the results obtained by Chang et al. Using this approach it is difficult to be accurate as tangents have to be drawn onto the experimental rate curves to obtain values of d(% S)/dt.

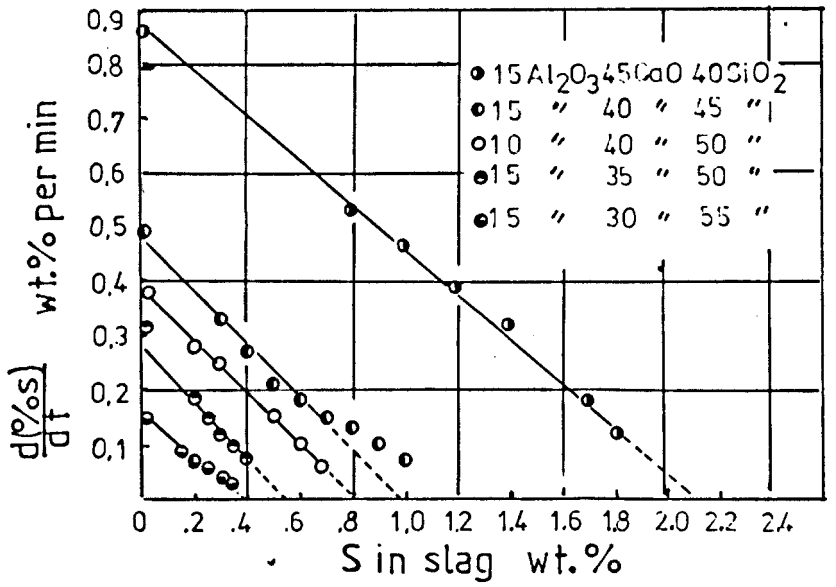

FIG.1.3. d(% S)/dt vs. (% S) PLOTS FOR FIVE SLAGS AT 1540°C. FROM CHANG AND GOLDMAN(3)

Ward et al.(14) plotted the integrated form of equation 5 instead of the differential form as above and this could remove the difficulty in calculation of the accurate tangent values of the rate curve. In the initial stages they assumed that sulphur content in the slag is negligible and hence equation 5 may be integrated to give ;

$$\mathrm{Ln}\,[\%\,S]_t - \mathrm{Ln}\,[\%\,S]_o = -\left(\frac{100A}{Wm} \cdot Km\right) t \qquad (6)$$

where Wm : weight of metal,

$[\%\,S]_t$, $[\%\,S]_o$: sulphur wt.% in metal at time t and o respectively.

Their plots show a linear relationship between Ln [% S] and time at least in the initial stages as predicted by equation 6. Some of their plots are shown in Fig.1.4.

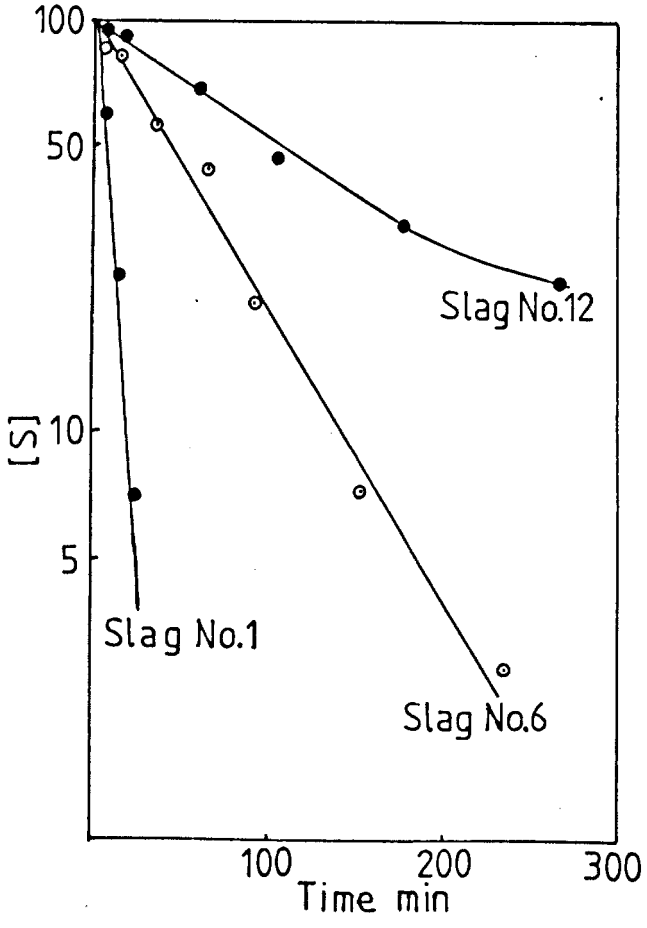

FIG.1.4. DESULPHURIZATION CURVES LOG S v TIME.
No. 12 SILICIOUS SLAG, No. 6 MODERATELY SILICIOUS SLAG, No. 1 ALUMINOUS SLAG. FROM WARD et al.(14)

Again the value of Km can be obtained from the slope of the graph.

It was found (3) (21) that Km rapidly increased with the slag basicity while Ks was not greatly affected as shown in Fig 1.5.

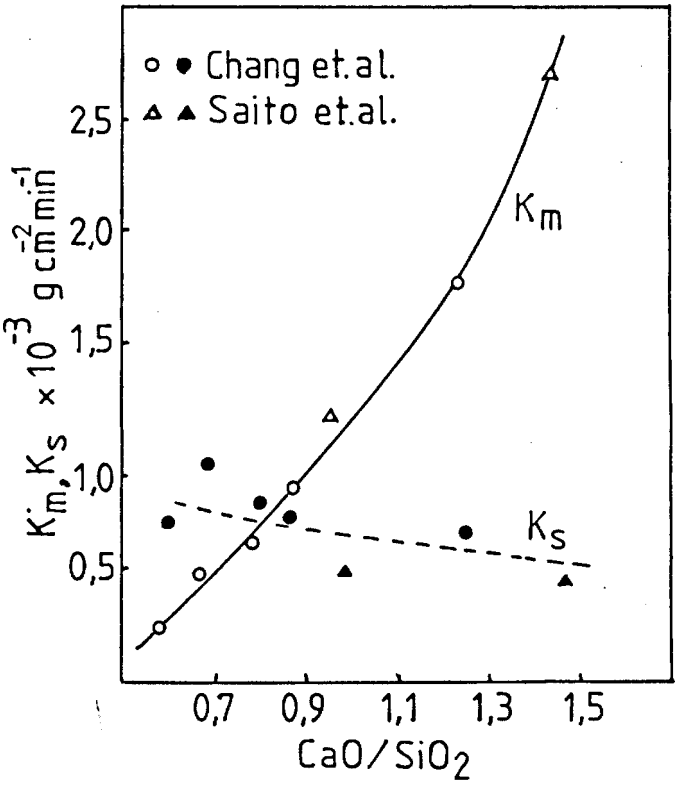

FIG.1.5. RELATION BETWEEN MASS TRANSFER COEFFICIENTS, Km, Ks AND BASICITY OF SLAG. FROM CHANG AND GOLDMAN(3) AND SAITO et al.(21)

It was also found (3) that the rate of sulphur transfer increased with increasing temperature. If sulphur transfer is a thermally activated process, the rate coefficients, Km, Ks, should follow the Arrhenius relation for such rate processes, i.e.

$$Km = Am \exp\left(\frac{-Em}{RT}\right) \qquad (7)$$

$$Ks = As \exp\left(\frac{-Es}{RT}\right) \qquad (8)$$

where Am, As : frequency factor for sulphur transfer from metal to slag and from slag to metal respectively. g cm^{-2} min^{-1}.

Em, Es : Activation energies for the respective transfer cal g mol^{-1}.

R : gas constant (1.987 cal $^{o}K^{-1}$ mol^{-1})

T : absolute temperature ^{o}K.

On taking logarithms, equations 7 and 8 become

$$Ln\ Km = Ln\ Am - \frac{Em}{RT} \qquad (9)$$

$$Ln\ Ks = Ln\ As - \frac{Es}{RT} \qquad (10)$$

Plots of the logarithm of the rate coefficient vs. 1/T should show the straight linearity. Chang et al. (3) found that Km was more temperature sensitive than Ks and the values of Es = 39000 cal mol^{-1} and Em = 79000 cal mol^{-1} were obtained from the plots.

In the second study by Derge et al.,(4) the details of the mechanism of this desulphurization reaction were investigated by observing changes in iron content in the slag during the sulphur transfer reaction. It was found that the iron content of the slag increased in the early stages, when sulphur transfer proceeded rapidly, passed through a maximum when the sulphur transfer slowed down and decreased to some steady low value.

To further investigate the role of iron in the slag they took some slag, which had been previously reacted with an iron-sulphur-carbon alloy to give a slag sulphur content of about 1 %, crushed it and magnetically separated any particles. When this was remelted in a graphite crucible iron beads formed which contained about 0.8 % C.

However if the slag was remelted in a refractory crucible no iron beads were formed. This demonstrates that the beads were formed by reduction of combined iron and not by agglomeration of small iron particles.

Further samples of the slag which had been reacted with the iron -carbon-sulphur alloy were used to study sulphur transfer from slag to metal. In the first experiment the slag was reacted with an iron-carbon alloy in a graphite crucible whilst in a second experiment the slag was prereduced in graphite before being reacted with the metal. The sulphur transfer rate from slag to metal was significantly slower in the second (low iron oxide) experiment.

In view of these observations Derge et al. thought that iron and sulphur leave the metal and enter the slag together and the sulphur then is stablized in the slag by combination with calcium, the iron oxide resulting from this slag phase reaction is in turn reduced to iron by carbon producing CO evolution. The process was described schematically as the following sequence;

$$[FeS] = (FeS) \qquad (11)$$

$$(FeS) + (CaO) = (CaS) + (FeO) \qquad (12)$$

$$(FeO) + C_{\substack{\text{crucible} \\ \text{or metal}}} = [Fe] + CO_{gas} \qquad (13)$$

They also measured the rate of CO evolution during sulphur transfer to get direct quantitative evidence which can confirm that CO evolution is a necessary part of the consecutive reactions of desulphurization. It was found that CO gas evolution increased with increase of temperature and sulphur content in metal. It is worth noting that Derge et al. (4) stated that they could not achieve a satisfactory material balance for CO evolution on the basis of conventional slag and metal analysis through the molecular reaction

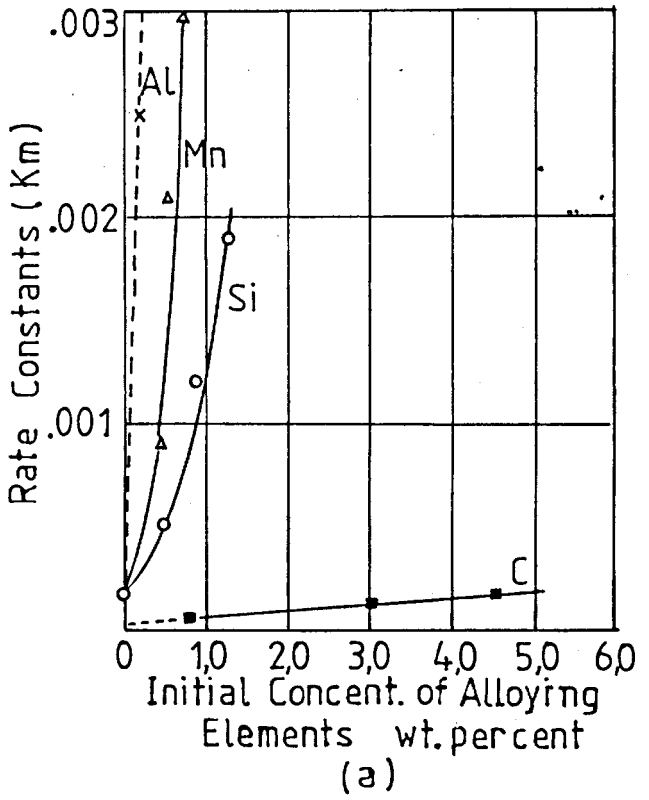

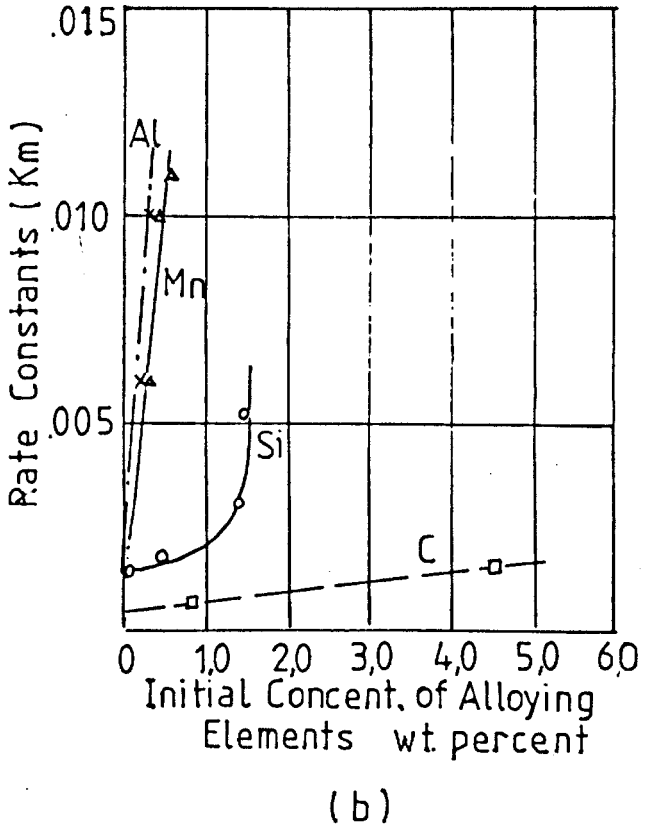

FIG.1.6. COMPARISON OF THE EFFECT OF ALLOYING ELEMENTS ON RATE CONSTANTS FOR SULPHUR TRANSFER.

(a) WITH ACID SLAGS (15 % Al_2O_3, 30 % CaO, 55 % SiO_2)

(b) WITH BASIC SLAGS(15 % Al_2O_3, 45 % CaO, 40 % SiO_2)

FROM K.M.GOLDMAN et al. (19)

equations. This problem was later overcome by King and Ramachandran with interpretation of data on the basis of an electrochemical reaction.

In the third study Goldman et al. (19) investigated the effect of addition of deoxidizing elements to the metal on the mechanism of sulphur transfer. It was found that C, Si, Mn, Al all increased the rate of sulphur transfer from metal to slag with increasing effectiveness in the order named and Cu, Ni, and P had no observable influence on the rate as shown in Fig.1.6. This was confirmed later by many other investigators. (6)(7)(17)(20). Therefore it seemed clear that in the unalloyed system iron was the principal carrier of sulphur across the slag-metal interface, but when manganese was present as an alloying element, it not only replaced iron, but caused the overall process to proceed more rapidly. The elements Si and Al appeared to act as a deoxidizer by supplanting carbon in removing oxygen from the system.

In view of the experimental evidences Goldman et al. (19) generalized the three step mechanism;

$$MS = (MS) \qquad (11a)$$

$$(MS)+(CaO) = (CaS)+(MO) \qquad (12b)$$

$$(MO)+ R = M + (RO) \qquad (13c)$$

where R = C, Si, Al, Mn(?) and M = Fe, Mn, Si(?).

They suggested that the limiting reaction in controlling the rate of desulphurization might be the heterogeneous reaction between carbon and FeO in the third reaction involving CO evolution.

But this mechanism received a strong opposition from Grant et al. (5) who investigated the effect of manganese and its oxide on desulphurization by blast furnace type slags. Grant et al. observed that MnO addition to slag during desulphurization caused an almost

immediate sulphur reversion into metal and the speed of desulphurization was directly related to the degree of oxidation of the slag. Discussing the effect of reduction of oxide in the slag on the desulphurization rate, they said that easily reducible oxides such as FeO offer little impediment to desulphurization whereas oxides such as the more refractory SiO_2 release oxygen slowly, maintaining an oxidized slag over a long period of time, thus preventing the desulphurization. This role of SiO_2 reduction on the desulphurization was investigated in a separate study (22) in which they observed that a more acid slag showed a higher silicon content in metal and that silicon addition to metal increased profoundly the rate of sulphur removal as in Fig.1.7. These results were interpreted as showing that silica in the slag is a sufficiently good oxidizing agent to interfere with the principal desulphurizing reaction, but when sufficient silicon is present to prevent further reduction, thus depriving the silica of its oxidizing power, the transfer of sulphur from metal to slag is extremely rapid. Therefore they concluded (5) that the limiting reaction in controlling the rate of desulphurization is probably the reduction of SiO_2 and not the heterogeneous reaction between C and FeO.

Nilas and Froberg (17) also suggested a similar explanation for the role of silica reduction in the desulphurization reaction on the basis of electrochemical reactions which is discussed below. Ionization of S in slag through its transfer from metal to slag needs electrons, i.e. $S + 2e^- \longrightarrow (S^{2-})$ while silica reduction also requires electrons, $(Si^{4+}) + 4e^- \longrightarrow Si$, thus they both proceed with consumption of electrons, therefore both the sulphur transfer and silica reduction reactions retard each other.

There was also another similar explanation for the role of

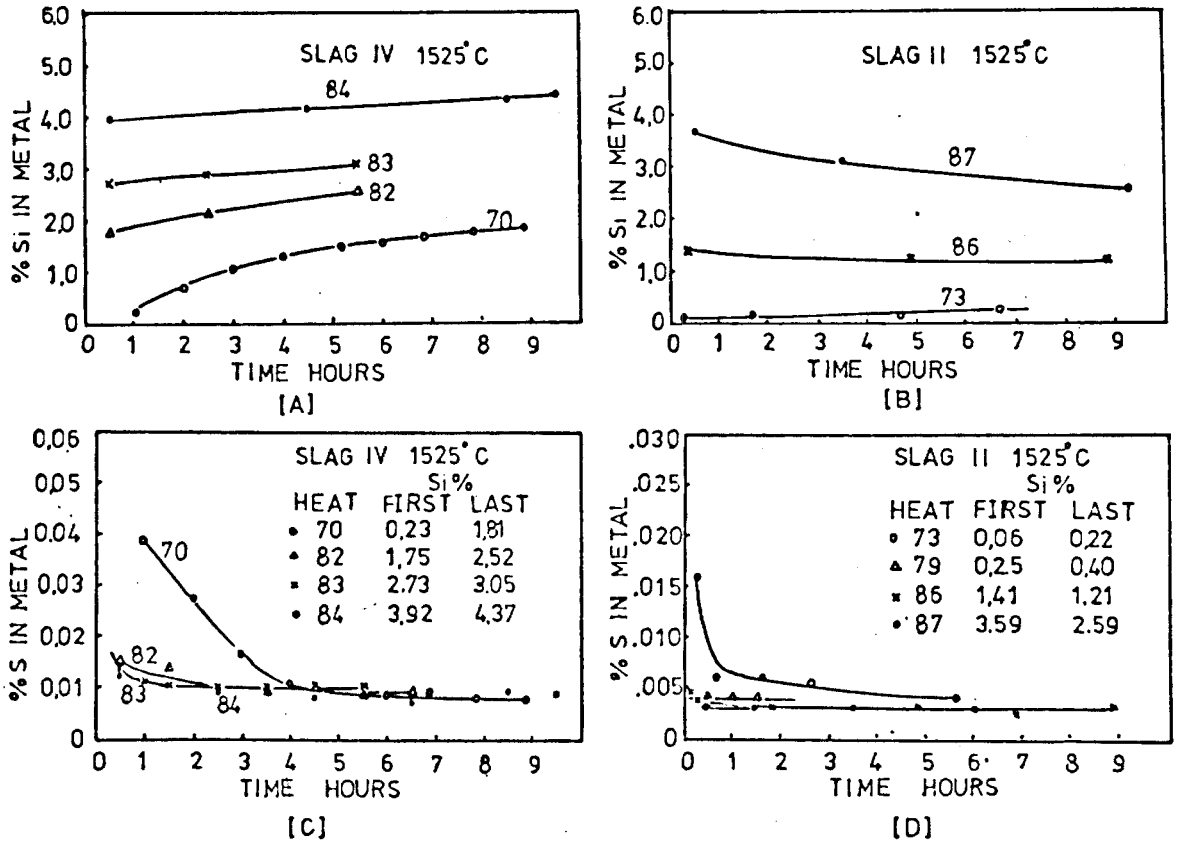

FIG.1.7. A : INCREASE IN SILICON CONTENT OF METAL WITH TIME FOR SLAG IV AT 1525° C

B : CHANGE IN SILICON OF METAL WITH TIME FOR SLAG II AT 1525° C

C : DECREASE IN SULPHUR IN METAL WITH TIME FOR SLAG IV AT 1525° C FOR HEATS AT DIFFERENT INITIAL CONTENT

D : THE SAME AS C BUT FOR SLAG II.

SLAG II : 50 % CaO, 10 % MgO, 25 % SiO_2, 15 % Al_2O_3

SLAG IV : 40 % CaO, 10 % MgO, 35 % SiO_2, 15 % Al_2O_3

FROM N.J.GRANT et al. (22)

silica reduction in sulphur transfer by Ward et al. (14) who observed the equality of the activation energies for silica reduction and sulphur transfer in acid slags. In view of these observations Ward et al. explained that the difficulty of sulphur transfer to acid slags, i.e. slags having few free O^{2-} ion, lies in the difficulty in breaking the Si - O bond in the tetrahedral coordination shell of (SiO_4^{4-}) to produce free oxygen ions which could then exchange with sulphur in the metal; and therefore sulphur transfer from metal to slag and silicon transfer from slag to metal are both controlled by a common factor, that is, the difficulty of breaking the Si - O bond, hence this can account for the equality of the activation energies for both transfers. But in basic slags the activation energy for sulphur transfer should be less than that for silicon due to the higher activity of free oxygen ions. However they couldn't get data to verify this as low silica activity made it difficulty to measure silicon transfer from slag to metal.

Later workers, however, have provided more evidence that it is heterogeneous CO evolution which is the barrier to sulphur transfer.

Turkdogan et al. (6) explained the influence of deoxidizing elements on the rate of desulphurization observed in their experiments as shown in Fig.1.8. using the concept of a sluggish carbon-oxygen reaction discussed elsewhere (23)(24).

They represented the first stage of the desulphurization reaction by the following equation ;

$$[Fe] + [S] = (Fe) + (S) \qquad (14)$$

and as a consecutive step the following reaction was supposed to take place in slags containing suspended carbon ;

$$(Fe) + (O) + C = [Fe] + CO_{gas} \qquad (15)$$

In the absence of carbon the above reaction can not occur and oxygen will dissolve in iron;

$$(Fe) + (O) = [Fe] + [O] \qquad (16)$$

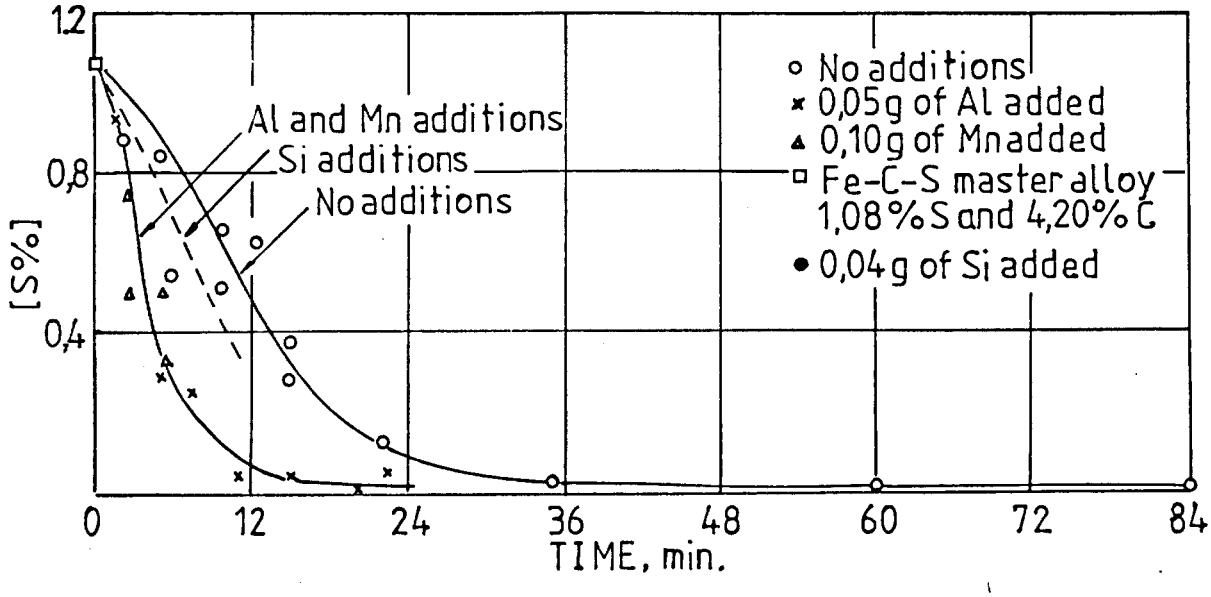

FIG.1.8. RATE OF DESULPHURIZATION OF CARBON-SATURATED IRON BY A CALCIUM ALUMINATE SLAG (50 % CaO, 50 % Al_2O_3) AT 1505° C. FROM E.T.TURKDOGAN et al. (6)

They omitted the ionic charges from the above equations, because of the uncertainty of the degree of ionization of solutes in slag. If the rate of reaction 15 were as fast as reaction 14, then reaction 16 could not have taken place; that is, if the oxygen activity in iron were not increased during the process of desulphurization because of reaction 15, it follows that additions of silicon, manganese, or aluminum should not have any effect on the rate of metal-slag sulphur transfer.

In view of the experimental evidence that deoxidants speed sulphur transfer it can therefore be stated that the oxidation of carbon suspended in the slag and dissoved in the metal is slow compared with the oxidation of other elements, the oxides of which are not gaseous, but which dissolve in the slag.

Later Ramachandran and King (7) also demonstrated CO evolution is the rate controlling reaction through the well known electrochemical reaction mechanism which is reviewed in the next section.

1.4. ELECTROCHEMICAL REACTION MECHANISM

The molecular reaction mechanism suggested by Derge et al. (4) (19) suffers from the following drawbacks;

(1) It is inconsistent with the ionic theory of slags and such molecular reactions can not explain the phenomena of the uphill sulphur transfer from a lower concentration of sulphur to a higher sulphur concentration by counter flow of oxygen, which was experimentally demonstrated by Turkdogan and Grieveson (25).

(2) The molecular reaction mechanism is also unable to explain the effect of applied current on the desulphurization kinetics (26)(27).

(3) A mass balance for CO evolution and the other transferred elements in slag and metal can not be achieved on the basis of molecular reactions.

Such an explanation therefore lost ground to a more fundamental explanation based on electrochemical reactions.

Rosenquist (28) is recorded as the first to suggest the electrochemical mechanism in the discussion on the paper of Derge et al. (4)

and it has since been discussed in great detail by Wagner (29) and Ramachandran and King (7). Ramachandran and King established the electrochemical reaction mechanism by following sulphur transfer using chemical analysis and measurement of CO evolution.

Sulphur exists in metal as a neutral atom, while slags are ionic and have very limited solubility for neutral atoms, although some such solubility does exists(30). At the oxygen potential of cast iron sulphur exists in slag primarily as S^{2-} ion (31). Therefore each sulphur atom which transfers from metal to slag must acquire two electrons at the slag-metal interface;

$$[S] + 2e = (S^{2-}) \qquad (17)$$

In order to preserve electroneutrality either a negative ion such as O^{2-} must be discharged at the interface;

$$(O^{2-}) = [O] + 2e^{-} \qquad (18)$$

Or an electropositive atom such as Fe, Si, or Al must transfer to slag;

$$Fe = (Fe^{2+}) + 2e^{-} \qquad (19)$$

$$1/2\,[Si] = 1/2(Si^{4+}) + 2e^{-} \qquad (20)$$

$$2/3\,[Al] = 2/3(Al^{3+}) + 2e^{-} \qquad (21)$$

Reaction 18 is responsible for the evolution of CO. It was suggested by Ramachandran et al. that this reaction takes place directly with carbon according to the reaction;

$$[C] + (O^{2-}) = CO_{gas} + 2e^{-} \qquad (22)$$

Thus, the condition of electroneutrality would imply that the rate of cathodic reactions such as equation 17 must be equal to the sum of all the anodic reactions such as equation 18 - 22. In other words;

$$2\,n_S = 2\,n_{CO} + 2\,n_{Fe} + 4\,n_{Si} + 3\,n_{Al} \qquad (23)$$

Where n_i is the rate of transfer(or evolution) of i from metal to slag in mole per sec. and the sign is reversed for slag to metal transfer.

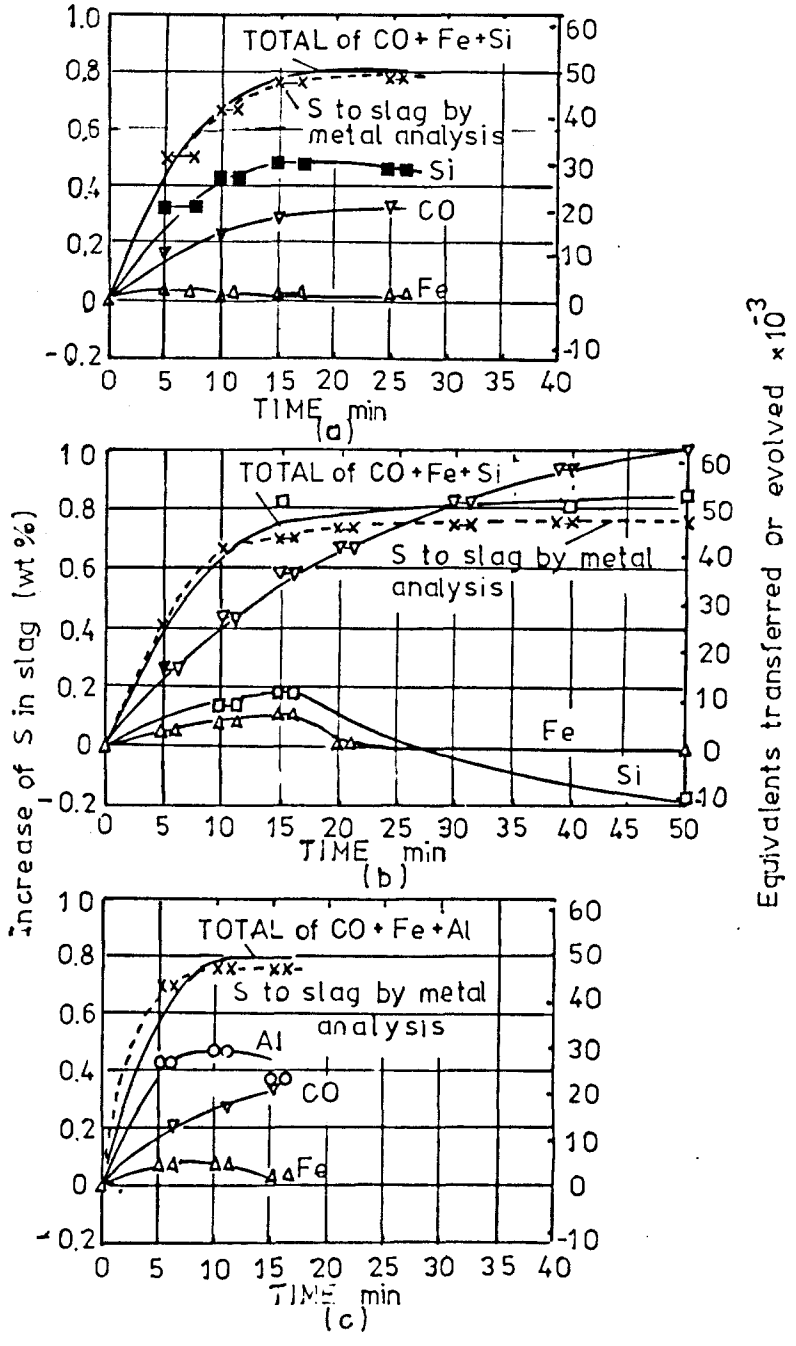

FIG.1.9. INCREASE OF SULPHUR IN SLAG, EQUIVALENTS OF S, Fe AND Si TRANSFERRED FROM METAL TO SLAG AND EQUIVALENTS CO EVOLVED

(a) SLAG 48 % CaO, 21 % Al_2O_3 AND 31 % SiO_2 ; INITIAL Si 0.38 %, EQUILIBRIUM Si , 0.5 % 1502° C,

(b) SLAG AS IN (a); INITIAL Si 0.1 % EQUILIBRIUM Si 0.5 %,

(c) SLAG 50 % CaO, 50 % Al_2O_3, INITIAL Al 0.53 % 1550° C.

FROM KING AND RAMACHANDRAN (32)

Or in terms of chemical equivalents;

$$n_S = n_{CO} + n_{Fe} + n_{Si} + n_{Al} \qquad (24)$$

This relationship was observed within experimental error in all the results of Ramachandran et al.(7) as in Fig.1.9. showing some typical results.

In Fig.1.9. (a) and (b) the initial silicon concentrations in the metal were less than 0.5 % which would have been in equilibrium with the slag in the presence of CO at 1 atm. and carbon. Yet silicon passed from metal to slag as sulphur was transferred. Iron moved into slag as well, despite the fact that at equilibrium the quantity of iron in the slag would have been negligible. At the same time as these reactions occurred, CO gas was evolved. Ultimately, however, the iron and silicon which passed into the slag were reduced back into the metal. In Fig.1.9. (c) where aluminum was present in the metal and silicon was absent, aluminum moved into the slag. A number of reactions were obviously occuring and King and Ramachandran summed up these reactions as below;

	Initial stages	Later stages
Anodic reactions	$[C] + O^{2-} = CO + 2e^-$	$[C] + O^{2-} = CO + 2e^-$
	$Fe = Fe^{2+} + 2e^-$	
	$1/2\,[Si] = 1/2\,Si^{4+} + 2e^-$	
	$2/3\,[Al] = 2/3\,Al^{3+} + 2e^-$	
Cathodic reactions	$[S] + 2e^- = S^{2-}$	$[S] + 2e^- = S^{2-}$
		$Fe^{2+} + 2e^- = Fe$
		$1/2\,Si^{4+} + 2e^- = 1/2\,[Si]$
		$2/3\,Al^{3+} + 2e^- = 2/3\,[Al]$

One of the above reactions is the slowest step and hence it is rate controlling. As the CO evolution reaction 22 is seen to involve three phases, so it is expected to be very slow. In fact it is because of this slow reaction that iron, silicon, and aluminum get oxidized initially irrespective of their equilibrium condition with slag,to keep pace with rapid sulphur transfer at the initial stages of desulphurization.

However the mechanism of CO evolution is yet not very clear. The evolution of CO could take place by any of the following mechanisms

(1) Oxygen may be transferred to the metal by equation 18 and reacted with carbon in the metal;

$$(O^{2-}) = [O] + 2e^{-} \qquad (18)$$

$$[C] + [O] = CO_{gas} \qquad (25)$$

(2) CO may be formed by discharge of O^{2-} at the slag-metal interface as;

$$[C] + (O^{2-}) = CO_{gas} + 2e^{-} \qquad (22)$$

This requires that C in metal, O^{2-} in slag react to form gaseous CO, which means a three phase reaction and hence it may take place along a line; most probably crucible - metal - slag line

(3) O^{2-} can react with the graphite crucible to form CO ;

$$C_{(graphite)} + (O^{2-}) = CO_{gas} + 2e^{-} \qquad (26)$$

and the electrons pass through the graphite crucible and metal to cathodic reaction site, i.e. local cell action as shown in Fig.1.10.

In discussion on the paper of King and Ramachandran (32) Darken strongly argued that the reaction involving carbon in the metal, Oxygen in the slag and CO in the gas phase was particularly difficult for him to visualize because of the very small interfaces involving three phases which could exist. He felt that a two phase reaction would be more reasonable.

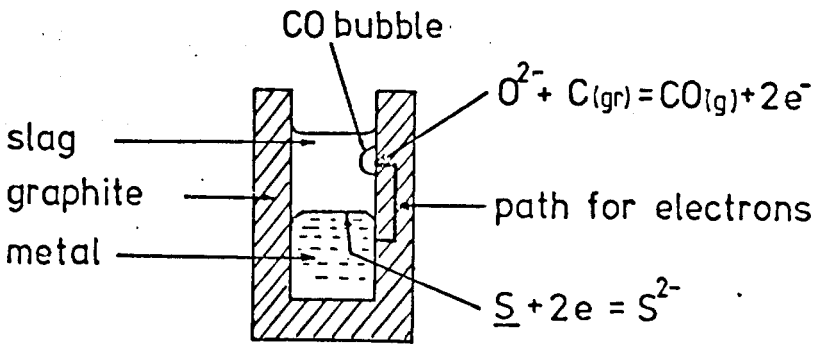

FIG.1.10. LOCAL CELL REACTION FOR SULPHUR TRANSFER IN GRAPHITE CRUCIBLE. FROM T.B.KING. (34)

In spite of Darken's argument King felt that it was not too improbable that a bubble could nucleate at the slag-metal interface, but he did not propose that the reaction was exclusively phase-boundary controlled. Instead it was partially phase boundary controlled and partly diffusion controlled. It may be considered that he could not neglect the possibility of diffusion control because he and his co-workers (16)(33) had observed some effect of stirring on the desulphurization rate.

Wagner reviewed the proposition that local cell action might be controlling, that is, there is a possibility at the slag-graphite interface that oxygen ions from the slag combined with carbon from the crucible to form CO, and the electrons from this reaction pass through the graphite crucible to the site of the reaction with sulphur. He also said that he felt that the nucleation problem was not a serious one in the system and cited the low overvoltage necessary for hydrogen evolution on a platinum electrode.

In this discussion Philbrook pointed out that the general results obtained in the experiments were similar to those that had been reported several years ago (4). In concluding the discussion King commented that they had proposed a mixed type of control for the reaction rather than simply phase-boundary control.

Much later King suggested in his review paper another possible explanation on the mode of CO evolution and sulphur transfer, schematically shown in Fig.1.11. which is based on the movement of CO bubbles through the slag metal interface through which the diffusion path for oxygen is greatly shortened.

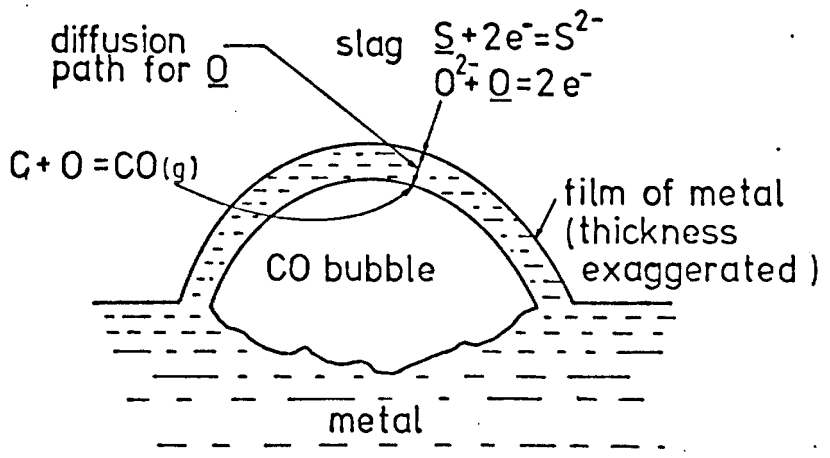

FIG.1.11. CO BUBBLE AT SLAG/METAL INTERFACE, CARRYING FILM OF IRON INTO SLAG PHASE. FROM T.B.KING. (34)

This explanation is based on Richardson's experimental demonstrations (35) which show that as bubble rises through the phase boundary a complete film of metal surrounds it and is carried into the slag and

eventually the film peels off and disintegrates into droplets. This new explanation seem to be more appropriate for explaining stirring effects.

However, in view of the experimental results of Ramachandran et al., Richardson(36) said that if the anodic reaction of CO evolution took place only at the points where the graphite crucible, slag, and metal met in their experiments, whilst the cathodic processes took place over the whole slag-metal interface, the uneven distribution of negative charges which would arise in the slag (because it conducts ionically and not electronically) would soon slow down both the anodic and cathodic processes and then the reactions would become dependent on the transport of ions in the slag, and the rates would be affected by stirring. This may be one of the reasons why stirring increased the reaction rates.

Recognition of the electrochemical nature of the sulphur transfer process has led to investigations of the effect of applying a potential difference between metal and slag (26)(27). Ward and Salmon (26) carried out investigations at 1400 ^{o}C with carbon saturated iron and passed current after metal and slag had come to equilibrium with respect to sulphur and silicon. They found that sulphur could be made to pass from metal to slag but that the current efficiency for sulphur transfer was low.

After it had been proved that the kinetics of sulphur reactions are electrochemical in nature, quantitative formulation of the exchange of various elements started. Hamptinne et al. (37) attempted to formulate some equations for the rates of iron and silicon transfer as a function of the rate of carbon monoxide evolution by assuming the

existence of an electrical potential difference between metal and slag, but their treatment was lacking in the effects of chemical potential differences of components and the electrical potential between slag and metal. The second important approach was made by Lu (38) with application of irreversible thermodynamics to the coupling of various reactions during desulphurization. It was followed by Frohberg et al. (39) who attempted to derive a mathematical transport model for sulphur transfer reactions in the similar way.

As a conclusion of this review, it is not still clear whether the sulphur transfer reaction is controlled by silica reduction or CO evolution reaction as described previously. Furthermore for the CO evolution reaction some suggestions of diffusion control could neither be ignored completely, nor can it be said that CO evolution is controlled only by electrochemical reaction.

CHAPTER 2.

EXPERIMENTAL

CHAPTER 2

EXPERIMENTAL

2.1 APPARATUS

2.1.1 FURNACE AND REACTION TUBE

A vertical Carbolite silicon carbide resistance furnace with an impervious mullite reaction tube was used for all experiments. The furnace was heated by six silicon carbide elements (Crusillite type X) connected in a series arrangement.

Temperature control was achieved by means of Eurotherm type PID / SCR thyristor controller with an accuracy of within $\pm$ 3 ^{o}C.

The actual reaction temperature in the mullite tube was measured by a Cambridge potentiometer with a Pt / Pt13%Rh thermocouple introduced in a mullite sheath which was inserted through the bottom of the reaction tube. This also supported the graphite reaction crucible at the desired position.

The temperature profile of the furnace was measured frequently by changing the position of this thermocouple sheath. This furnace had a 3 cm long hot zone at the reaction temperature of 1460 ^{o}C and the temperature variation within the hot zone was $\pm$ 1 ^{o}C.

The mullite reaction tube, vertically set in the furnace, was of 50 mm I.D., 900 mm in length and open at both ends. The top of the reaction tube was sealed using high temperature "O" rings compressed on to the walls of the tube by a water cooled brasshead containing a central hole for sampling and another for gas inlet. The bottom of the tube was sealed in the same way and the brasshead contained one gas outlet hole and one central hole for insertion of the thermocouple sheath. For experiments under reduced pressure the surfaces of mullite tube at both ends were polished with fine emery paper on a lathe to improve sealing.

CO gas (Air Products Ltd. N_2 = 0.3 %, O_2= 0.075 %, CH_4 = 30 v.p.m.) was passed through this reaction tube to keep a reducing atmosphere and the pressure in the reaction zone was kept constant at any predetermined value by using of a Cartesian Manostat.

2.2. MATERIALS

2.2.1. SLAG PREPARATION

Lime silica slags, with different basicities, containing 6 wt.% magnesia to lower the melting temperature were used in the most experiments. In one experiment a 20 % lime - 80 % calcium fluoride slag was used as this is used commercially to remove sulphur.

The lime silica slags were prepared by melting mixtures of " analar " calcium carbonate, silica sand washed with hydrochloric acid, and " analar " magnesia in the desired proportions, in a graphite crucible using a high frequency induction furnace.

For the lime-calcium fluoride slag calcium carbonate was calcinated first in a graphite crucible at 1000°C by low induction heating and then BDH high purity calcium fluoride was added gradually and the temperature raised until the slag was completely melted.

The slag melts were cast into an iron mold and ground to - 60 mesh.

For slags containing FeO or MnO the desired weight of the oxide prepared by ignition was added and thoroughly mixed.

FeO was made by heating ferrous oxalate in an iron tube first at 600°C until almost all gas evolution had finished and, after that at 900°C. The gas mixture which was mainly CO and CO_2 was passed through water and thus the progress of gas evolution was followed. When the gas evolution had ceased completely, the iron tube was

quenched in water and the FeO thus produced was ground to - 150 mesh, demagnetized, and analysed to determine its iron content.

MnO was prepared by heating manganous oxalate in a silica tube, using the same technique as described above for FeO, except that hydrogen was allowed to pass through the tube before increasing the temperature to 1100°C.

2.2.2. METAL PREPARATION

Carbon saturated iron - sulphur alloy was made by melting Japanese electrolytic iron 99.9 % purity in graphite crucibles, then adding ferrous sulphide stick, stirring well with a graphite rod, and casting into water. The alloy thus quenched was crushed, dried after washing in acetone and analysed for sulphur and carbon. Sulphur analysis showed that approximately 20 % of the sulphur added was lost during the melting.

Carbon saturated Fe - S - Si alloy was prepared in the same way described above except that pure silicon lump 99.9 % was placed on the bottom of the graphite crucible under the electrolytic iron before melting.

In a few occasions carbon saturated Fe - S - Si alloy and Fe - S - Mn alloy were made by melting carbon saturated Fe - S alloy and pure silicon or electrolytic manganese 99.9 % purity directly in graphite reaction crucibles and a metal sample was taken from this melt for analysis using a silica tube with an aspirator.

2.2.3. GRAPHITE CRUCIBLES

Three different sizes of crucibles with the dimensions in table 2.1. were machined from Morganite AGTS high purity graphite rods.

Table 2.1.

Crucible designation	Dimensions (mm) I.D.	O.D.	Length	Bottom thickness
1 1/4 in.	31.8	38.1	90	23
3/4 in.	19	25.4	75	3
3/8 in.	9.5	25.4	55	3

The 1 1/4 in. crucible had a hole of 10 mm dia. and 20 mm depth at its bottom to be fixed on the end tip of a thermocouple sheath.

For supporting 3/4 in. and 3/8 in. crucibles in the reaction tube an 1 1/4 in. crucible 20 mm wall height was used as a container for these small crucibles. The 1 1/4 in. crucible was used for 100g of metal and 30 - 60 g of slag and the 3/4 in. crucible was used for 35 g of metal and 10 g of slag.

The 3/8 in. crucibles were used to study the effect of crucible diameter on the depulphurization rate, with 8.75 g of metal and 2.5 g of slag whilst keeping the heights of metal and slag as constant.

2.3. PROCEDURE

The required amount of alloy was premelted into the bottom of a graphite reaction crucible and the preweighed powdered slag was added.

The experimental technique varied with the size of crucible. With small diameter crucibles, 3/4 in. and 3/8 in., the charge was introduced at the bottom of the furnace and slowly raised up to a predetermined position just below the hot zone with a temperature of 1100^{o}C and held at the position until the crucible achieved the same temperature.

It then was raised up quickly to the hot zone and the experimental time was measured from this time. After the experimental

time had elapsed, the assembly was rapidly removed out to the air (less than 5 secs.) causing an effective quench of the specimen. The complete slag sample was ground in an agate mortar and the metal sample was sectioned transversely ready for chemical analysis.

With the larger crucible, 1 1/4 in., the procedure was identical except that slag samples were taken at predetermined time intervals using a copper sampling rod with an end tip of 4 mm dia. The average size of slag samples was about 0.6 g.

The majority of experiments were conducted under a flowing carbon monoxide atmosphere, whilst for those under reduced pressure atmospheres a static atmosphere was necessary. Constant low pressures were maintained using a cartesian manostat to vent the evolved gas to waste.

In all cases the ground slag samples were treated by magnet to separate any iron particles before analysis.

Slag samples were analysed for sulphur, ferrous oxide, and manganous oxide in the cases where manganese was present.

In the early experiments the metal sample was totally sectioned and each section was analysed to study a concentration gradient, but in most of the later experiments a few selected sections from the top and bottom of the sample were analysed for sulphur, silicon, carbon, and manganese.

2.4. ANALYSIS

2.4.1. ANALYSIS OF SULPHUR IN SLAG

Sulphur in slag was analysed by the stoichiometric combustion method with carbon dioxide gas developed by Fincham and Richardson (40).

A horizontal carbolite furnace with an 1 in. dia. mullite combustion tube was used for the analysis. The gas used for combustion was commercial CO_2 (Distillers Co.Ltd) which oxidised the sulphur in the slag to SO_2 and the outgoing combustion gas was bubbed through the absorbents,which were contained in two tall narrow vessels fitted with bubblers and burettes, connected in series to ensure complete absorption of SO_2. Titration was carried out in each vessel as analysis proceeded. The absorbing solution consisted of 100 ml of deionized water, 5 ml of 1 : 4 dilute hydrochloric acid, and 1 ml of freshly prepared 0.9 % starch solution containing 1.5 % potassium iodide.

0.1 - 0.3 g of slag was placed on preignited fire clay combustion boats and introduced quickly into the combustion tube. The combustion temperature was 1400 °C and the flow rate of CO_2 was 300 c.c./min. Sulphur given off as SO_2 was absorbed in the acid solution and standard potassium iodate solution of 0.2225 g/l concentration (such that 1 ml of solution was equivalent to 0.0001 g of sulphur) added from the burette to maintain the initial neutral blue starch colour. Analysis was complete when continued gas bubbling produced no further colour change.

Periodically the method was checked by analysing B.C.S. slag standards and excellent reproducibility and accuracy were obtained. The accuracy of the sulphur analysis is considered to be $\pm$ 2 % of the total sulphur.

2.4.2. ANALYSIS OF SULPHUR IN METAL

The combustion method with CO_2 gas is not suitable for the analysis of metal as the combustion is not only far too slow for routine analyses, but in this time normal combustion boats are

destroyed by the iron oxide produced.

A rapid combustion method with air for the determination of sulphur in iron and plain carbon steel, and the apparatus suggested by R.F.Jones et al.(41) were adapted for analysis of sulphur in carbon saturated iron in the present experiments.

The advantage of this method is that the combustion can be completed within 5 minutes and formation of the troublesome ferric oxide dust which reduces the yield of titratable sulphur by reacting with some of the sulphur gases is almost completely eliminated. But this was only true for iron and plain carbon steel. When the carbon content in metal was more than 1 %, vigorous ferric oxide fume was observed in the outgoing combustion gas. This problem could be overcome simple by diluting the metal sample to less than 1 % carbon content with electrolytic pure iron powder.

With a 1 g sample and using N / 160 sodium tetraborate as titrant the method was suitable for metal having sulphur contents in the range of 0.01 - 0.15 %. By suitable adjustment of sample weight this range could be extended.

The material to be analysed was placed on a preignited fire clay combustion boat and burnt in a stream of air with 1 l/min. flow rate at a temperature of 1400 ^{o}C in a horizontal carbolite furnace. The sulphur gases were absorbed in 40 ml neutralized hydrogen peroxide solution and the sulphuric acid formed was titrated with N / 160 standard sodium tetraborate solution. Screened methyl red was used as the indicator. The absorbtion solution was made by adding 30 ml of hydrogen peroxide (20 vols) to deionized water, making up 1 liter and adding 0.5 ml of screened methyl red indicator. The sodium tetraborate titrate solution was standardized with British chemical

standard metal samples for each analysis. The accuracy of this method is estimated to be ± 2 % of the total sulphur.

2.4.3. ANALYSIS OF CARBON IN METAL

1 g of finely milled metal sample was placed in a pre-ignited fire clay combustion boat with tin foil as a flux and burnt in a stream of purified oxygen with 300 - 325 ml per minute flow rate at a temperature of 1000 - 1050°C in a horizontal carbolite furace.
Oxygen was purified by passing through a purification tower, the upper portion being charged with soda asbestos and the lower with calcium chloride (12 - 30 mesh).

Combustion gas produced was passed through a prolong tube charged with anhydrone for the final dehydration of the gas stream and then passed through precipitated manganese dioxide to remove sulphur from the gas.

CO_2 in the finally purified combustion gas was collected by passing through a Nesbitt absorption bulb, 80 ml capacity and 6.5 ins. overall height, charged with anhydrone followed by soda asbestos, these fillings being held in position by small ignited asbestos plugs. It was preferable to allow oxygen flow for 15 to 20 minutes after combustion period of approximately 1 min., during which time the Nesbitt absorption bulb returned to room temparature.
The Nesbitt bulb then was detached and weighed. The increase in weight was converted to present the weight of carbon.

This method was checked with B.C.S. metal samples and good accuracy was obtained within ± 2 % of total carbon.

2.4.4. ANALYSIS OF IRON IN SLAG

Slag powder samples were thoroughly treated by a magnet to

separate any iron particles iron analysis.

0.2 g of sample was dissolved in 25 ml boiling 1 : 1 dil. hydrochloric acid with few drops of hydrofluoric acid added to dissolve insoluble silica. A few drops of 5 % stannous chloride solution in 5 % dil. hydrochloric acid was added to reduce any ferric iron to ferrous iron while the solution was boiling. The solution was then cooled quickly to room temperature under tap water and 20 c.c. of saturated mercuric chloride solution added to remove the excess stannous chloride as a silky white precipitate. This was followed by the addition of 10 c.c. of 15 % orthophosphoric - 15 % sulphuric acid mixture and 8 drops of 0.2 % sodium diphenylamin-sulphonate solution as an internal indicator.

The solution was then titrated against N/100 standard potassium dichromate solution to an intense purple end point (42).

The total iron determined was converted to a ferrous oxide content in the slag eventhough this way did not fully reflect the way the iron was present.

2.4.5. ANALYSES OF SILICON AND MANGANESE IN METAL

1 g of metal sample was dissolved in 50 ml of boiling 8 % sulphuric acid and a few drops of nitric acid were carefully added until the solution changed color. The solution was then boiled for 2 - 3 minutes to expel excess nitric acid fumes, cooled to room temperature, then transferred to a 100 c.c. graduated flask and made up to the volume with deionized water. The solution was left standing for a 2 - 3 hours for the graphite flakes in the solution to settle.

Standard solutions were prepared in the same way with British chemical standard metal samples containing a suitable range of

concentrations for silicon and manganese.

The silicon and manganese contents were determined using a Perkin Elmer model 103 atomic absorption spectrometer by comparison with calibration curves obtained using standard solutions. Manganese was determined with an air/acetylene flame and silicon using a nitrous oxide/acetylene flame. All conditions were as specified in the Perkin Elmer analysis manual.

2.4.6. ANALYSIS OF MANGANESE OXIDE IN SLAG

0.1 g of slag was fused in a platinum basin with about 0.3 g of prefused sodium tetraborate and about 0.7 g of sodium carbonate to make the silicate slag soluble in acid solution.

After fusion the melt was cooled and taken into solution by the addition of 20 ml of 1 : 1 nitric acid followed by a few drops of 20 vols. hydrogen peroxide. The solution was transferred into a 500 ml graduated flask and made up to the volume with deionized water.

Solutions of British chemical standard slags, with a suitable range of MnO concentration, were prepared in the same way as sample slags. The manganese oxide concentration was determined by atomic absorption by comparison with the standard samples. Conditions were the same as for the determination of manganese in metal.

2.4.7. ANALYSES OF SILICA, LIME, AND MAGNESIA IN MASTER SLAGS

Because it was very difficult to get standard slags with the same slag component as the present master slags, artificial standard slag solutions were prepared.

Silica stock standard solutions were prepared by fusing 0.1 g of acid washed silica sand with 0.3 g of sodium tetraborate and 0.7 g of sodium carbonate, dissolving in 20 ml 1 : 1 nitric acid with a few drops of hydrogen peroxide and making up to 200 ml.

Lime stock standard solutions were prepared by adding 0.1784 g of " analar " calcium carbonate, 0.3 g sodium tetraborate and 0.7 g of sodium carbonate into 50 ml of water and dissolving with addition of 10 ml of nitric acid and making up to 200 ml.

Magnesia stock standard solution was prepared by dissolving 0.1 g of " analar " magnesia with sodium tetraborate and sodium carbonate in the same way as the lime standard solution.

To eliminate interferences standards were prepared from these stock solutions to contain all three components in the concentration range of the experimental slag.

To make a standard slag solution with composition of 70 % SiO_2, 20 % CaO, 10 % MgO 70 ml of silica standard solution taken from the prepared stock standard solution was mixed with 20 ml of lime standard solution and 10 ml of magnesia standard solution making up to 100 ml. In the same way 50 % SiO_2, 43 %CaO, 7 % MgO and 30 % SiO_2, 66 % CaO, 4 % MgO slag solutions were prepared covering the whole range of master slag compositions.

For analysis of silica in the master slag 0.1 g of the slag was made up to 200 ml solution in the same way as the silica stock standard solution. Silica was determined by atomic absorption by comparison with the standard solutions. The conditions were the same as those used for silicon in metal.

For the analysis of lime and magnesia the same standard solutions and sample solutions used for silica analysis had to be

used at 10 times dilution as the working linear ranges of the instrument for lime and magnesia were far smaller than that for silica.

In the analysis of lime 1 % lanthanum oxide additions to the standards and samples were necessary to avoid the interference of silica. Both were determined by atomic absorption using a air/acetylene flame.

The accuracy of master slag analyses is estimated to be $\pm$ 0.5 wt. percent.

2.4.8. COMPARISON OF RESULTS FROM SLAG AND METAL ANALYSES.

The analysed final metal sulphur content in each run was compared with a metal sulphur content calculated by mass balance (taking into account the changing slag weight due to sampling) from the analysed sulphur content of the slag. In all cases very good agreement between the two was obtained within $\pm$ 5 % of total sulphur (see tables at appendix). This demonstrates the validity of the slag sampling technique for following the desulphurization of metal under these experimental conditions, and the accuracy of the analyses.

CHAPTER 3

RESULTS AND DISCUSSIONS

CHAPTER 3

RESULTS AND DISCUSSIONS

3.1. INTRODUCTION

Because of the apparent lack of agreement about reaction mechanisms by previous workers, it was decided to try to obtain enough data to correlate the previously observed rates and establish a reasonable mechanism for sulphur transfer. Previous workers have not come to clear conclusion about the rate controlling step suggestions being mass transport in the slag, mass transport in the metal or an interfacial chemical reaction.

The effect of slag basicity and metal sulphur content was studied initially. Previous workers had indicated that sulphur transfer rates increased with increasing basicity and the reaction was initially a first order reaction with respect to sulphur content in metal. This was confirmed in the present work.

During studies(43) into silica reduction using the same slags as the present investigation it was found that melt geometry had an effect on transfer rate. Previous workers have used a variety of crucible diameters, slag depths, and metal depths and it was thought important to study the effect of these parameters on the transfer rate of sulphur. The effect of geometry can be fed into various proposed mechanisms for the rate controlling step and can help to eliminate some of them.

It has also been claimed that the addition of deoxidants (Si, Mn, Al etc.) to the metal enhances desulphurization rates whilst the addition of oxides (FeO, MnO) to the slag decreases the rate of desulphurization. These effects led to a chemical reaction mechanism

for sulphur transfer reaction and a diffusion control mechanism. Both of these effects have been studied in the present investigation.

Finally the effect of ambient pressure has been studied. As the sulphur transfer reaction involves CO evolution as an important concurrent reaction, the gas phase reaction must be affected by ambient pressure change. A knowlege of the behaviour under different pressures can also help to eliminate some proposed rate controlling steps.

3.2. EFFECT OF METAL COMPOSITION

In view of the overall reaction for sulphur transfer; $[S] + (O^{2-}) = [O] + (S^{2-})$, the effect of sulphur concentration in metal on the rate of the sulphur transfer from metal to slag was investigated initially.

100g of carbon saturated iron alloys containing different amounts of sulphur and 30g of a slag (45 % SiO_2, 6 % MgO, 49 % CaO) were used in a graphite crucible of inner diameter 31.8 mm at a temperature of 1460 °C ± 5 °C. The progress of the reaction was followed by sampling the slag and analysing for sulphur and iron in the slag samples. The detailed experimental results are shown in table 1. Fig 3.1. shows sulphur transfer rate curves for different initial sulphur contents in metal plotted as the change in sulphur content of slag with time.

It is clear from the rate curves that a higher sulphur content, that is, higher driving force for the transfer, shows higher sulphur transfer rate as expected from the general reaction rate theory, that the reaction rate is proportional to the concentration of a reactant, i.e. Rate = Const. x Force. In order to show directly the rate of desulphurization and compare the apparent rate constants, it was considered better to plot the change in sulphur concentration in metal

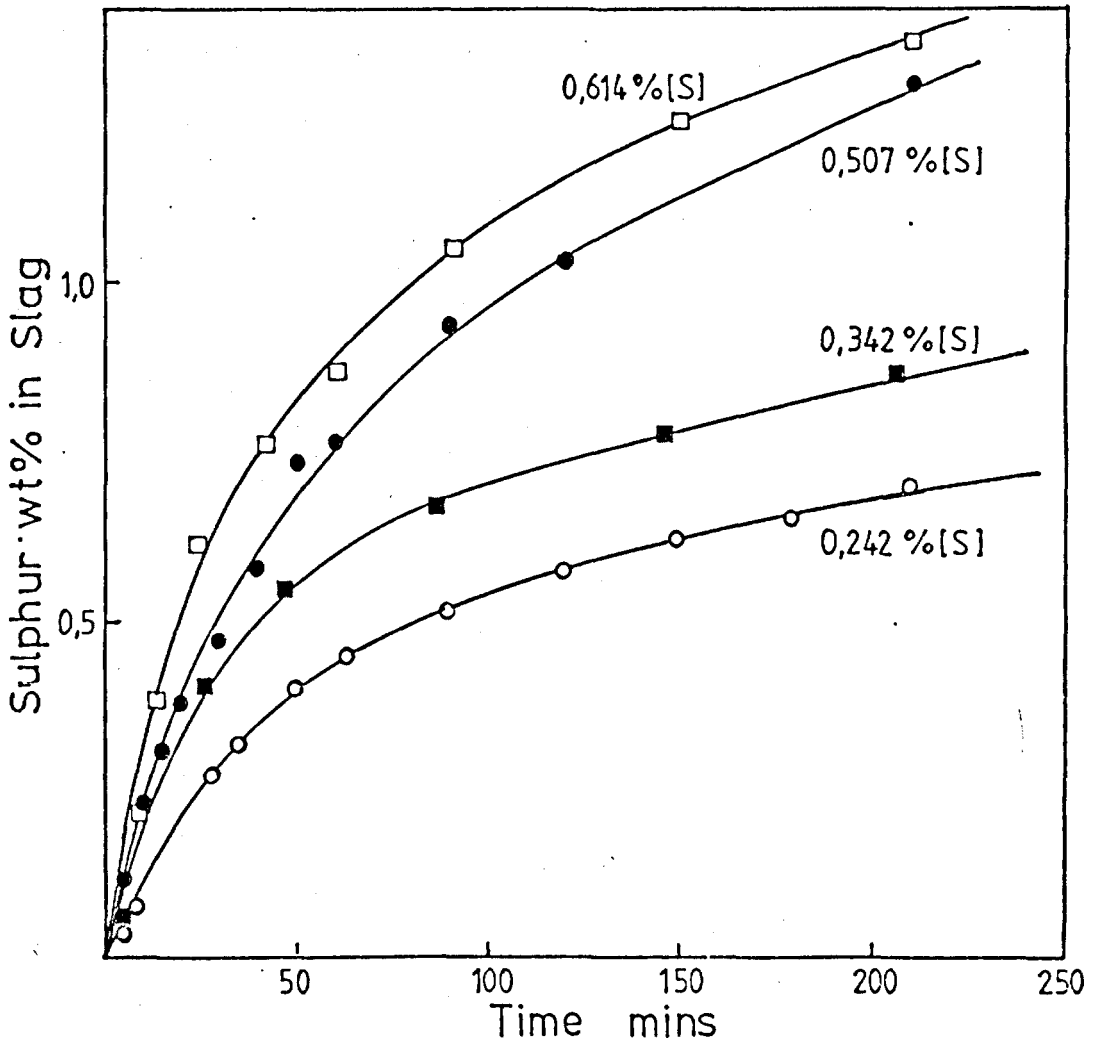

FIG. 3.1. COMPARISON OF SULPHUR TRANSFER CURVES FOR DIFFERENT INITIAL SULPHUR CONTENT IN METAL.

SLAG COMPOSITION : 45 % SiO_2, 6 % MgO, 49 % CaO

TEMPERATURE : 1462 - 1469 °C

EXPS. 1, 3, 46, AND 4 (TABLE 1)

against time. Because slag samples only were taken during a run, the sulphur content of the metal was calculated by a mass balance from the change in the sulphur content of the slag taking into account the change in the slag weight due to the samples removed;

$$[\%\ S]_{t_2} = [\%\ S]_{t_1} - \frac{Ws^{t_2}}{Wm}\ (\%\ S)_{t_2} - (\%\ S)_{t_1} \qquad (3.1)$$

where $[\%\ S]_{t_1}$, $[\%\ S]_{t_2}$; sulphur content in metal at time t_1 and t_2 respectively,

$(\%\ S)_{t_1}$, $(\%\ S)_{t_2}$; sulphur content in slag at time t_1 and t_2 respectively,

Wm ; metal weight (constant),

Ws^{t_2} ; slag weight remaining before sampling at time t_2.

This was based on the assumption that the weight of sulphur in the slag was the same as the weight of sulphur removed from the metal. This can be verified by comparison of the calculated value of the final sulphur content in metal with the analysed sulphur content of the final metal at the end of the run. In all cases good agreement between the two values was obtained (see table 3.1.). In Fig.3.2. desulphurization rate curves for the same experiments as in Fig.3.1 are plotted as the change in sulphur content of metal with time. All curves show almost the same curvature implying that the rate constant does not vary as sulphur content in metal changes and only the flux of sulphur is affected due to the change of driving force. From this point of view it was considered worthwhile to calculate the rate constant as this can be used for comparison of transfer reactions under different experimental conditions.

Basically we can assume that the rate of sulphur transfer from

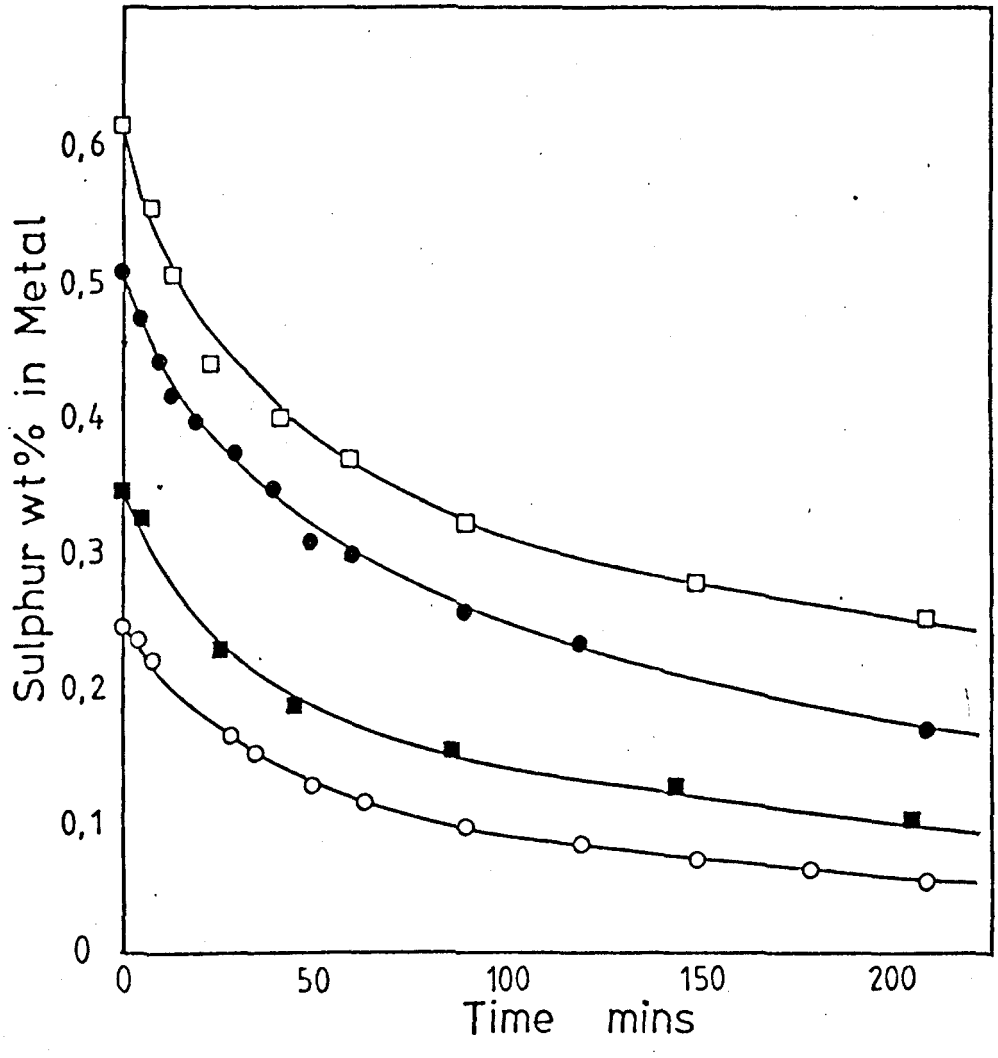

FIG. 3.2. THE SAME SULPHUR TRANSFER CURVES AS FIG. 3.1. SHOWN AS THE CHANGE IN SULPHUR CONCENTRATION IN THE METAL.

metal to slag is proportional to the concentration of sulphur in the metal and that the rate from slag to metal is proportional to the sulphur concentration in the slag. Thus the net transfer rate of sulphur from metal to slag can be expressed as follows;

$$-\frac{d[\%\,S]}{dt} \cdot \frac{Wm}{100A} = Km\,[\%\,S]^m - Ks\,(\%\,S)^n \qquad (3.2)$$

where $[\%\,S]$, $(\%\,S)$; concentration of sulphur in metal and slag respectively wt.% ,

Km, Ks ; rate coefficient of sulphur transfer from metal to slag and from slag to metal, g cm^{-2} min^{-1} ,

Wm ; weight of metal, g,

A ; the area of the slag metal interface,

m.n ; the orders of the forward and reverse transfer reactions.

Assuming the reactions are first order,

$$-\frac{Wm}{100A} \cdot \frac{d[\%\,S]}{dt} = Km\,[\%\,S] - Ks\,(\%\,S) \qquad (3.3)$$

At equilibrium the forward and reverse reactions become equal;

$$Km\,[\%\,S]_e = Ks\,(\%\,S)_e$$

$$Ks = \frac{[\%\,S]_e}{(\%\,S)_e} \cdot Km \qquad (3.4)$$

where $[\%\,S]_e$, $(\%\,S)_e$; sulphur concentration in metal and slag at equilibrium.

and according to mass balance

$$(\%\,S)_e = \frac{Wm}{Ws}\,(\,[\%\,S]_o - [\%\,S]_e\,) \qquad (3.5)$$

$$\text{and } (\%\,S) = \frac{Wm}{Ws}\left([\%\,S]_o - [\%\,S]\right) \qquad (3.6)$$

where Wm, Ws ; weight of metal and slag respectively,

Combining Eq. 3.3, 3.4, 3.5, and 3.6

$$-\frac{Wm}{100A}\cdot\frac{d[\%\,S]}{dt} = Km\,[\%\,S] - Km\,\frac{Ws}{Wm}\cdot\frac{[\%\,S]_e}{[\%\,S]_o - [\%\,S]_e}$$

$$\cdot\frac{Wm}{Ws}\left([\%\,S]_o - [\%\,S]\right)$$

$$= Km\,\frac{[\%\,S]_o}{[\%\,S]_o - [\%\,S]_e}\left([\%\,S] - [\%\,S]_e\right) \qquad (3.7)$$

Integrating Eq. 3.7,

$$\text{Ln}\,\frac{[\%\,S]_t - [\%\,S]_e}{[\%\,S]_o - [\%\,S]_e} = -\frac{[\%\,S]_o}{[\%\,S]_o - [\%\,S]_e}\cdot Km\cdot\frac{100A}{Wm}\cdot t \qquad (3.8)$$

Eq. 3.8 is an integration form of the rate equation.

If the assumptions made during derivation of the rate equation 3.8 are true, then the plots of Ln $\left([\%\,S]_t - [\%\,S]_e / [\%\,S]_o - [\%\,S]_e\right)$ vs time t must show a straight line and from the slope of the line a value of rate coefficient Km can be obtained

$$Km = \text{slope}\cdot\frac{Wm}{100A}\cdot\frac{[\%\,S]_o - [\%\,S]_e}{[\%\,S]_o} \qquad (3.9)$$

This is demonstrated in Fig. 3.3, plotted as Ln $\left([\%\,S]_t - [\%\,S]_e / [\%\,S]_o - [\%\,S]_e\right)$ vs time for the same experiments as shown in Fig. 3.1 and 3.2. All of the curves for different initial sulphur contents of metal are linear and of identical slope for an initial fast reaction period, indicating that the sulphur transfer reaction in the initial period is first order and the rate coefficient is independent of the

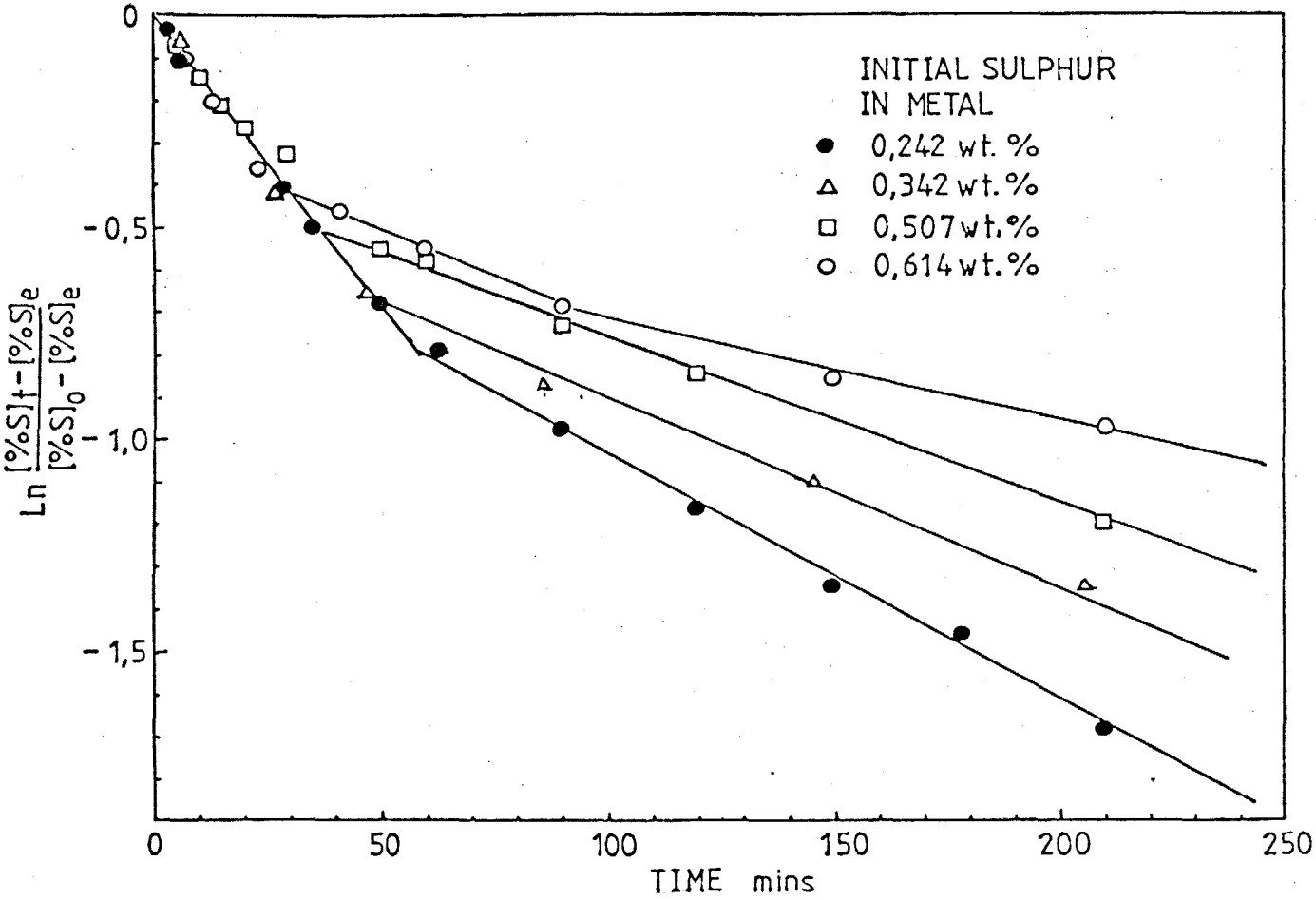

FIG. 3.3. Ln ($[\%\,S]_t - [\%\,S]_e$ / $[\%\,S]_o - [\%\,S]_e$) vs TIME PLOTS FOR DIFFERENT INITIAL SULPHUR CONTENTS. EXPS. 1, 3, 46, AND 4 (TABLE 1)

initial sulphur content of metal. A first order reaction was also observed by previous workers. (3)(7)(14)

Ward et al.(14) used the same rate equation as Eq. 3.3, but they simplified the equation to

$$-\frac{d[\%\,S]}{dt} = \frac{100A}{Wm} \cdot Km\,[\%\,S],$$

assuming that the sulphur content in slag at the beginning of experiments was negligible. Integrating the above equation gives

$$Ln\ \frac{[\%\,S]_t}{[\%\,S]_o} = -\frac{100A}{Wm} \cdot Km \cdot t \qquad (3.10)$$

as mentioned previously in the literature review. From the slope of the curve plotted as Ln ($[\%\,S]_t$ / $[\%\,S]_o$) vs time t Ward et al. calculated the value of Km.

If $[\%\,S]_e$ in equation 3.8 is assumed to be negligibly small as compared with $[\%\,S]_o$ in the beginning of transfer reaction, then the equation simplifies to the same as Ward et al's equation 3.10. Fig. 3.4 shows the plots of Ln $[\%\,S]_t$ vs time according to the equation 3.10. The values of Km obtained from the slopes of these curves were found to be exactly the same as the values calculated from the curves plotted according to the equation 3.8 for the fast initial period. However it must be pointed out that the curves plotted according to the simplified equation 3.10 become unreal at the later stage of reaction because the slag sulphur content would be no longer negligible and it is preferable to use equation 3.8 derived taking account of the reverse transfer reaction from slag to metal for examination of the later stage of reaction.

It is very interesting that after a fast reaction period all of the curves in Fig. 3.3 show a break point from a fast stage to a

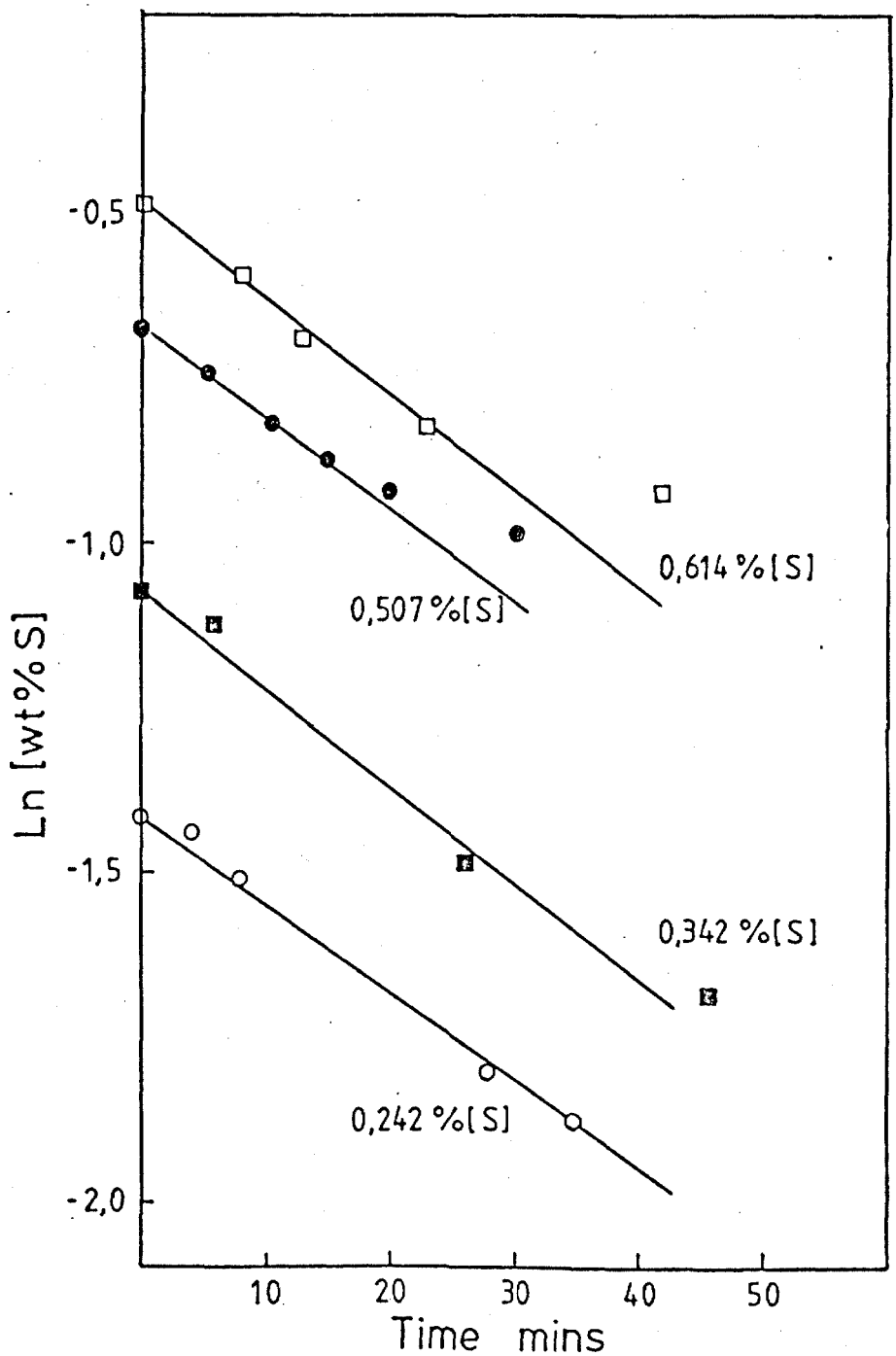

FIG. 3.4. Ln [% S] vs TIME PLOTS FOR THE SAME EXPERIMENTS AS FIG. 3.3.

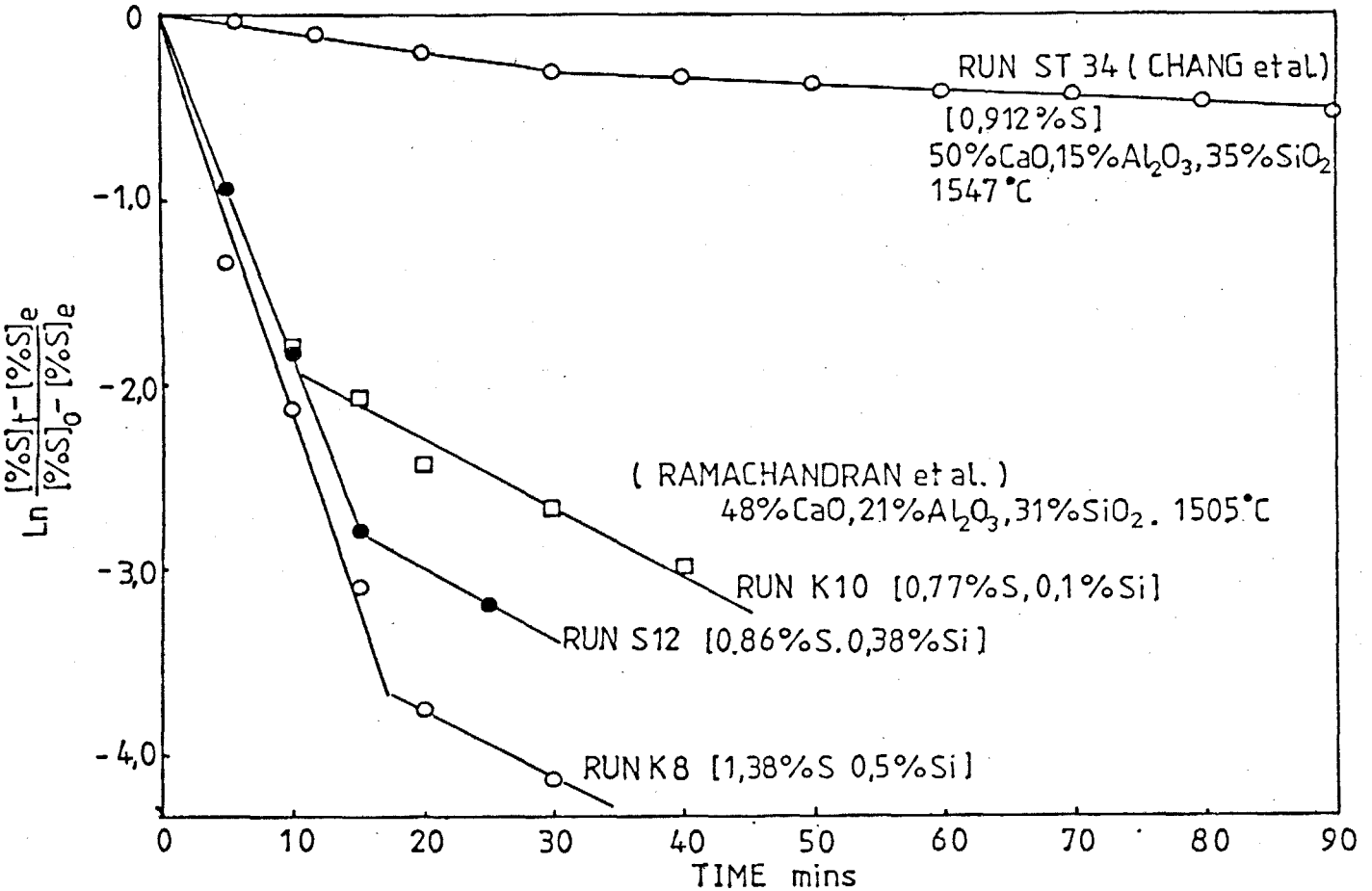

FIG. 3.5. SOME PLOTS OF Ln ($[\%S]_t - [\%S]_e$ / $[\%S]_o - [\%S]_e$) vs TIME

(CALCULATED FROM STUDIES OF CHANG et al. (3) AND RAMACHANDRAN et al. (7))

slow stage and the second stage of the curves also show a linear change as the first fast stage. The two stages seem to belong to different reaction regimes. The same trend of change in the reaction rate after the fast period was also found in the previous worker's data (3)(14) as shown in Fig. 3.5. The plots were made with calculated values from the previous worker's data obtained under various experimental conditions. At the present stage however it is not clear why such a transition from a fast stage to a slow one appeared. It will be discussed later with other experimental results.

For the calculation of equation 3.8, the equilibrium sulphur concentration in metal, $[\% S]_e$, was obtained using the following equations (44);

$$\log \frac{(\% S)_e}{[\% S]_e} = 5.55 - \frac{725}{T} + \log Cs + \log f_s - \log \frac{Pco}{a_c} \qquad (3.11)$$

$$\log Cs = -5.57 + 1.39\,(R) \qquad (3.12)$$

$$R = \frac{N\,CaO + (N\,MgO / 2)}{N\,SiO_2 + (N\,Al_2O_3 / 3)} \qquad (3.13)$$

where Cs ; sulphide capacity

f_s ; activity coefficient of sulphur in metal

T ; absolute temperature, ^oK

Pco, a_c ; partial pressure of CO and activity of carbon in metal respectively ; these were assumed to be unity for the present calculation

N ; mole fraction.

The equilibrium partition ratio $Ls = (\% S)_e / [\% S]_e$ obtained by equation 3.11 and mass balance relation, $(\% S)_e \cdot Ws = Wm\,([\% S]_o - [\% S]_e)$, gives

$$[\% S]_e = \frac{[\% S]_o}{\frac{Ws}{Wm} \cdot Ls + 1} \qquad (3.14)$$

where Ws, Wm ; weight of slag and metal respectively,

$[\% S]_o$; initial sulphur content in metal.

3.3. EFFECT OF SLAG COMPOSITION

From the overall reaction for sulphur transfer it is to be expected that an increase in the activity of free oxygen ions in slag will increase the desulphurization rate. It follows that an increase in the slag basicity increases the desulphurization rate as more basic slags have higher activity of free oxygen ions. This was observed by many previous investigators (3)(4)(7)(12)(14).

In the present investigation the effect of slag composition on the desulphurization rate was studied for lime-silica slags over a wide range of silica activities to obtain some basic data for further comparisons with other worker's results. Four lime silica slags, with different basicities, containg 6 % MgO to lower the melting point and in one experiment 20 % lime, 80 % calcium fluoride which is used commercially as a desulphurizer were used. The compositions of the slags used are as below;

Slag designation	Composition wt. %	Log Cs
SL 456	45 % SiO_2, 6 % MgO, 49 % CaO	- 3.81
SL 476	47 % SiO_2, 6 % MgO, 47 % CaO	- 3.95
SL 556	55 % SiO_2, 6 % MgO, 39 % CaO	- 4.40
SL 646	64 % SiO_2, 6 % MgO, 30 % CaO	- 4.77
SL CaF_2	20 % CaO, 80 % CaF_2	- 1.38

The experimental conditions are summarised in table A .

TABLE A

Exp. No.	Temp. ^{o}C	Crucible Dia. cm	Slag Composition	wt. g	Metal S wt. %	wt. g	Detailed Results
6	1460	3.18	SL 476	30	0.252	100	table 2
10	1463	3.18	SL 476	30	0.252	100	table 2
9	1465	3.18	SL 476	30	0.456	100	table 2
15	1463	3.18	SL 556	30	0.252	100	table 3
14	1465	3.18	SL 556	30	0.456	100	table 3
2	1465	3.18	SL 646	30	0.242	100	table 4
13	1469	3.18	SL 646	30	0.456	100	table 4
60	1464	1.91	SL CaF_2	10	0.493	35	table 18

Exp. No 10 was carried out under the exactly same condition as Exp. No 6 to check the present experimental technique. Both data on the change in sulphur content of metal with time were identical within experimental error, which indicates that the present technique gives consistent results.

All of the results except the one for the calcium fluoride slag are plotted together in Fig.3.6 as the change in sulphur content of metal with time. The sulphur content of metal was calculated from the slag analysis as detailed above. It is clear from Fig. 3.6 that the more basic slags shows a higher rate of desulphurization and the rate seems to be entirely dependent on slag composition irrespectively of sulphur content of the metal. This is clearly demonstrated in Fig. 3.7, plotted as Ln $[\% S]_t$ vs time for different initial sulphur contents of metal and different slag compositions, for a fast initial

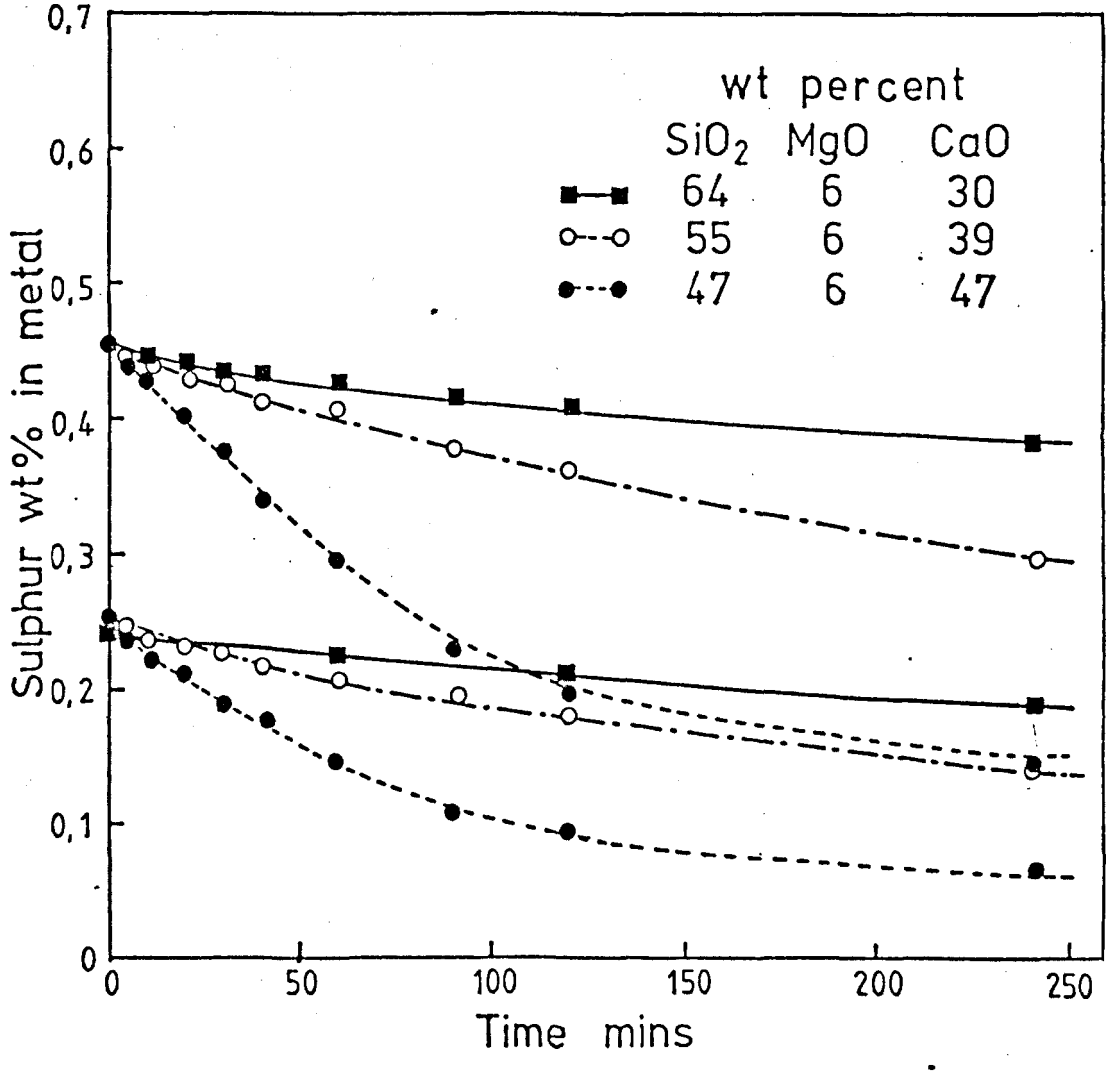

FIG. 3.6. EFFECT OF SLAG COMPOSITION ON RATES OF SULPHUR TRANSFER.

EXPS. 6, 9, 14, 15, 2, AND 13. (TABLES 2, 3, 4)

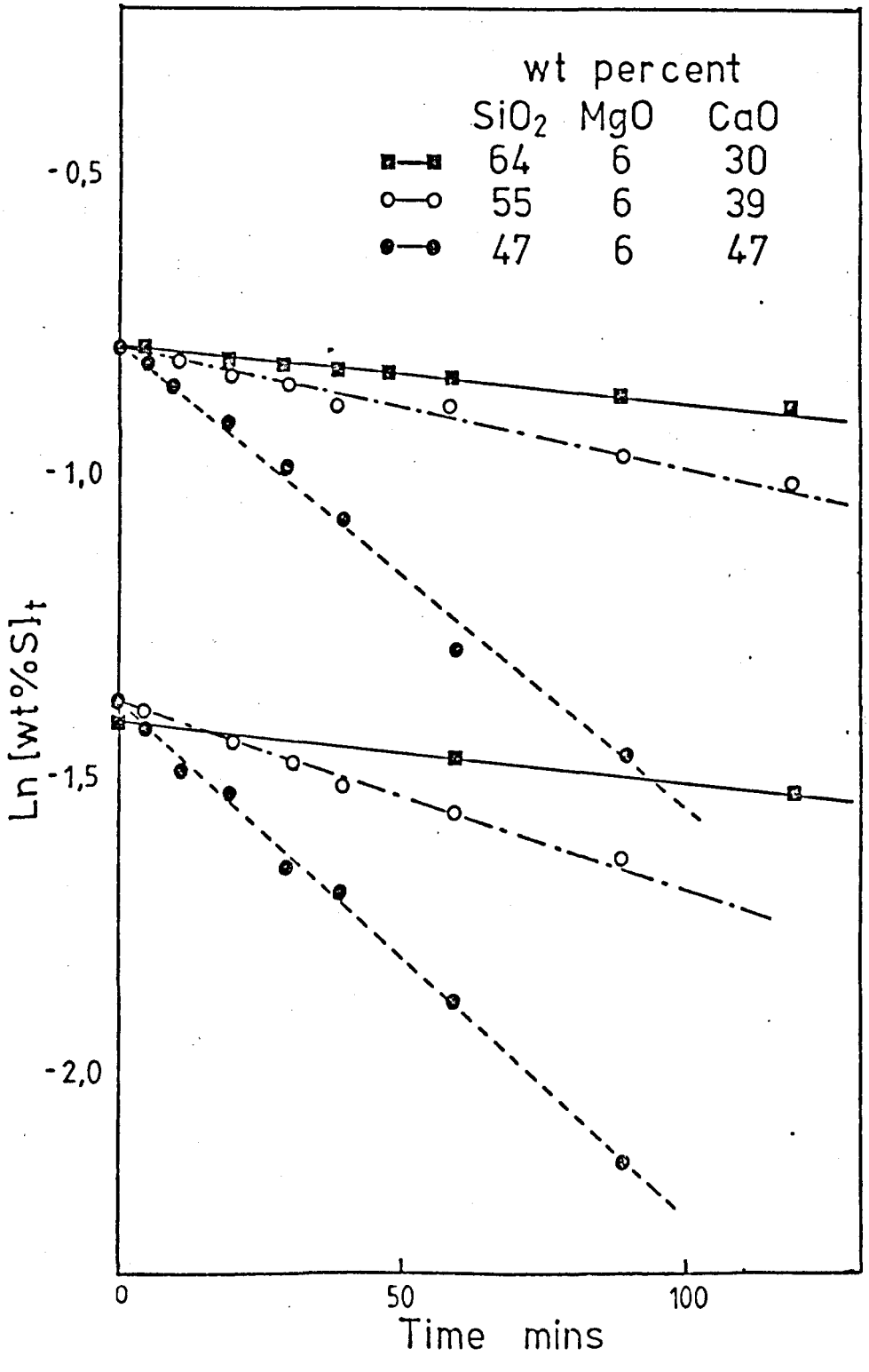

FIG. 3.7. Ln [wt % S] vs TIME PLOTS FOR DIFFERENT SLAG COMPOSITION AND INITIAL SULPHUR CONTENT IN METAL.

TEMPERATURE : 1460 - 1469 °C.

EXPS. 6, 9, 14, 15, 2, AND 13 (TABLES 2, 3, 4)

reaction period. The parallel lines for different initial metal sulphur contents with a given slag give identical rate coefficients, Km. The results for different slag basicities with a metal containing 0.456 % S are once again plotted as Ln $([\% S]_t - [\% S]_e / [\% S]_o - [\% S]_e)$ vs time in Fig. 3.8 to show the later reaction stage. The value of Km obtained from these curves for the initial stage was exactly the same as that obtained from the plots of Ln $\% S_t$ vs time as mentioned previously. The plots in Fig. 3.8 also show a break point but the difference between the slopes for the fast stage and the slow stage becomes very small as the slag basicity decreases. This change of the reaction rate is more clearly shown in Fig. 3.9 plotted for the calcium fluoride slag as Ln $([\% S]_t - [\% S]_e / [\% S]_o - [\% S]_e)$ vs time t. Some rate data for the most basic slag SL 456 and for the same SL 456 slag but with 1.89 % Si alloy under 1/4 atmosphere were included in Fig. 3.9 for comparison. The latter one is the highest desulphurization rate observed during the present experiment with the lime-silicate slags under consideration. The plots for the 20 % lime, 80 % calcium fluoride slag show an extremely fast reaction period showing 95 % desulphurization within 5 minutes of reaction time and then a very sharp change into a slow stage. Because of the speed of reaction, slag analyses were incapable of following the rate and the curve has been obtained from metal analyses. This implies strongly that the two stages of different reaction rates are controlled by different reaction mechanisms. The initial fast rate of the calcium fluoride slag is nearly five times faster than the highest rate obtained in the experiments with lime-silica slags which proves that this slag based on calcium fluoride is a good desulphurizer. All data compared in Fig. 3.9 were obtained from the experiments using a smaller graphite crucible

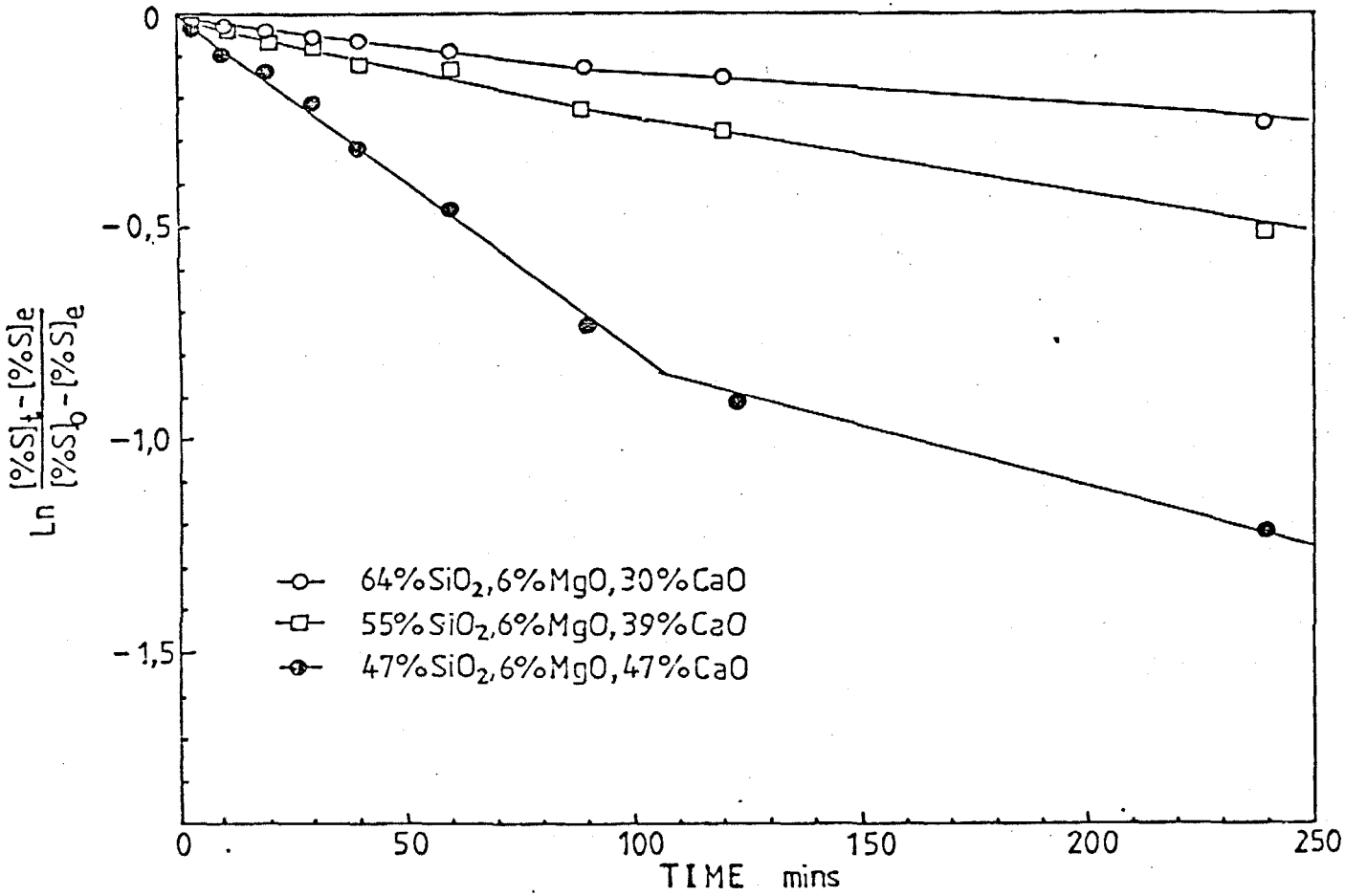

FIG. 3.8. Ln ($[\%\,S]_t - [\%\,S]_e$ / $[\%\,S]_o - [\%\,S]_e$) vs TIME PLOTS FOR DIFFERENT SLAG COMPOSITIONS EXPS. 9, 14, AND 13 (TABLES 2, 3, 4)

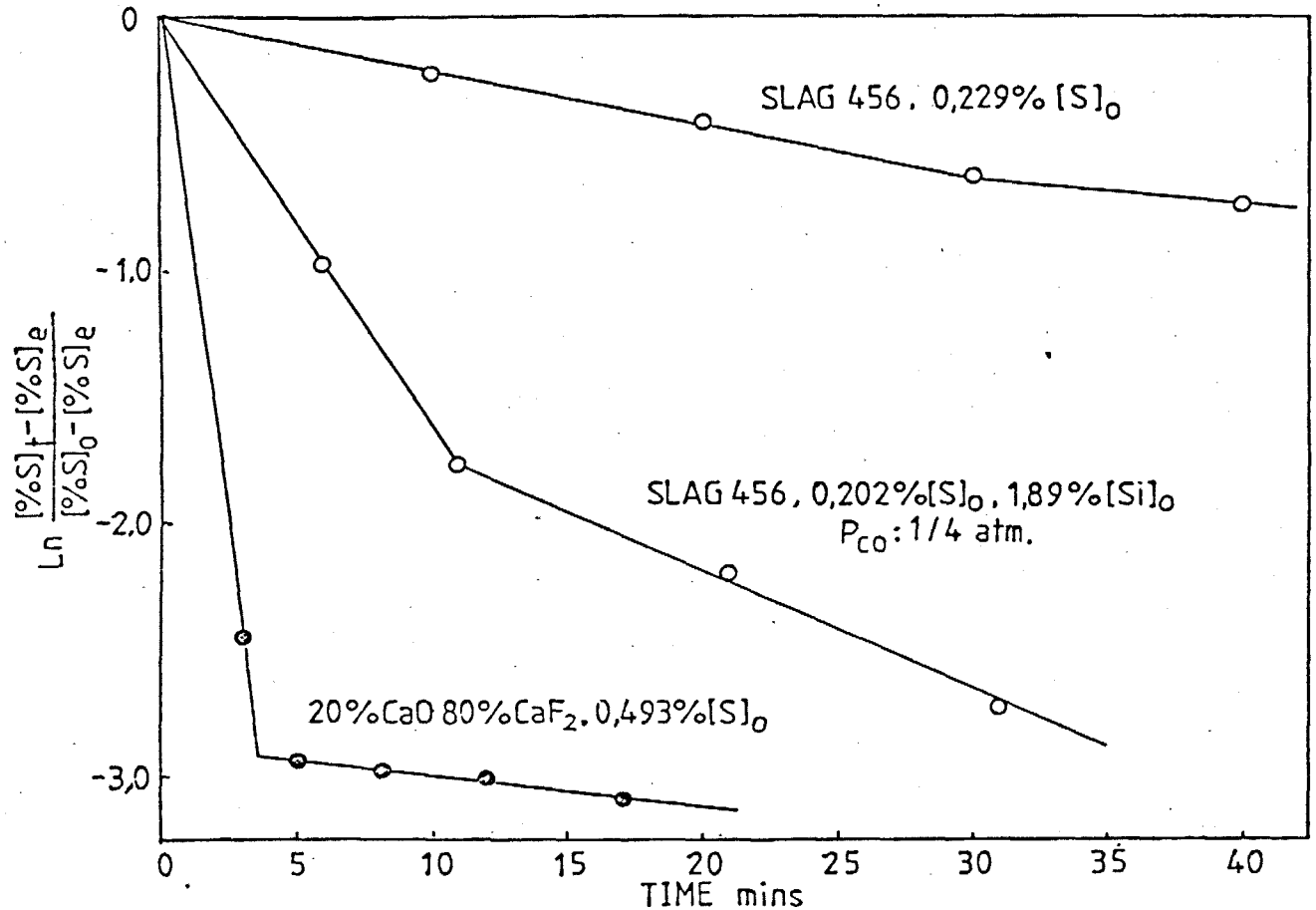

FIG. 3.9. Ln ($[\%\,S]_t - [\%\,S]_e$ / $[\%\,S]_o - [\%\,S]_e$) vs TIME PLOTS FOR A CALCIUM FLUORIDE SLAG AND A LIME SILICATE SLAG WITH DIFFERENT METAL COMPOSITION. EXPS. 60, 29, AND 32A. (TABLES 18, 12, 9)

(dia. 19 mm). The effect of crucible size on the reaction rate will be discussed later.

The effects of slag composition are summarised in Fig. 3.10 plotted as the change in rate coefficient of sulphur transfer from metal to slag, Km, with sulphide capacity of slag. The data from Chang et al.(3) were included with the present results for comparison. The original data of Chang et al. were plotted as Km against CaO / SiO_2 ratio of slag as Fig. 1.5 in the literature review chapter.

It is more convenient and accurate to use sulphide capacity in describing the ability of slag to pick up sulphur as sulphide ions instead of using one of the expressions for slag basicities, which have been suggested in various forms, in relation to the sulphur partition reaction between metal and slag. The concept of such a slag basicity is based on the fact that a more basic slag has a higher activity of free oxygen ions and the desulphurization reaction is strongly related to the activity of free oxygen ions in the slag as mentioned above. However very few measurements are available on the activity of free oxygen ions in the slag and there is some disagreement between the available data while there are extensive data on sulphide capacities of liquid slags (45)(46)(47). Sulphide capacities are obtained by equilibrating liquid slags with a gas mixture with known sulphur and oxygen potential pressures, i.e.

$$(O^{2-}) + 1/2\ S_2 = (S^{2-}) + 1/2\ O_2 \qquad (3.15)$$

$$K_{3.15} = \frac{\gamma_{S^{2-}}}{(a_{O^{2-}})} \cdot (\%\ S) \left(\frac{Po_2}{Ps_2}\right)^{\frac{1}{2}} \qquad (3.16)$$

and the sulphide capacity is defined by the expression;

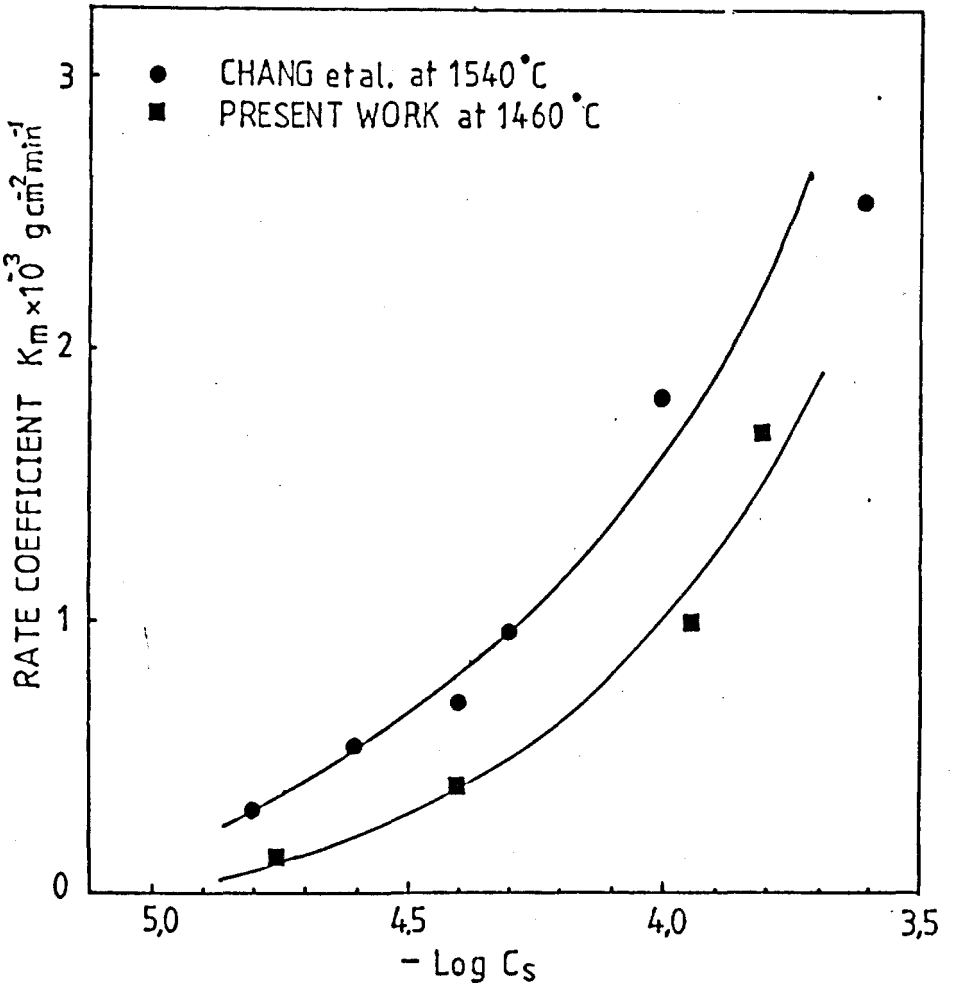

FIG. 3.10. TRASFER RATE COEFFICIENT VERSUS LOG Cs (SULPHIDE CAPACITY) FOR PRESENT WORK AND FOR DATA OBTAINED FROM CHANG et al. (3).

$$Cs = (\%\ S)\ \left(\frac{Po_2}{Ps_2}\right)^{\frac{1}{2}} \qquad (3.17)$$

and from Eq. 3.16 and 3.17

$$Cs = \frac{a_o{}^{2-}}{\gamma_s{}^{2-}}\ K_{3.15} \qquad (3.18)$$

For a small concentration of sulphide in a silicate slag of fixed oxide composition containing substantial amount of O^{2-} ions, $\gamma_s{}^{2-}$ and $a_o{}^{2-}$ in Eq. 3.18 should be independent of the sulphur content. Thus Cs can be used to express the sulphur affinity of a slag. From Eq. 3.18 it can be expected that the Cs value will increase as the activity of oxygen ions increases provided the activity coefficient of sulphur in slag, $\gamma_s{}^{2-}$, does not increase similarly. In fact $\gamma_s{}^{2-}$ does not vary so (48). In the present work the sulphide capacity of a slag was computed by the empirical equation 3.12 and 3.13 obtained from extensive sulphide capacity measurements; except for the calcium fluoride slag, for which the sulphide capacity value was taken directly from experimental data (48). As shown in Fig. 3.10, the rate coefficents, Km, for the present experiments change with slag sulphide capacity in a similar way to Chang et al's results, which were obtained at a temperature 80 °C higher than in the present study.

It may be reasonable to start to examine a mechanism for sulphur transfer from the observed results. The transfer reaction steps can be separated into the following steps:

(1) Transport of sulphur from metal to the metal-slag interface

(2) Reaction at the interface

(3) Transport of sulphur from the interface to slag.

The first and third steps of sulphur transport are diffusion control.

However, according to the observed facts that the rate of sulphur transfer from metal to slag changes as the slag composition varies, it can be concluded that a possible explanation on the transport of sulphur from metal to metal-slag interface as a rate controlling step is ruled out. This elimination of diffusion control of sulphur in metal is supported by the experiment with the calcium fluoride slag and a 0.493 % S alloy where the sulphur was reduced to less than 0.03 % within 5 minutes. If the sulphur transfer reaction is limited by diffusion of sulphur in the metal phase then such an extremely fast desulphurization could not be achieved simply by changing a slag into the calcium fluoride slag. Thus it can be considered that the desulphurization reaction is controlled either by a chemical reaction at the interface or by diffusion of sulphur from the interface into the bulk of the slag. Using the observed rate data, diffusion of sulphur in the slag phase as a controlling step will be examined firstly.

When a reaction at the slag metal interface is limited by a slow diffusion step in a phase the rate can be defined mathematically by applying the boundary layer theory adopted to metallurgical problems by C. Wagner(29);

$$\frac{dn_i}{dt} = \frac{DA}{\delta}\left[C_i \text{ (Interface)} - C_i \text{ (Bulk)} \right] \qquad (3.19)$$

where n_i ; mole of component i

D ; diffusion coefficient of component i, $cm^2\ sec^{-1}$

A ; interface area, cm^2

δ ; effective boundary layer thickness, cm

C_i ; concentration of component i, mole cm^{-3}

Adapting Eq. 3.19 to the sulphur transfer reaction from metal to slag where the diffusion of sulphur in the slag is considered as the rate limiting step;

$$\frac{dn_s}{dt} = \frac{DA}{\delta}\left[C_s\ (\text{Interface}) - C_s\ (\text{Bulk}) \right] \tag{3.20}$$

Changing concentration into weight percentages

$$\frac{d(\%\ S)}{dt} = \frac{D}{\delta\ h_s}\left[(\%\ S)_i - (\%\ S)_b \right] \tag{3.21}$$

where h_s ; height of slag, cm.

If at the interface the concentration of sulphur in the slag is in equilibrium with that in the metal, then

$$(\%\ S)_i = Ls\ [\%\ S] \tag{3.22}$$

where $$Ls = \frac{(\%\ S)_e}{[\%\ S]_e} \tag{3.23}$$

By material balance

$$(\%\ S)_b = \frac{Wm}{Ws}\left[[\%\ S]_o - [\%\ S] \right] \tag{3.24}$$

$$(\%\ S)_e = \frac{Wm}{Ws}\left[[\%\ S]_o - [\%\ S]_e \right] \tag{3.25}$$

$$\frac{d(\%\ S)}{dt} = -\frac{Wm}{Ws} \cdot \frac{d[\%\ S]}{dt} \tag{3.26}$$

where Wm, Ws ; weight of metal and slag respectively

$[\% S]_o$, $[\% S]_e$; sulphur concentration in metal at initial and equilibrium states respectively.

Substituting from Eq. 3.22 - 3.26 into Eq. 3.21 and rearranging gives

$$-\frac{d[\% S]}{dt} = \frac{D}{\delta h_s} \cdot \frac{[\% S]_o}{[\% S]_e} \cdot [\,[\% S] - [\% S]_e\,]$$

By integrating,

$$\text{Ln}\ \frac{[\% S]_t - [\% S]_e}{[\% S]_o - [\% S]_e} = -\frac{D}{\delta h_s} \cdot \frac{[\% S]_o}{[\% S]_e} \cdot t \qquad (3.27)$$

If the reaction is diffusion controlled then the plots of Ln ($[\% S]_t - [\% S]_e$ / $[\% S]_o - [\% S]_e$) vs time t should show a straight line. This is exactly the same plot as the previous plots according to Eq. 3.8. Thus directly plotting the experimental data using any of the equations 3.8 and 3.27 does not directly provide a means for assessing the rate limiting mechanism. It is necessary to compare the rate constants obtained under different experimental conditions to examine consistency of the postulated rate controlling mechanisms. From the equation 3.27 the slope of a line plotted as Ln ($[\% S]_t - [\% S]_e$ / $[\% S]_o - [\% S]_e$) vs time t can be expressed as

$$\text{Slope} = -\frac{D}{\delta h_s} \cdot \frac{[\% S]_o}{[\% S]_e} \qquad (3.28)$$

Substituting Eq. 3.14, $[\% S]_e = \dfrac{[\% S]_o}{Ws/Wm \cdot Ls + 1}$, derived previously using the same equations as Eq. 3.23 and 3.25, into Eq. 3.28 gives

$$\text{Slope} = -\frac{D}{\delta h_s}\left(\frac{Ws}{Wm} \cdot Ls + 1\right) = -\frac{D}{\delta h_s}\left(\frac{\rho_s \cdot h_s}{\rho_m \cdot h_m} \cdot Ls + 1\right)$$

and thus

$$-\text{Slope} = \frac{D}{\delta} \cdot \frac{\rho_s}{\rho_m} \cdot Ls \cdot \frac{1}{h_m} + \frac{D}{\delta} \cdot \frac{1}{h_s} \qquad (3.29)$$

where ρ_s, ρ_m ; densities of the slag and metal respectively

h_m ; height of metal phase.

In Eq. 3.29 the densities of a slag and metal can be assumed constant over a small change of sulphur concentration and the mass transport constant, D/δ, can not be affected by a change in the slag or metal depth. The equilibrium partition ratio of sulphur between the slag and the metal given by equation 3.11, is constant for a given temperature and ambient pressure. Thus, from equation 3.29, it must follow that, if the sulphur transfer reaction is controlled by diffusion of sulphur in the slag the slope will be changed inversely to the change in the height of the slag phase or the metal phase, all other experimental conditions remaining constant.

Sulphur transfer experiments were carried out varying the depth of the slag or the depth of the metal to check for the consistency of the postulated diffusion control mechanism, which will be discussed in the next section.

However, the values of the effective boundary layer thickness, evaluated from the slope of the curves for the present results with lime silicate slags are in the range of 0.001 — 0.0014 cm which are not unreasonable values for a diffusion control mechanism as estimated thicknesses ranging from 0.001 to 0.2 cm have been obtained by substituting various measured kinetic data in diffusion rate equations similar to Eq. 3.19 (49). Therefore at the present stage without further results under different experimental conditions as mentioned.

above it is very difficult to say whether the sulphur transfer is controlled by diffusion of sulphur in the slag or not.

The elimination of the diffusion of sulphur in the metal phase as a possible rate controlling step can be confirmed simply by using a diffusion equation derived by the same procedure as for slag diffusion; if the diffusion of sulphur in the metal is the rate controlling step, then the basic equation will be:

$$-\frac{d[\%\,S]}{dt} = \frac{D}{\delta\, h_m}\,[\%\,S]_b - [\%\,S]_i \qquad (3.30)$$

Employing the same steps for the diffusion of sulphur in the slag and using the same basic relationships yields the final rate equation:

$$\mathrm{Ln}\,\frac{[\%\,S]_t - [\%\,S]_e}{[\%\,S]_o - [\%\,S]_e} = -\frac{D}{\delta\, h_m}\cdot\frac{[\%\,S]_o}{[\%\,S]_o - [\%\,S]_e}\cdot t \qquad (3.31)$$

The plot of the left side of this equation against time shows exactly the same straight line as for the previous cases. The slope of a plot is expressed:

$$\text{Slope} = -\frac{D}{\delta\, h_m}\cdot\frac{[\%\,S]_o}{[\%\,S]_o - [\%\,S]_e} \qquad (3.32)$$

Substituting $[\%\,S]_e = \dfrac{[\%\,S]_o}{Ws/Wm \cdot Ls + 1}$ into Eq. 3.32 gives

$$\text{Slope} = -\frac{D}{\delta}\cdot\frac{1}{h_m}\cdot\left(1 + \frac{Wm}{Ws}\cdot\frac{1}{Ls}\right) \qquad (3.33)$$

In Eq. 3.33 the diffusion coefficient of sulphur in the metal, D, and the effective boundary layer thickness in the metal phase, δ, must remain constant irrespective of changes in metal depth, slag weight or slag composition. If the postulated mechanism is true,

according to Eq. 3.33 the slope should be decreased as the equilibrium partition ratio, Ls, increases. Thus by changing to a more basic slag, all other experimental conditions remaining constant, this predicts that the slope should decrease; which is completely opposite to the observed results in the present studies and all other worker's investigations (3)(4)(7)(12)(14). therefore there is no doubt in eliminating the diffusion of sulphur in the metal as a rate controlling step.

This conclusion is contrary to the argument of O.V.Travin et al. who observed a thick concentration gradient of sulphur at the metal slag interface in the metal and suggested this as a direct evidence for the diffusion of sulphur in the metal as a rate controlling step.

During the present experiments the sulphur concentration gradients in the metal at different reaction times have been examined for some of the experiments, stopped at different reaction times. The sulphur concentration was analysed in each segment (thickness : 1.3 mm) machined from the metal and plotted against the segment level as shown in Fig. 3.11. These results do not show a concentration gradient of sulphur in the narrow range near to the slag metal interface, but a general concentration gradient of sulphur in the bulk of the metal. Except in the very early stages of the reaction there is not a significant concentration gradient, which indicates that the bulk of the metal is well stirred, possibly by convection caused by CO gas bubbles accompanied by a chemical reaction.

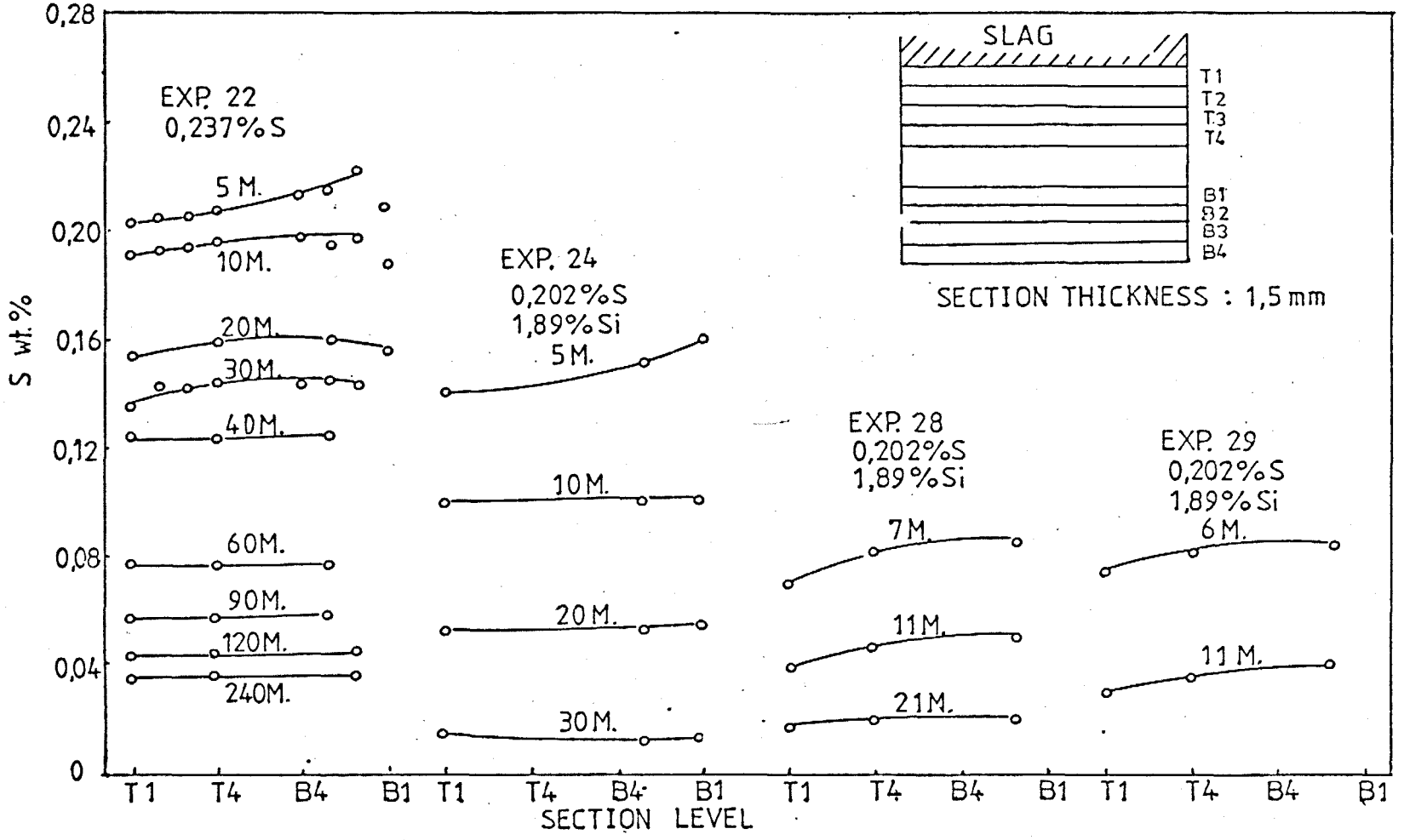

FIG. 3.11. SULPHUR CONCENTRATION GRADIENTS IN METAL

3.4. EFFECT OF MELT GEOMETRY

3.4.1. EFFECT OF SLAG AND METAL DEPTHS.

As the reaction rate equation, Eq. 3.8, and the diffusion rate equation, Eq. 3.27, have geometry factors in them, the reaction rate coefficient, Km, and the mass transport constant, D/δ, both should not be affected by a change in the melt geometry. Some experimental results of the transfer rates obtained by varying only the melt geometry (the slag depth, the metal depth or the diameter of a crucible holding the slag-metal melts) will enable us to check for the consistency of the postulated rate controlling mechanism.

At first the effect of slag and metal depth on the sulphur transfer rate was studied. The different experimental conditions employed for this study and the results are summarised in table B. The slag depth was doubled with the metal depth remaining constant and then the metal depth was reduced to half keeping the slag depth constant.

TABLE B

Exp. No	Slag Composition	Initial % S	Slag Weight (depth)	Metal Weight (depth)	Slope	Results
55	SL 476	0.491	30 g (1.8 cm)	100 g (1.8 cm)	0.009	table 5
56	SL 476	0.491	60 g (3.6 cm)	100 g (1.8 cm)	0.019	table 5
58	SL 476	0.491	60 g (3.6 cm)	100 g (1.8 cm)	.0.019	table 5
57	SL 476	0.491	30 g (1.8 cm)	50 g (0.9 cm)	0.017	table 5

Experiment No. 58 was carried out under the exactly same conditions as experiment No. 56 to confirm the observed result. The duplicate experiments are in close agreement on the change in sulphur content of metal with time, indicating that the present experimental

technique gives consistent results and the observed results are not suspicious.

The desulphurization rates for experiments No. 55 —58, with the slag SL 476, were plotted in Fig. 3.12 as Ln ($[\% S]_t - [\% S]_e$ / $[\% S]_o - [\% S]_e$) vs time. As mentioned above these plots apply both to the diffusion rate equation, Eq. 3.27, and to the reaction rate equation, Eq. 3.8. Thus from the change in the slope of these plots according to the variation of the melts depth the diffusion control mechanism will be examined first.

If the sulphur transfer is controlled by diffusion of sulphur in the slag, then the slope is expressed as Eq. 3.29 discussed above:

$$\text{Slope} = \frac{D}{\delta} \cdot \frac{\rho_s}{\rho_m} \cdot Ls \cdot \frac{1}{h_m} + \frac{D}{\delta} \cdot \frac{1}{h_s}$$

According to this equation the slope should be decreased by an increase of the slag depth, keeping all other experimental conditions constant, whilst the slope should be increased by a decrease of the metal depth.

However the observed results from Exps. 55 and 56 show that the slope was almost doubled by doubling the slag depth, which was confirmed in the duplicate experiment, Exp. No. 58. These results are completely opposite to the prediction from slag diffusion control. On the other hand, when the metal depth was reduced to half as in the experiment No. 57, the slope was increased as compared with the slope for the experiment No. 55, which seems to follow the above prediction.

However when Exp. No. 56 with 60 g of slag and 100 g of metal is compared with Exp. No. 57 with 30 g of slag and 50 g of metal, the slope for Exp. 57 is smaller than that for Exp. 56 even though both the slag and metal depths were halved in Exp. 57; which is completely

contrary to the condition of the above Eq. 3.29. Thus it can be concluded that sulphur transfer is not controlled by the rate of diffusion of sulphur in the slag.

A similar experiment to the present study using a double slag depth was carried out by J.C.Fulton and J.Chipman(16). Their results shown in Fig.1.2 (chapter 1) indicate that the slope of the plot for the experiment with double the amount of the slag is bigger than that with normal amount of the slag, even though the difference between the two slopes is not as big as in the present study.

This conclusion derived is contrary to the suggestion of a diffusion control mechanism for sulphur in slag made by M.Hatano(8) where direct evidence of a thick concentration layer of sulphur in the slag was shown.

The slower second stage during the desulphurization reaction which has been observed in most of the transfer experiments is unlikely to be controlled by diffusion of sulphur in the metal and the slag. This is because most of the plots according to the rate equations for the second stage show nearly parallel lines as shown in Fig. 3.12 instead of significant changes in the slope due to varying experimental conditions, which can not be true for the diffusion control mechanism as discussed above.

The only possible explanation left for the rate controlling step is a reaction at the slag metal interface. This reaction control mechanism must be examined with respect to the data obtained by varying the melt geometry to prove its consistency.

From the reaction rate equation, Eq. 3.8, the slope of the plot of this equation is expressed:

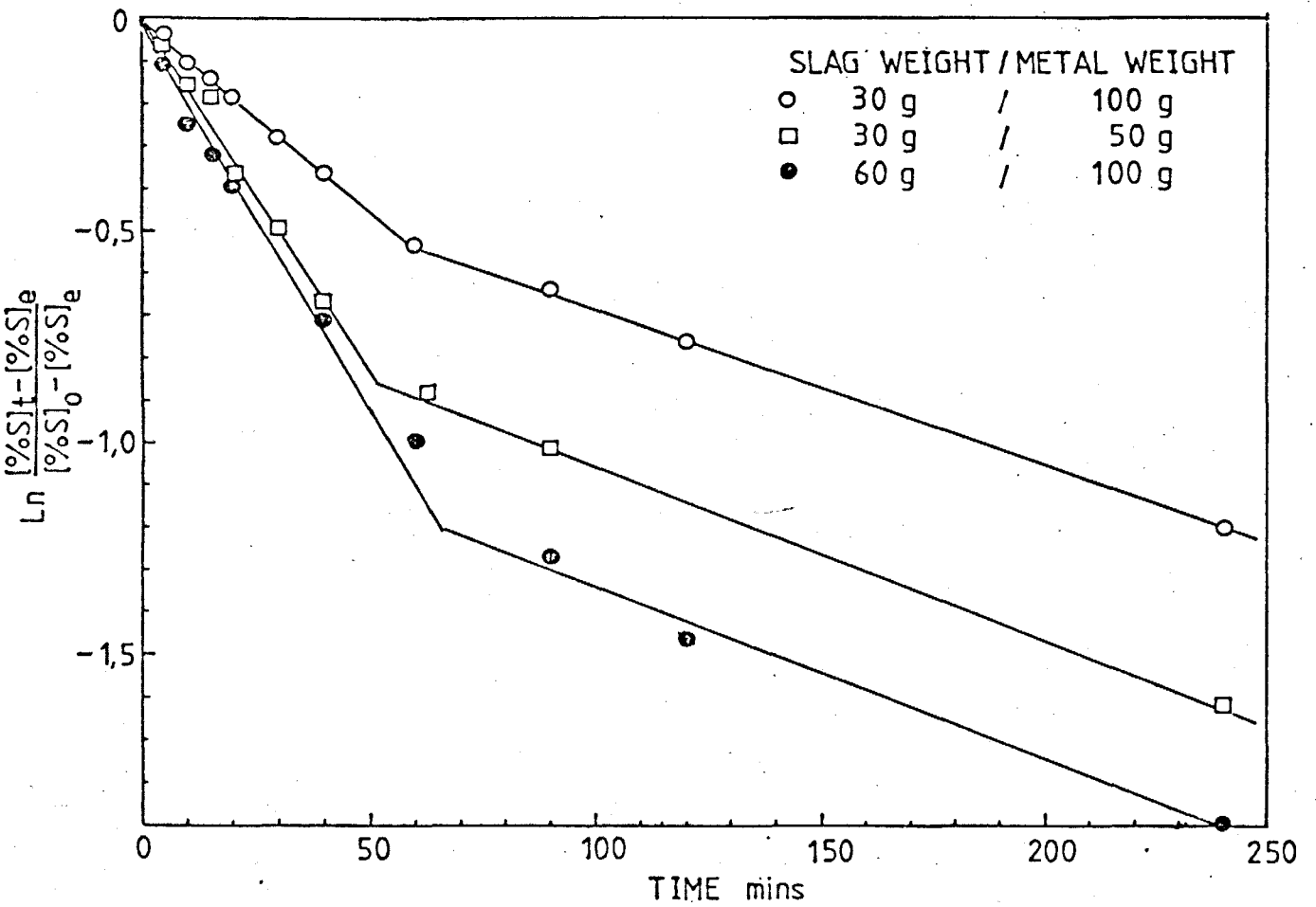

FIG. 3.12 Ln ($[\%\,S]_t - [\%\,S]_e$ / $[\%\,S]_o - [\%\,S]_e$) vs TIME PLOTS FOR DIFFERENT DEPTH OF SLAG AND METAL.

EXPS. 55 - 58 (TABLE 5)

$$\text{Slope} = -\frac{100A}{Wm}\ Km\ .\ \frac{[\%\ S]_o}{[\%\ S]_o - [\%\ S]_e} \qquad (3.34)$$

Substituting $[\%\ S]_e = \dfrac{[\%\ S]_o}{Ws/Wm\ .\ Ls + 1}$ into Eq. 3.34 and

rearranging gives

$$\text{Slope} = 100A\ .\ Km\ \frac{1}{Wm} + \frac{1}{Ws\ Ls} \qquad (3.35)$$

As the slag, SL 476, under consideration has Ls = 57, $\frac{1}{Ws\ Ls}$ in Eq. 3.35 is negligibly small. Thus Eq. 3.35 becomes

$$\text{Slope} = \frac{100A}{Wm}\ .\ Km \qquad (3.36)$$

Therefore if the sulphur transfer reaction is controlled by a reaction at the slag-metal interface, then the slope should be inversely proportional to the metal weight as the rate coefficient can not be affected by a melt depth. However the data in table B shows that the slope was increased about twice by reducing the metal weight to half, keeping the slag depth constant, but the slope was also increased nearly twice by doubling the slag depth with a constant depth of the metal. The latter case does not seem to follow the relationship of Eq. 3.36. However the reaction rate equation was derived on the basis of the fact that the rate is proportional to the area of the slag-metal interface. If a local cell reaction between the slag, the graphite crucible and the metal, suggested by C. Wagner(29), contribute to the desulphurization reaction along with the main slag-metal interface reaction, then the area in the rate equation, Eq. 3.8, must include some contribution from the area of the slag graphite crucible interface.

This assumption about the area of reaction interface can not be applied to any diffusion control mechanism, but only to an electrochemical reaction mechanism, because diffusion processes proceed across only the slag-metal interface. If the above assumption is available for the present study, then the puzzling fact that the slope was increased by increasing slag depth with a constant metal weight can be explained on this assumption; the contribution of the slag-graphite crucible interface area to the area for the observed desulphurization reaction becomes bigger due to the increase of the slag depth and the slope can be increased as a result.

The ratio of the slag-graphite crucible interface area to the slag-metal interface area becomes bigger as the diameter of crucible decreases keeping the slag depth constant, which leads to the necessity of the study on the effect of crucible diameter on the desulphurization rate.

3.4.2. EFFECT OF CRUCIBLE DIAMETER

The reaction rate equation (Eq. 3.8) was derived on the basis of the fact that the reaction rate is proportional to the area of the reaction interface. If the area is considered as only the slag-metal interface area, then the slope of the plot of the rate equation can be expressed as

$$\text{Slope} = \frac{100}{\rho_m \cdot h_m} \cdot Km \qquad (3.37)$$

Thus if the metal depth is kept constant the slope would be constant irrespectively of the crucible diameter assuming the sulphur transfer is controlled by a reaction over the slag-metal interface. Hence a study

on the effect of the crucible diameter was carried out using three different diameter crucibles, keeping the slag and the metal depths constant.

The experimental conditions employed and the results are summarised in table C.

TABLE C

Exp.No	Crucible dia. cm.	Slag wt. g (height cm)	Metal wt.g (height cm)	Initial S wt. %	Slope	Results
61	0.95	2.5(1.8)	8.75(1.8)	0.229	0.0250	table 6
32A	1.91	10 (1.8)	35 (1.8)	0.229	0.0195	table 6, 9
22	1.91	10 (1.8)	35 (1.8)	0.237	0.0195	table 9
1	3.18	30 (1.8)	100 (1.8)	0.242	0.0135	table 1, 6
4	3.18	30 (1.8)	100 (1.8)	0.614	0.0143	table 1
34	1.91	10 (1.8)	35 (1.8)	0.242 (0.44 % Si)	0.0627	table 11
25	3.18	30 (1.8)	100 (1.8)	0.242 (0.44 % Si)	0.0372	table 8

Slag SL 456 was used for all of these experiments. Exp. No. 34 and 35 were carried out with a metal containing 0.44 % Si, but the results are included here as the only difference between the two experiments is the crucible size. The effect of silicon in metal on the desulphurization rate will be discussed later.

The rate data for three typical experiments with different size of crucibles are plotted in Fig. 3.13 as Ln $([\% S]_t - [\% S]_e / [\% S]_o - [\% S]_e)$ vs time. The slope of the plot for the initial fast stage is clearly increased as the diameter of a crucible is decreased. This is contrary to the relationship predicted by Eq. 3.37 but the observed effect is the same as the effect of the increase of the slag

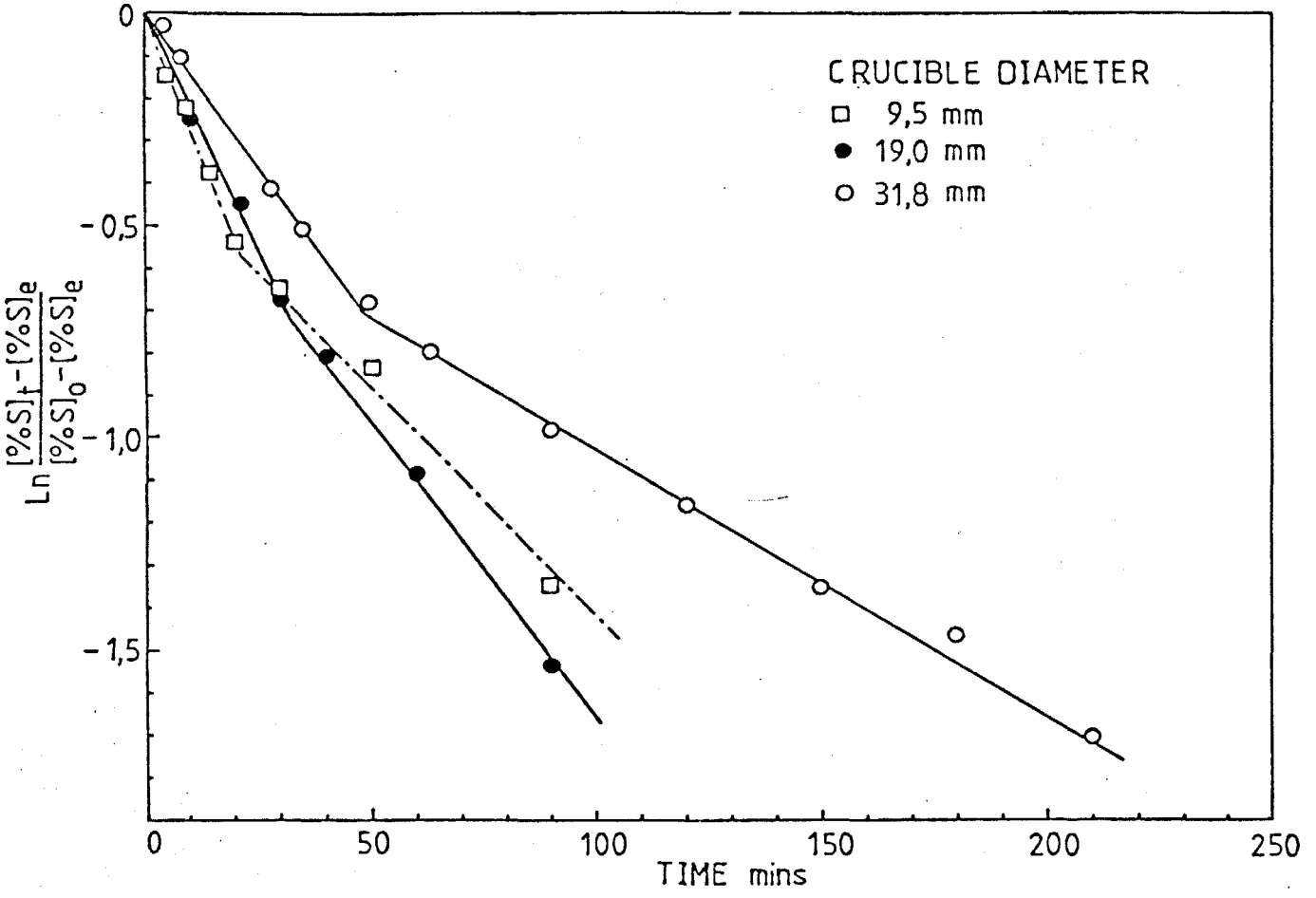

FIG. 3.13. Ln ($[\%\,S]_t - [\%\,S]_e$ / $[\%\,S]_o - [\%\,S]_e$) vs TIME PLOTS FOR DIFFERENT CRUCIBLE DIAMETER. EXPS. 61, 32, AND 1 (TABLE 6)

depth discussed above. Thus on the basis of the assumption of the local cell reaction for the sulphur transfer, and if the slag-graphite crucible interface area is considered to be as active as the slag-metal interface and both areas are assumed to be the reaction areas for the observed desulphurization reaction, then the values of the rate coefficient Km are evaluated from the above equation, Eq. 3.37, using the slope of the plots as in Fig. 3.13 as below

TABLE D

Exp.No	Crucible dia. cm.	A Slag/Metal Area cm^2	B Slag/Crucible Area cm^2	Slope	Km using A Area.	Km using A+B Area
61	0.95	0.71	5.4	0.0250	0.0031	0.00036
32	1.91	2.85	10.8	0.0195	0.0024	0.00050
1	3.18	7.92	18.0	0.0135	0.0017	0.00052
34	1.91	2.85	10.8	0.0627	0.0077	0.00016
25	3.18	7.92	18.0	0.0372	0.0047	0.00014
	Slag depth					
55	1.8 cm	7.92	18.0	0.009	0.0011	0.00035
56, 58	3.6 cm	7.92	36.0	0.019	0.0024	0.00043

Data for Exp. 55 and 56(58) with different slag depths discussed in the previous section are included here to compare the values calculated in the different ways. Table D shows that the values of Km, evaluated using the area of the slag-metal interface, vary by more than a factor of two, but Km values calculated using the sum of the areas of the slag-metal and the slag-crucible interface show a reasonable consistency, considering the possible error in obtaining the slope of a plot. According to this apparent consistency of Km values the assumption of local cell reaction as one of the desulphurization reactions seems to be

reasonable for explaining the observed results by a reaction control mechanism.

It is an interesting point that when the Km values calculated using only the slag-metal interface area are plotted against the diameter of the crucible, it shows a better linear relationship than the plots of the same Km values against the area of the slag-metal interface as shown in Fig. 3. 14. This seems to indicate that the contribution of the area of the slag-graphite crucible interface to the observed desulphurization rate becomes bigger as the diameter of the crucible decreases when the desulphurization rate is accounted by only the slag-metal interface area.

Fulton et al. (16) obtained different values of the slope for a doubled amount of slag as compared to the normal amount of slag, whilst Derge et al. (4) reported nearly constant Km values for different crucible diameters with a constant melt depth by calculating with the slag-metal interface area. But the data of Derge et al. were calculated from the rate data within 7 minutes of very initial stage and so the data might have uncertainty.

The difference in experimental techniques employed for the large crucible (3.18 cm dia.) and for the medium (1.91 cm dia.) and small (0.95 cm dia.) crucible as described in the experimental procedure section could be a possible reason for yielding different rates. However when the same experimental techniques as used in the present study were employed for a study into the kinetics of reduction of MnO from silicate slags by carbon in molten iron, using 3.18 and 1.91 cm dia. crucibles, no effect of crucible size on the reduction rate was observed (50). This indicates that there is no effect of the difference in experimental technique on the transfer rate. However

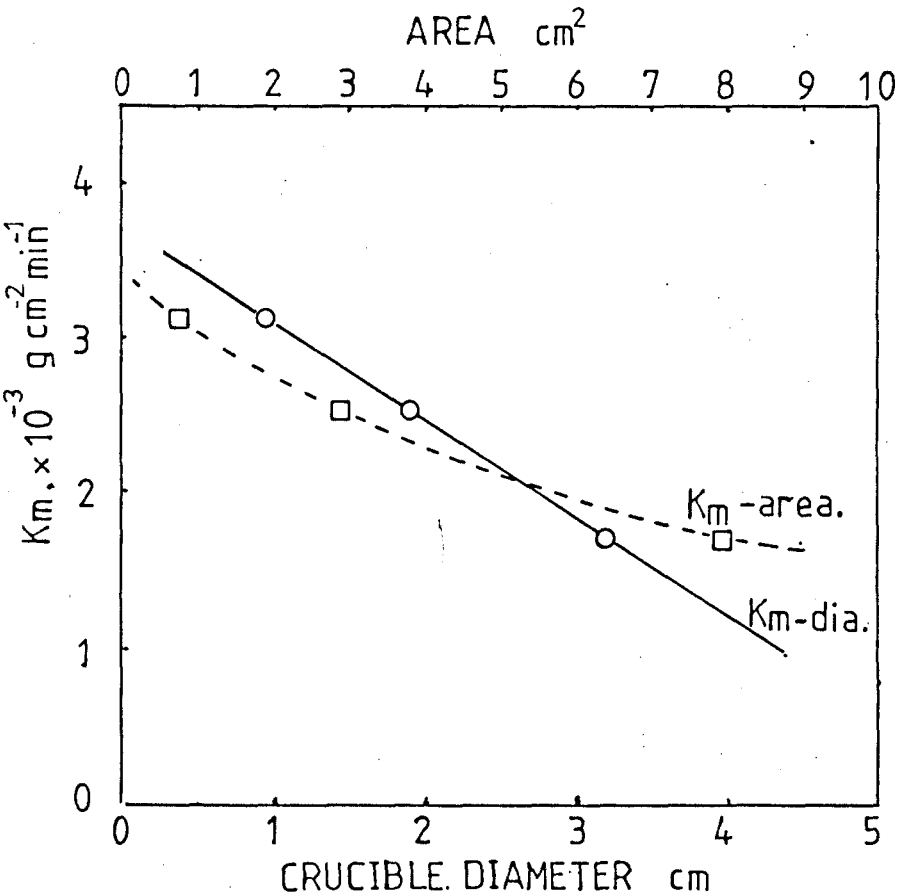

FIG. 3.14. TRANSFER RATE COEFFICIENT VERSUS CRUCIBLE DIAMETER AND SLAG / METAL INTERFACE AREA FOR THE SAME EXPERIMENTS AS FIG. 3.13.

the effect of melt geometry was observed during studies (43) into silica reduction as mentioned before. Therefore the observed effect of melt geometry is a characteristic phenomena of the desulphurization reaction which can be reasonably explained by assumption of a local cell reaction mechanism for desulphurization process. In the present study all values of Km recorded in tables were calculated using the slag-metal interface area as the reaction area unless stated otherwise, thus when a Km value is compared with others, the geometrical conditions for melt must be considered. The conclusion derived from the study of the effect of melt geometry is that the sulphur transfer reaction for the fast initial stage is not controlled by diffusion of sulphur in the slag or in the metal but by a reaction which is assumed to occur electrochemically at the slag-metal interface and at the slag graphite interface.

3.5. IRON TRANSFER

Iron transfer to slag during the metal / slag sulphur transfer reaction was thought to be an important concurrent reaction by many previous workers (4)(7)(19)(20). Derge et al. (4) explained the iron transfer by an assumption that sulphur is carried into the slag combined with iron as a compound whilst King and Ramachandran explained iron transfer as a component of their electrochemical reaction model as mentioned above.

In the present study iron transfer was investigated by analysing the total iron content of the slag, after magnetic separation of metallic iron, for every sulphur transfer experiment. The total iron determined by analysis was assumed to be as ferrous oxide in the

slag even though iron can be presented in other forms in slag. All of the data are recorded in the tables of results (see appendix). Some typical iron transfer curves are shown in Fig. 3.15 ; where the transferred amount of sulphur and iron to slag are plotted against reaction time for experiments No. 1 and 4. It can be seen from the curves that the iron content of the slag increases rapidly, for the fast initial stage of desulphurization, and then decreases as the desulphurization rate slows down, indicating that the iron transfer accompanies the sulphur transfer (the level reached after 240 minutes is however still above the final equilibrium with carbon / carbon monoxide). The rate curves also show that a higher sulphur transfer rate results in a higher rate of iron transfer for a given slag composition. Fig. 3.16 shows the iron and sulphur transfer rate curves for different slag compositions (SL 476 and SL 556) and indicates that the iron transfer rates for both slags are nearly the same, even though the sulphur transfer rate for the acid slag (SL 556) is much lower than that for the basic slag (SL 476). This can be explained by the fact that the reduction of ferrous oxide by carbon in iron is more difficult in an acid slag than in a basic slag (51) and that the activity coefficient of ferrous oxide in an acid slag is much lower than that in a basic slag ; thus a relatively high weight percentage of FeO is found in the acid slag even though there is less sulphur transfer. As seen in Fig. 3.16 the sulphur transfer rate seems to be the same as the iron transfer rate, on a molar basis, for the acid slag during the initial period of reaction ; but such a trend is not so clear for the basic slag, except at the very beginning of the reaction (which was also observed by Derge et al. (4)). Derge

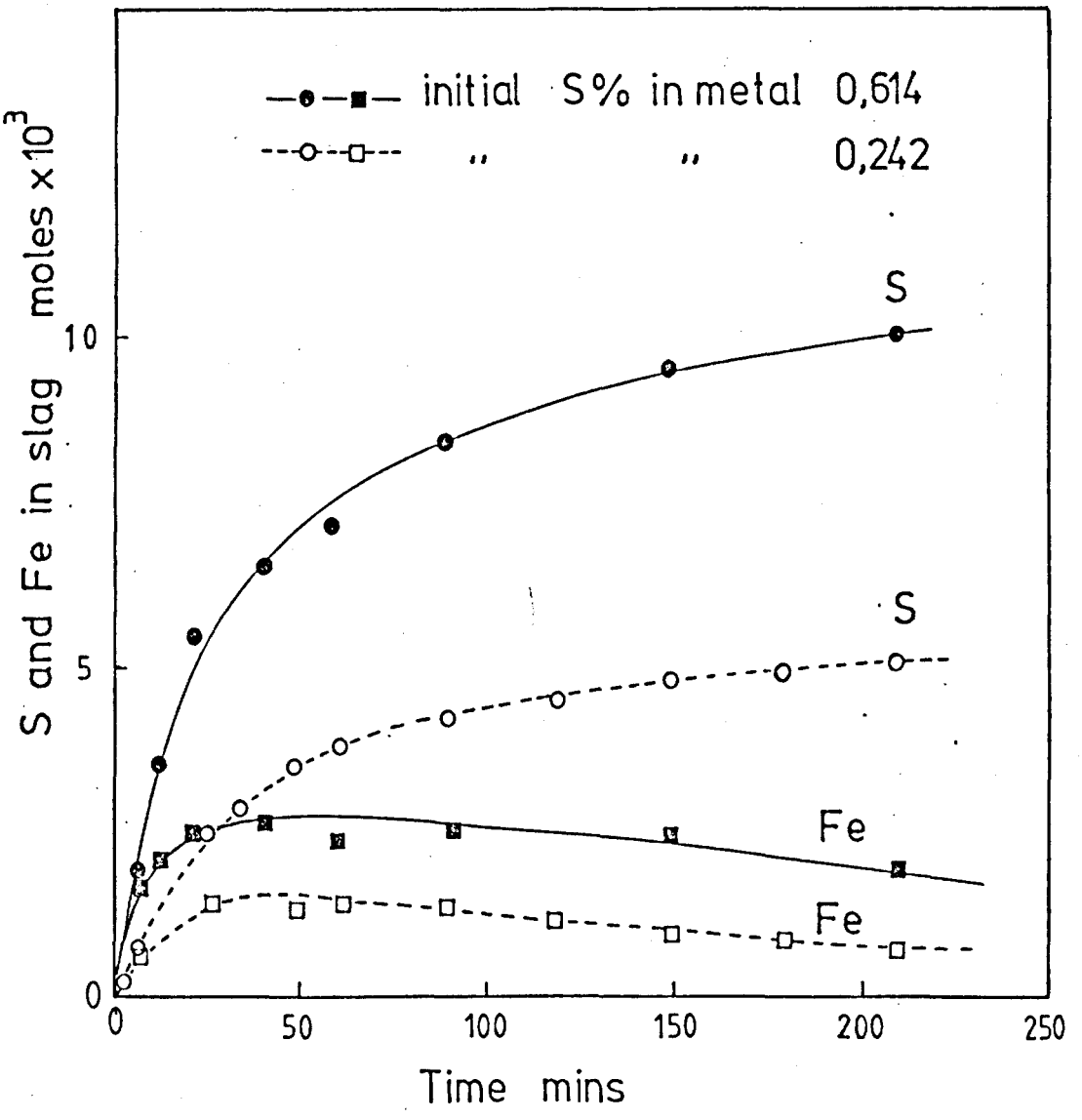

FIG. 3.15. EFFECT OF SULPHUR IN THE METAL ON RATES OF IRON TRANSFER TO SLAG.

EXPS. 1 AND 4 (TABLE 1)

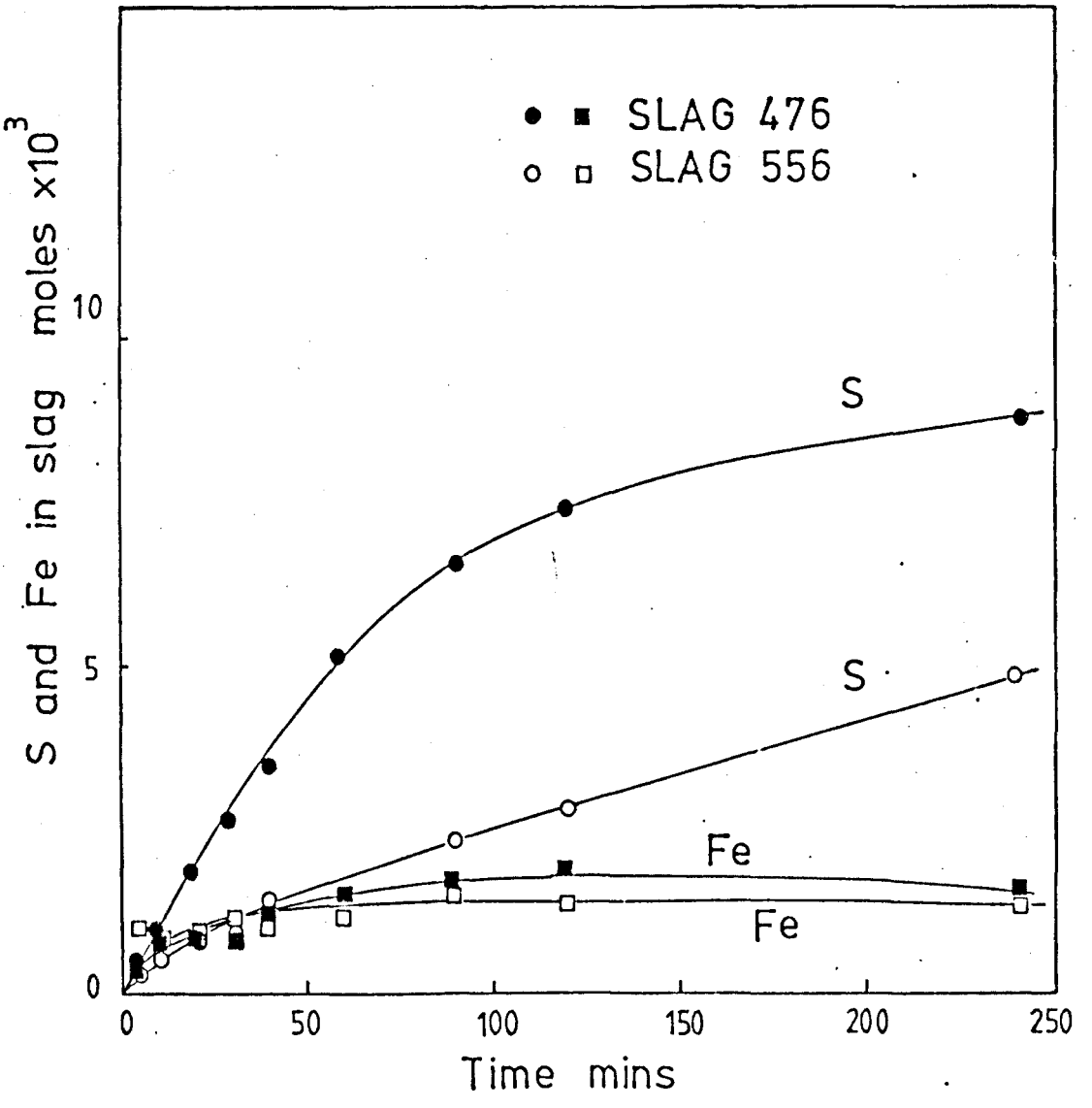

FIG. 3.16. EFFECT OF SLAG COMPOSITION ON RATES OF IRON TRANSFER

SLAG 476 : 47 % SiO_2, 6 % MgO, 47 % CaO, EXP. 9 (TABLE 2)

SLAG 556 : 55 % SiO_2, 6 % MgO, 39 % CaO, EXP. 14 (TABLE 3)

INITIAL S % IN METAL : 0.456 %

thought that the unit ratio of sulphur transfer rate to iron transfer rate on a molar basis observed in an acid slag, where the reduction of iron oxide is slow, indicated that sulphur is transferred to slag combined with iron as iron sulphide which in turns reacts with lime in slag to give ferrous oxide.

However, in view of the ionic character of slags, the desulphurization process is better explained by electrochemical reactions. The over all reaction for desulphurization, $[S] + (O^{2-}) = (S^{2-}) + [O]$, can be divided into half cell reactions;

$$[S] + 2e = (S^{2-}) \qquad (3.38)$$

$$(O^{2-}) = [O] + 2e \qquad (3.39)$$

As the reaction system of the present study is carbon saturated, reaction 3.39 is followed by:

$$C_{\text{metal or graphite crucible}} + [O] = CO \qquad (3.40)$$

Combining reaction 3.39 and 3.40 gives:

$$C + (O^{2-}) = CO + 2e \qquad (3.41)$$

Thus the over all reaction can be written as:

$$[S] + (O^{2-}) + C = (S^{2-}) + CO \qquad (3.42)$$

Reaction 3.38 is a cathodic reaction which needs two electrons for the ionization of sulphur whilst reaction 3.41 is an anodic reaction releasing two electrons and evolving CO gas. Thus reaction 3.41 is expected to be the slow step limiting the over all reaction as the reaction involves metal (or graphite crucible), slag and gas phases. This is substantiated by the iron transfer; i.e. despite the fact that

at C - CO equilibrium the quantity of iron in the slag would have been negligible, iron passed from metal to slag to provide electrons for the ionization of sulphur helping the delayed supply of electrons from reaction 3.41. Thus another anodic reaction, that of iron, accompanies sulphur transfer for the initial fast stage of desulphurization;

$$Fe = (Fe^{2+}) + 2e \qquad (3.43)$$

This anodic reaction is reversed to become a cathodic reaction later during the slow stage of desulphurization as seen in Fig. 3.15 and 3.16.

If there is Si, Mn, or Al in the metal, then, by the same reason as for iron, it will provide electrons for the sulphur reaction, reducing the necessity for the slow reaction of CO evolution, and thus enhancing the rate of desulphutization during the initial fast reaction period;

$$[Si] = (Si^{4+}) + 4e \qquad (3.44)$$

$$[Mn] = (Mn^{2+}) + 2e \qquad (3.45)$$

$$[Al] = (Al^{3+}) + 3e \qquad (3.46)$$

It is to be expected that the above forward reactions will be reversed to cathodic reactions due to their final equilibrium conditions as the desulphurization rate slows down later. This was demonstrated by Ramachandran and King (7). However,among the above reactions concurrent with sulphur transfer,the silicon reaction was considered to be the most important step for rate control of the desulphurization reaction because blast furnace slags have considerable amounts of silica as a major constituent thus requiring transfer of silicon to attain slag / metal equilibria; which is known to be a very slow step.

Silica reduction in the slag proceeds with consumption of electrons, eventually competing with the sulphur cathodic reaction for electrons, according to the reverse reaction of reaction 3.34 which is simplified for convenience of explanation;

$$(SiO_4^{-4}) = (Si^{4+}) + 4\ (O^{2-}) \qquad (3.47)$$

$$(Si^{4+}) + 4e = [Si] \qquad (3.44)$$

Thus Frohberg et al. pointed out that this silica reduction retards sulphur transfer. Grant et al. argued strongly that the desulphurization reaction is controlled by the silica reduction, not by the CO evolution as suggested by Derge et al.(4).

In view of this strong argument on the rate limiting step it was considered to be necessary to study the effect of silicon addition to the metal on the desulphurization reaction.

3.6. EFFECT OF SILICON ADDITION TO METAL

The addition of a deoxidant, such as Si, Al or Mn, to metal was observed to enhance the desulphurization rate by many previous workers (5)(6)(7)(19). In the present study the effect of silicon additions to metal on the desulphurization rate was investigated to help in understanding the rate controlling reaction step for the over all reaction; which is not clear from the disagreements between previous workers (4)(5)(7)(20). The experimental conditions employed for this study and the results are summarised in table E. The present experiments are into the effect of silicon addition to metal on desulphurization by different slag compositions (Exps. 12 and 16), the effect of the amount of silicon added (Exps. 31 and 25 - 27) and the

TABLE E

Exp. No	Slag	Initial % S	Initial % Si	Crucible dia. cm	Km g cm^2 min^{-1}	Result
9	SL 476	0.456	0	3.18	0.0011	table 2
11	SL 476	0.256	2.10	3.18	0.0050	table 7
12	SL 476	0.450	1.91	3.18	0.0048	table 7
14	SL 556	0.456	0	3.18	0.0003	table 3
16	SL 556	0.450	1.91	3.18	0.0014	table 7
1	SL 456	0.242	0	3.18	0.0017	table 1
31	SL 456	0.230	0.06	3.18	0.0032	table 8
25	SL 456	0.242	0.42	3.18	0.0047	table 8
26	SL 456	0.226	0.98	3.18	0.0059	table 8
27	SL 456	0.184	2.40	3.18	0.0065	table 8
22	SL 456	0.237	0	1.91	0.0024	table 9
32A	SL 456	0.229	0	1.91	0.0024	table 9
33	SL 456	0.106	0.125	1.91	0.0071	table 10
34	SL 456	0.242	0.42	1.91	0.0077	table 11
24	SL 456	0.202	1.89	1.91	0.0078	table 12

change in the silicon content of metal during desulphurization (Exps. 22, 24, and 32 - 34).

The study on the effect of silicon addition for different slag compositions was carried out by using a basic slag (SL 476) and an acid slag (SL 556) with a metal containing 1.91 % Si and 0.45 % S. The results are shown in Fig. 3.17, plotted as the change in sulphur content of metal with time; the results for the silicon free experiments 9 and 14 are included as super-imposed dashed curves for

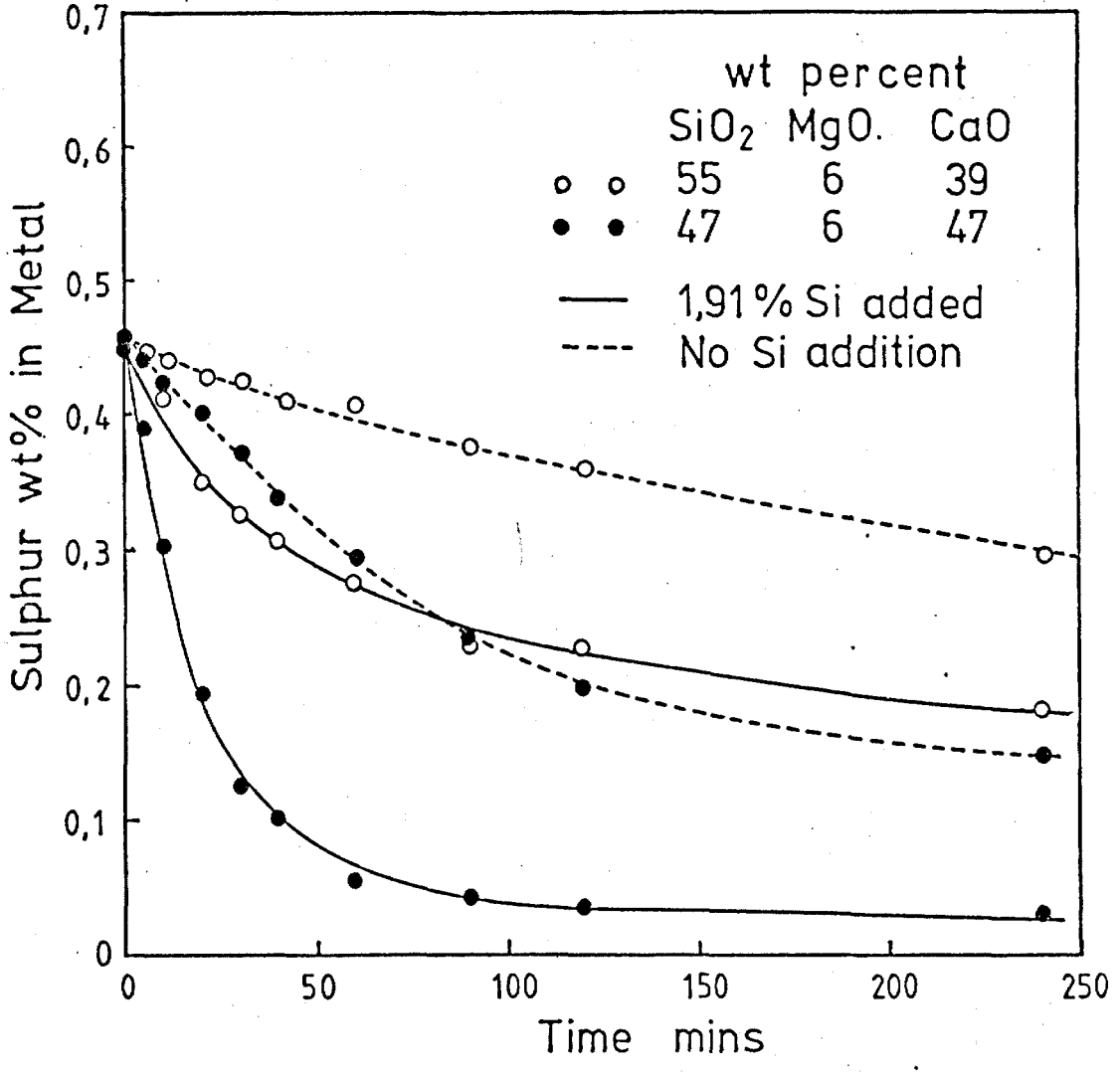

FIG. 3.17. COMPARISON OF EFFECT OF SILICON ADDITIONS TO THE METAL ON SULPHUR TRANSFER.

TEMPERATURE : 1465 - 1468 °C

EXPS. 12, 16, 9, AND 14 (TABLES 7, 2, 3)

comparison. It is seen from the rate curves that a 1.91 % Si addition seems to increase the rate of desulphurization by the same extent for both the basic slag and the acid slag. This is more clearly seen in Fig. 3.18, plotted as Ln $[\% S]_t$ against time for the same results in Fig. 3.17. The fact that 1.91 % silicon increases the rate by the same amount for the two different slags can be explained by an assumption on the effect of silicon addition; i.e. there may be a limit of silicon addition above which there is no further measurable effect on the sulphur transfer rate, such a limit being lower for a basic slag than for an acid slag due to the difference in equilibrium silicon level in metal for both the two slags. Thus 1.9 % Si may be near to the limit for the basic slag but still far below the limit for the acid slag. This limited effect of 1.91 % Si addition for the basic slag can be seen from the results of experiment No. 11 using a 2.1 % Si, 0.256 % S metal, shown in Fig. 3.19, where the results of silicon free experiment No. 6 and Exps. 9 and 12 are plotted together. The plots of Ln $[\% S]_t$ against time for these results are also included in Fig. 3.18. It is clear from Figs. 3.18 and 3.19 that 1.91 % and 2.1 % Si additions both increased the desulphurization rate coefficient to the same value, indicating that 0.2 % difference in silicon addition does not make any difference in increasing the rate. Thus it is considered that about 2 % Si is nearly the limit amount for the slag SL 476.

The above observations led to the necessity of a study into the effect of the amount of silicon added on the desulphurization rate. For this study Exps. 31 and 25 - 27 were carried out using the most basic slag SL 456 and varying the addition amount of Si from 0.06 to 2.4 %. The results are shown in Figs. 3.20 and 3.21. Both rate

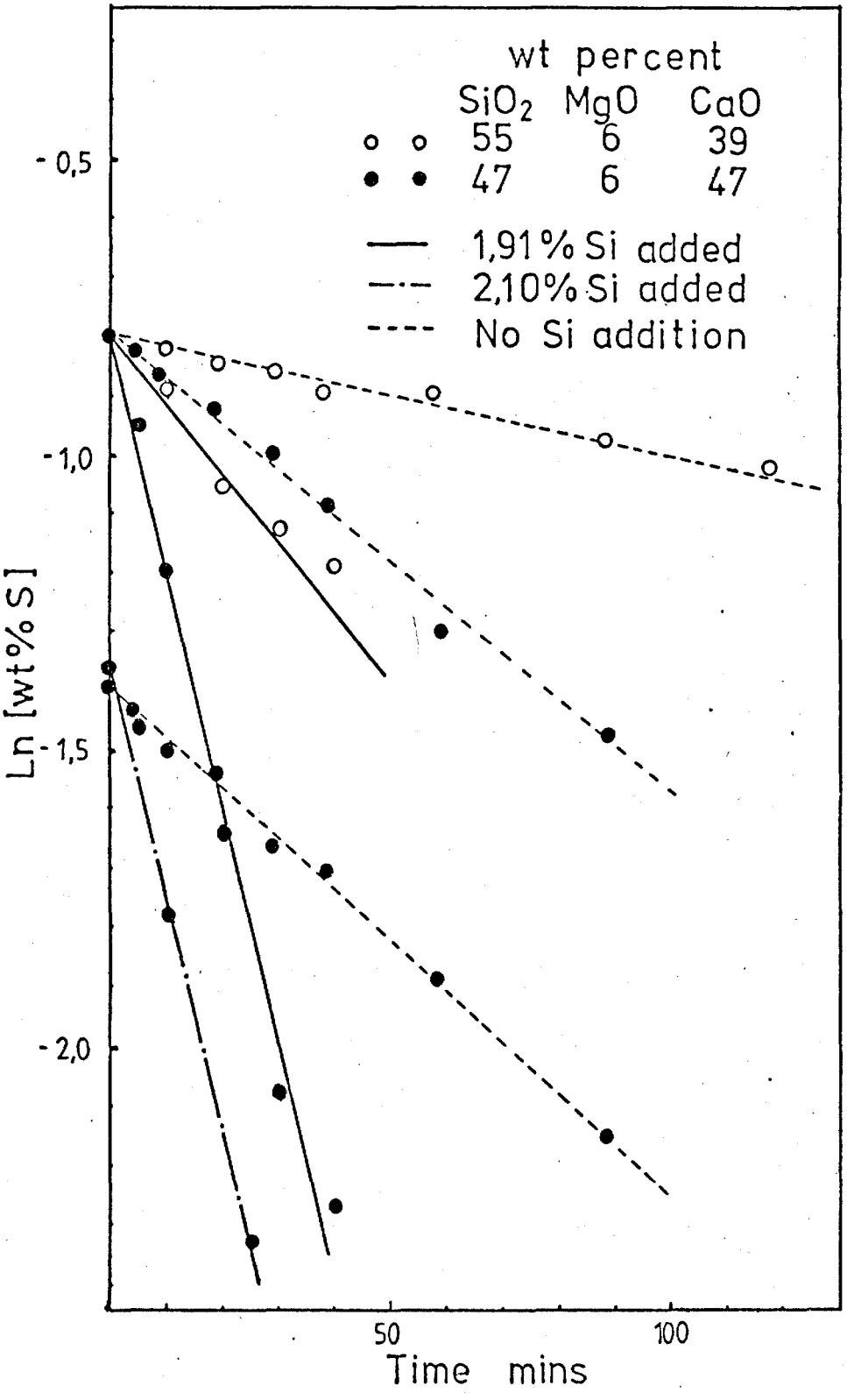

FIG. 3.18. Ln [wt % S] vs TIME PLOTS FOR

EXPS. 6, 9, 14, 11, 12, AND 16. (TABLES 2, 3, 7)

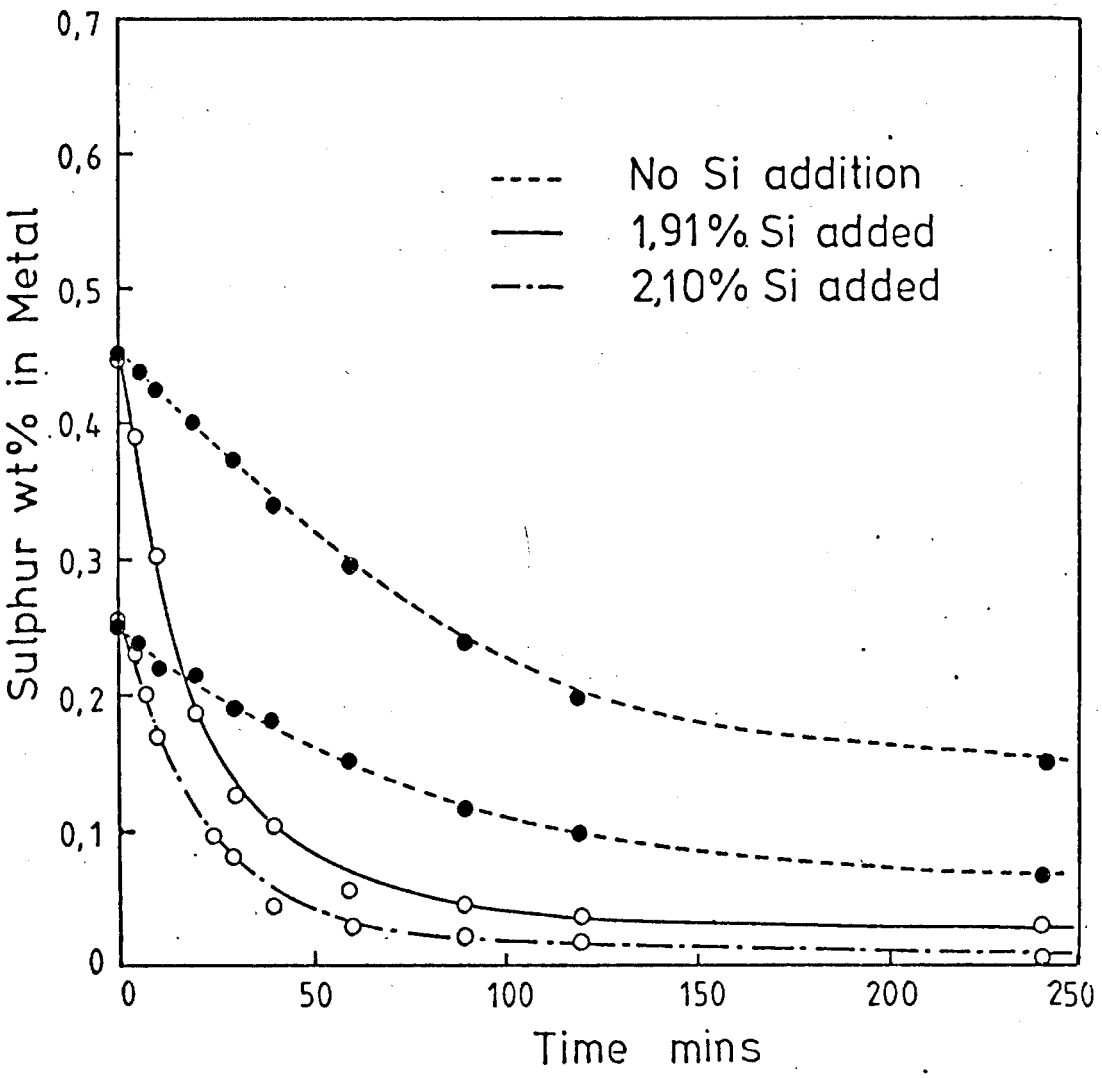

FIG. 3.19. COMPARISON OF EFFECT OF ALLOYED SILICON ON SULPHUR TRANSFER WITH DIFFERENT INITIAL SULPHUR CONTENT IN THE METAL.

SLAG COMPOSITION : 47 % SiO_2, 6 % MgO, 47 % CaO

EXPS. 11, 12, 6, AND 9. (TABLES 7, 2)

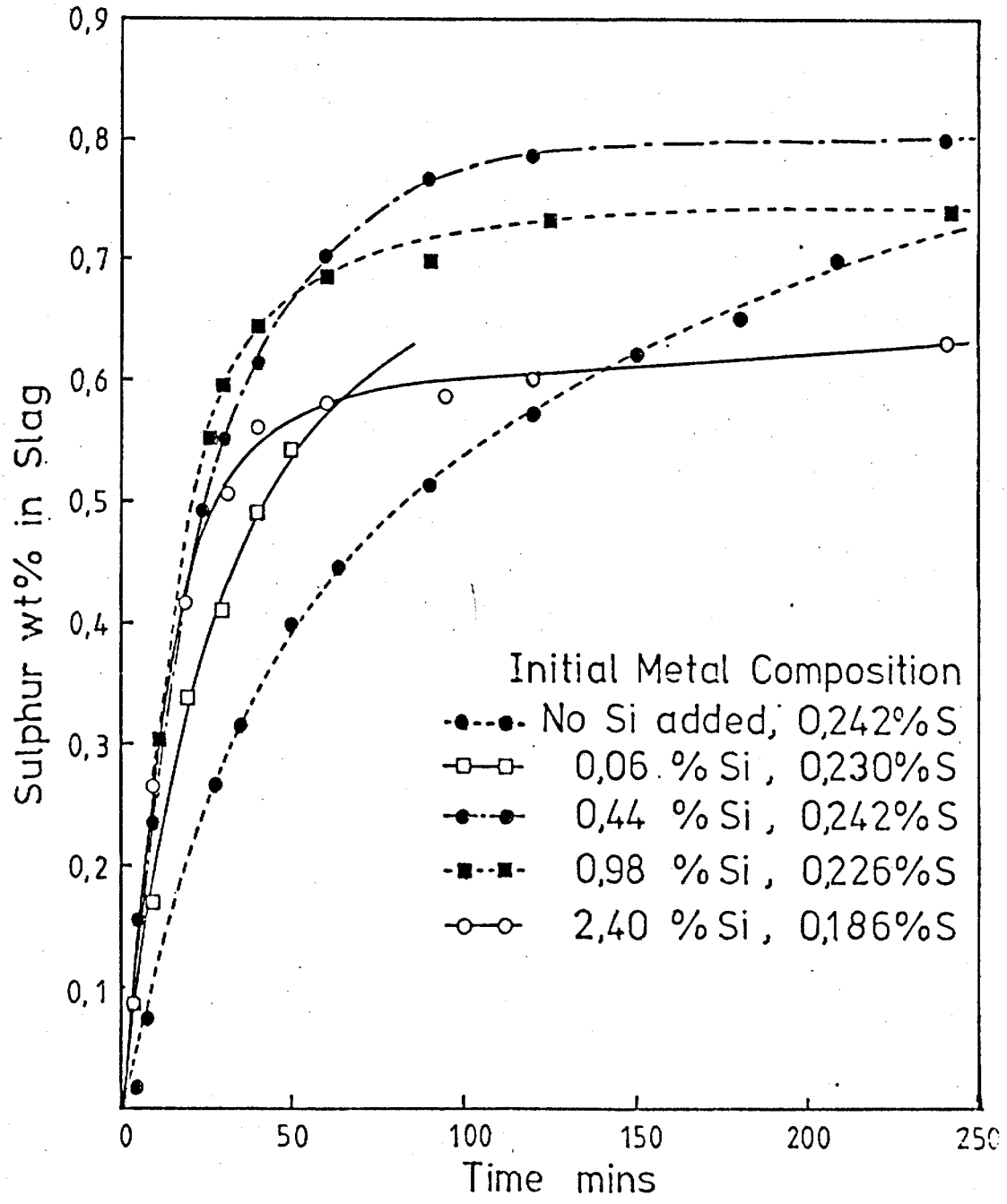

FIG. 3.20. THE EFFECT OF THE AMOUNT OF ADDED SILICON ON THE RATE OF SULPHUR TRANSFER.

SLAG COMPOSITION : 45 % SiO_2, 6 % MgO, 49 % CaO.

EXPS. 25, 26, 27, 31, AND 1. (TABLES 8, 1)

curves indicate clearly that there is a limit of silicon addition above which there is no effect on desulphurization rate as assumed above. From the rate data shown in Fig. 3. 21. Ln ($[\% S]_t - [\% S]_e$ / $[\% S]_o - [\% S]_e$) was plotted against time in Fig. 3.22. The value of $[\% S]_e$ was calculated by Eqs. 3.11 - 3.14 taking into account the increased activity coefficient of sulphur by silicon addition which was derived from the results of Ban-ya and Chipman (52). This demonstrates that increasing the silicon level from 1 % to 2.4 % does not increase the rate as much as the initial addition of 0.06 % Si. However it is interesting to notice that the plots for the slow second stage are nearly parallel irrespectively of amount of silicon, which will be discussed later. The effect of silicon addition is summarised in Fig. 3.23, plotted as the change in the rate constant against the added amount of silicon. Goldman et al.(19) measured the change in the rate coefficient with different amount of Si addition for a basic slag, 15 % Al_2O_3, 45 % CaO, 40 % SiO_2 and an acid slag, 15 % Al_2O_3, 30 % CaO, 55 % SiO_2 at 1500 ^oC as seen in Fig. 1.6 in chapter 1. Their data are reproduced in Fig. 3.23 as dotted curves. The rate coefficient for the acid slag increases almost proportionally to the amount of silicon addition, which proves the above assumption on the effect of silicon for the slag SL 556. But their results for the basic slag (which are very different from the present data) are doubtful as they show a sudden increase toward an infinitive value at about 1.5 % Si, which is quite improbable.

It must be noted that the effect of silicon addition to metal on the desulphurization rate coefficient can not be explained by the fact that alloyed silicon increases the activity of sulphur in metal,

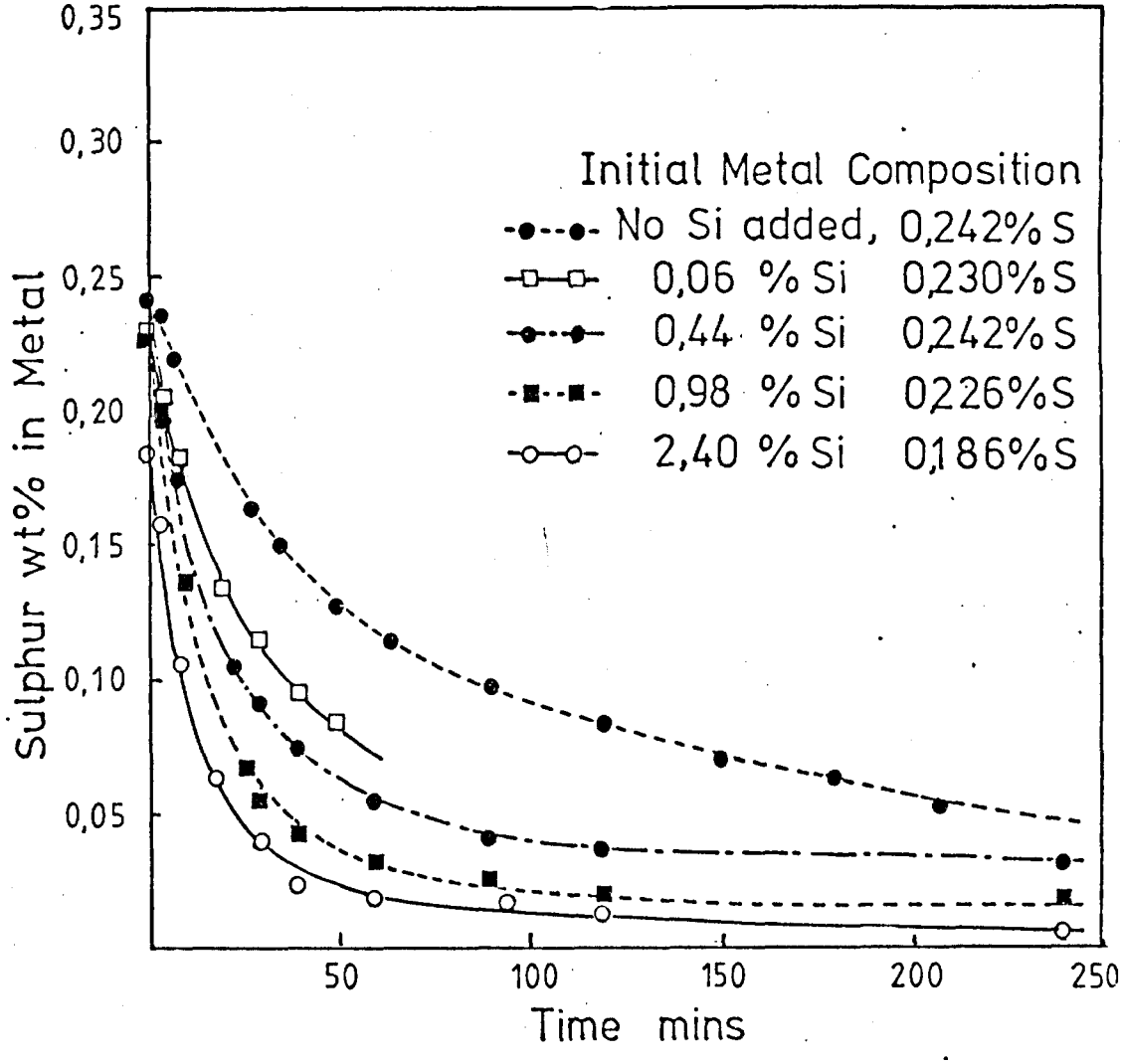

FIG. 3.21. COMPARISON OF DESULPHURIZATION RATES WITH DIFFERENT SILICON CONTENTS OF METAL FOR THE SAME EXPERIMENTS AS FIG. 3.20.

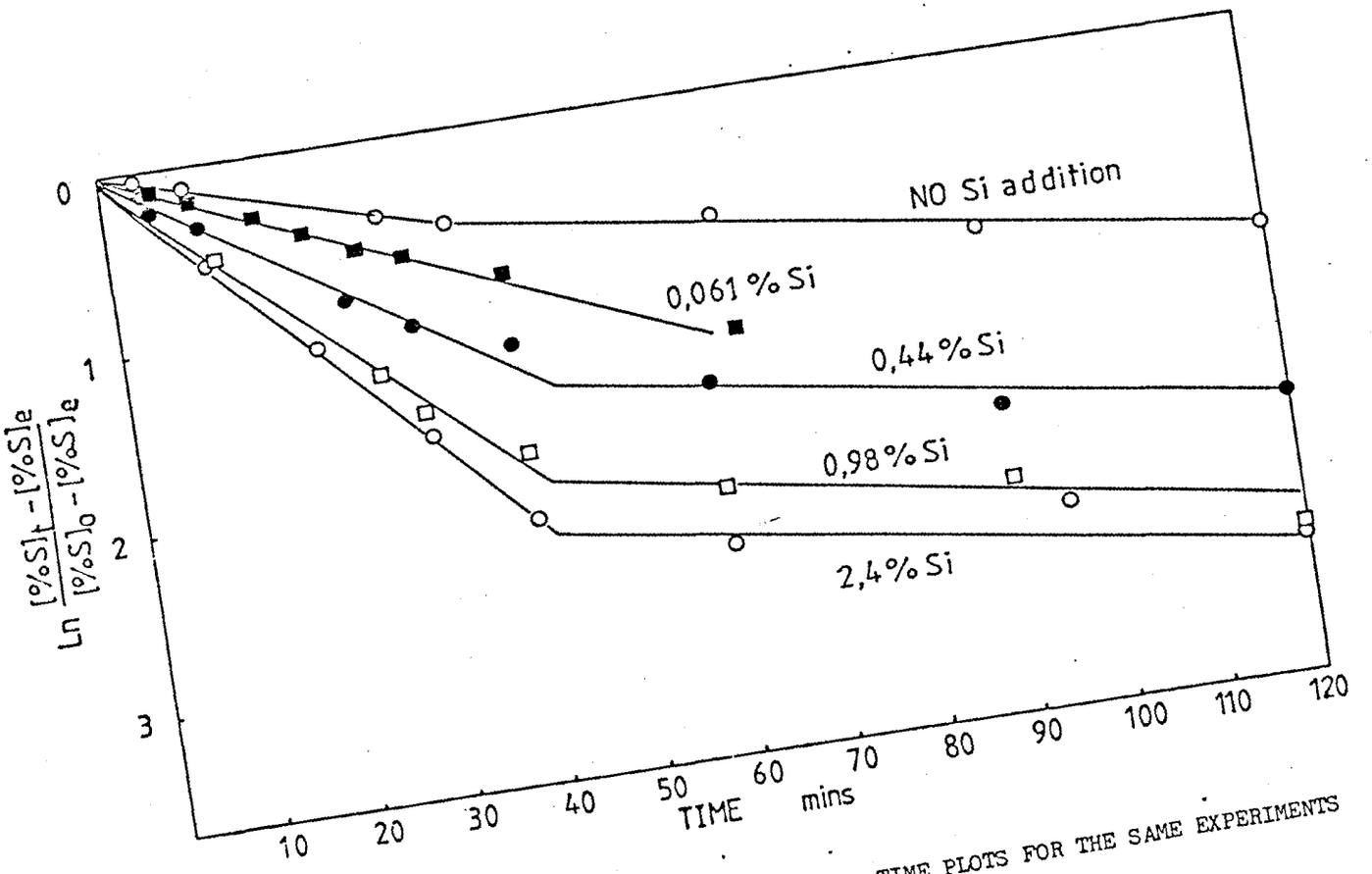

FIG. 3.22. Ln ($[\%\,S]_t - [\%\,S]_e$ / $[\%\,S]_o - [\%\,S]_e$) vs TIME PLOTS FOR THE SAME EXPERIMENTS AS FIG. 3.21.

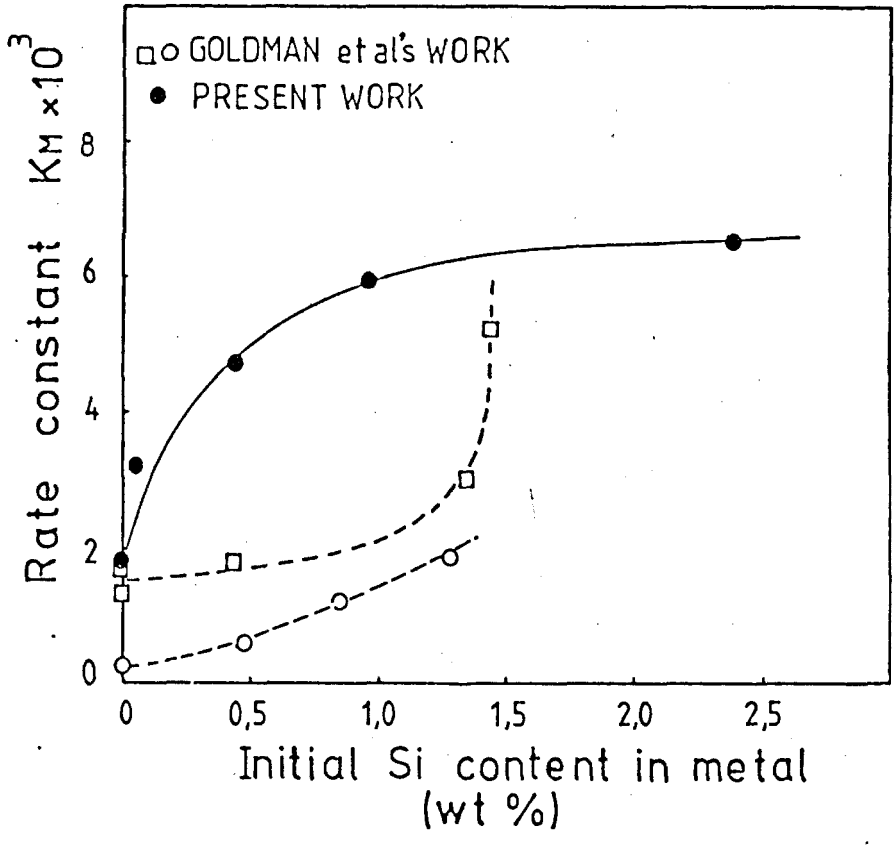

FIG. 3.23. EFFECT OF ALLOYED SILICON ON THE RATE COEFFICIENT OF SULPHUR TRANSFER FOR

A BASIC SLAG : 45 % SiO_2, 6 % MgO, 49 % CaO (AT 1465 °C) —●—

A BASIC SLAG : 15 % Al_2O_3, 45 % CaO, 40 % SiO_2 (AT 1500 °C) --□--

AN ACID SLAG : 15 % Al_2O_3, 30 % CaO, 55 % SiO_2 (AT 1500 °C) --○--

because the rate constant is not affected by the initial sulphur content of metal as discussed in the previous section 3.2. Furthermore Mn decreases the activity of sulphur in metal but Mn addition to metal increases the desulphurization rate as it will be shown in Fig. 3.36. Thus for the study into the effect of alloying elements on the desulphurization rate the use of activity instead of concentration of sulphur does not make any difference in showing the variation of the rate constant with alloying composition for a given alloy.

In order to explain the role of silicon in desulphurization the change in the silicon content of the metal during the reaction must be examined. As the above experiments were carried out by sampling only the slag, the change in silicon content could not be followed. The only available silicon concentrations are those in the initial metal and in the final metal after the run and these do not show any significant differences except for the experiment using the very low concentration of 0.06 % Si (see table 8). Thus experiments 22, 24, and 32 - 34 were carried out with 1.91 cm dia. crucibles by stopping the reaction after a predetermined time elapsed and analysing the metal. Typical result of these experiments are shown in Fig. 3.24 where the transferred amounts of silicon and sulphur from the metal to the slag (as number of moles) are plotted against the reaction time for the experiments using a 0.44 % Si, 0.242 %.S metal and a silicon free, 0.229 % S metal, the negative values meaning transfer from the slag to the metal. As seen in Fig. 3. 24, for Exp. 34, using a silicon containing alloy, silicon is transferred from metal to slag for the fast initial stage of desulphurization, then starts to recover as the reaction rate slows down and rises above the initial concentration towards the equilibrium level for the slag

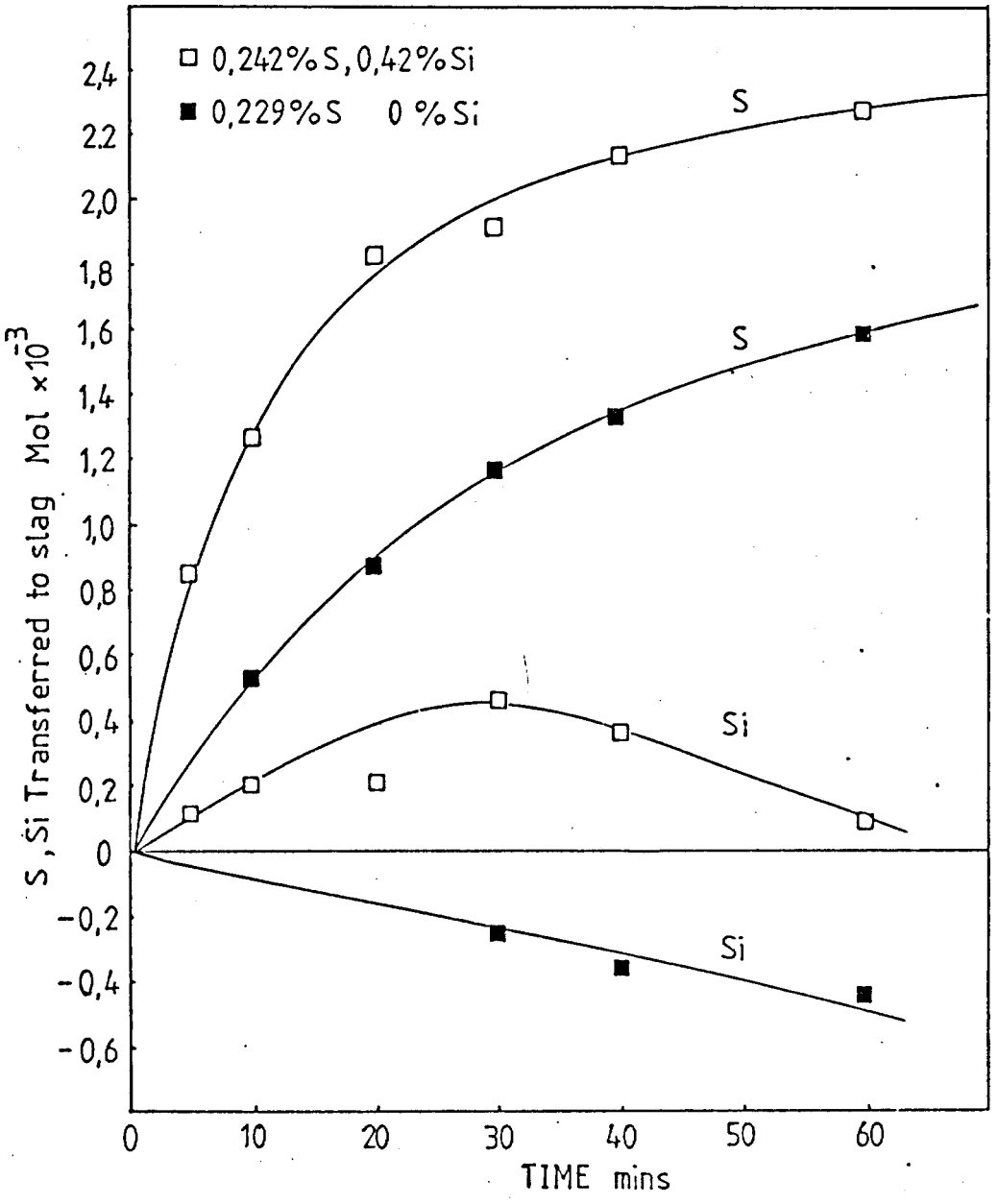

FIG. 3.24. SULPHUR AND SILICON TRANSFERS

EXPS. 32A AND 34 (TABLES 9AND 11)

SL 456 during the slow second stage of desulphurization. The equilibrium concentration of silicon in metal for the slag SL 456 is estimated as about 3 % by using a silicon distribution equation suggested by Turkdogan(53) and the silica activity value derived from the data of Rein and Chipman (54). Therefore the decrease of silicon content of the metal for the fast initial stage of desulphurization is in the opposite direction to that required by equilibrium and must be forced by the requirements of the sulphur transfer.

Ramachandran and King (7) observed the same trend of silicon transfer as the present study during desulphurization reaction as shown in Fig. 1.9. Grant et al. (5) also observed the silicon transfer along with sulphur transfer but their observations were only for the slow second stage of desulphurization, missing the changing mode of silicon in metal for the fast initial period of desulphurization as shown in Fig. 1.7.

The reason for the increasing effect of alloyed silicon can be demonstrated by the change in iron content of slag as shown in Fig. 3.25 where the rate of iron transfer to slag for Exp. 1 using a silicon free metal is compared with those for Exps. 25 - 27 using metals containg various silicon amounts; the iron transfer rate data for the silicon alloy experiments are erratic but the general iron contents are very low considering the increased high sulphur transfer rate. Thus it can be concluded from both the observations of silicon and iron transfer that for the initial fast desulphurization period the silicon in the metal is transferred to slag to provide electrons for sulphur cathodic reaction, reducing the amount of iron transfer and the necessity of the difficult anodic reaction 3.41, $C + (O^{2-}) = CO + 2e$, and thus increasing the sulphur transfer rate. This explanation implies

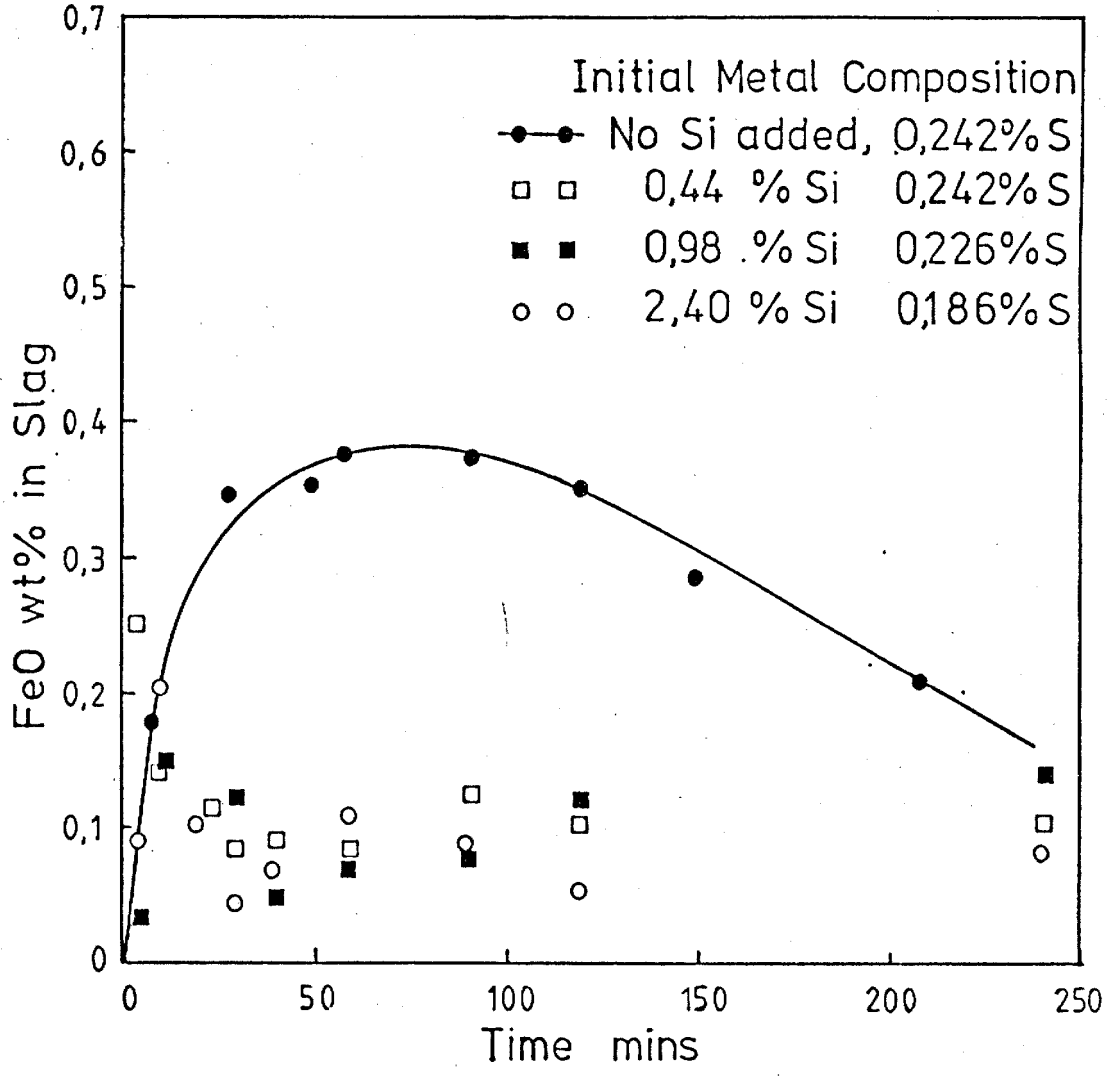

FIG. 3.25. EFFECT OF SILICON IN METAL ON IRON TRANSFER.

(SAME EXPERIMENTS AS FIG. 3.20)

SLAG COMPOSITION : 45 % SiO_2, 6 % MgO, 49 % CaO.

EXPS. 1, 25, 26, AND 27. (TABLES 1, 8)

that the slow reaction step limiting the sulphur transfer is the sluggish anodic reaction of CO evolution.

However it must be pointed out in Fig. 3.24 that for Exp. 32, using a silicon free metal, silica reduction proceeds from the initial stage of reaction but for Exp. 34, using a silicon alloy, the silicon in the initial metal is oxidized instead of silica being reduced during the fast stage of desulphurization. From the fact that silica reduction may retard the desulphurization reaction, as mentioned before, the effect of silicon addition could be explained by the retardation of silica reduction. This explanation implies that the desulphurization reaction is controlled predominantly by silicon reduction. Thus two different reactions, the sluggish CO evolution reaction and silica reduction, are both available for the rate controlling step for desulphurization reaction.

In order to destinguish which one of the above two reactions is more predominant in controlling desulphurization, it might be helpful to study the effect of the addition of oxide, such as MnO and FeO, which are more easily reduced than silica and thus more actively compete with sulphur for the electrons available for the transfer reaction, and to investigate the effect of ambient pressure which can affect the gas phase reaction.

However, the slow second stage of desulphurization must be considered in relation to silica reduction. Fig. 3.26 shows plots of $\mathrm{Ln}\left([\%\,S]_t - [\%\,S]_e \,/\, [\%\,S]_o - [\%\,S]_e \right)$ against time for the Exps. 24 and 32 - 34 carried out to study the change of silicon content in metal during desulphurization. Once again all the plots for the second slow stage of reaction are parallel within experimental error as also seen in Fig. 3.22, indicating that the rate for the second

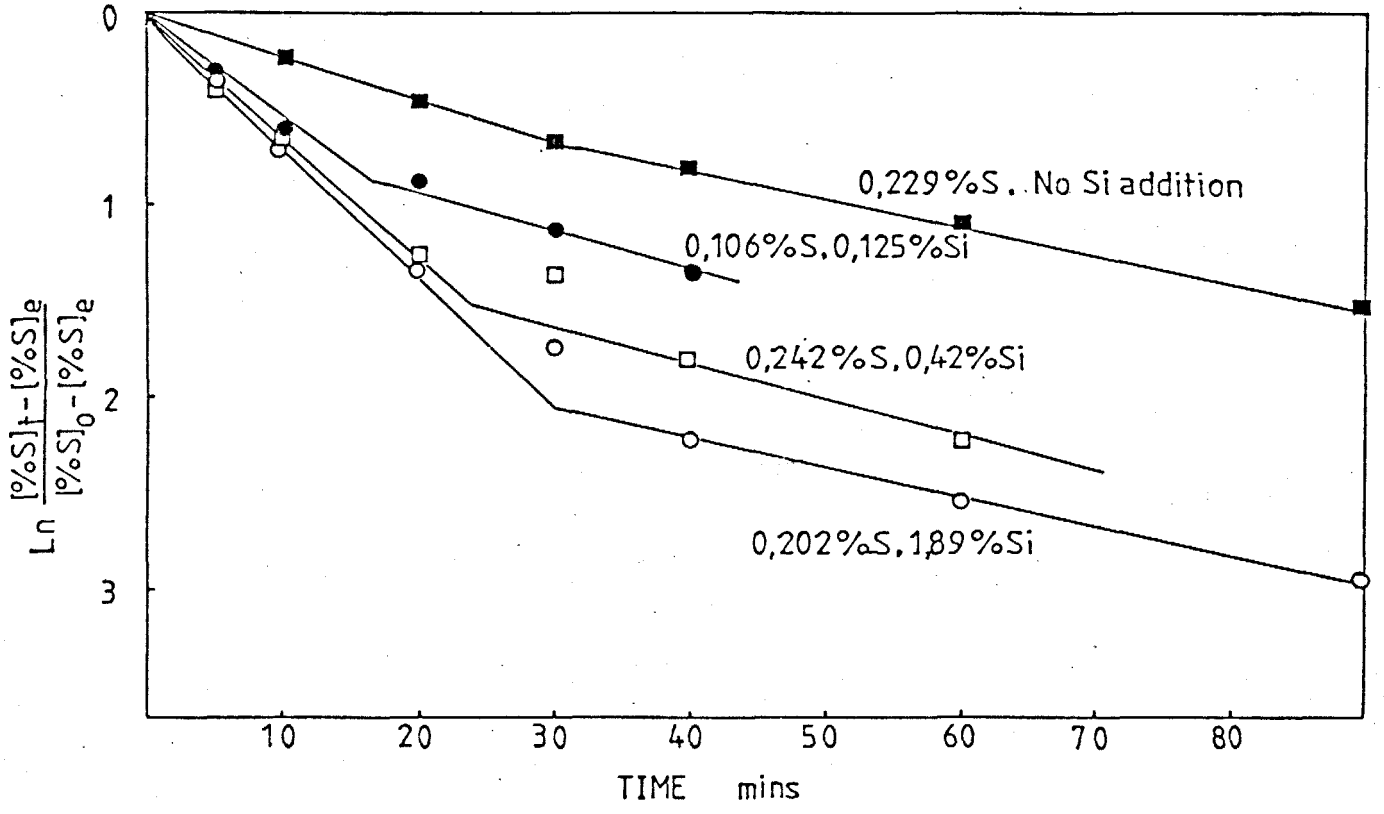

FIG. 3.26. Ln ($[\%S]_t - [\%S]_e$ / $[\%S]_o - [\%S]_e$) vs TIME PLOTS FOR EXPS. 24 AND 32 - 34. (TABLES 9, 10, 11 AND 12)

slow stage seems to be independent of the metal composition for a given slag and experimental condition. The same trend can be seen in Fig. 3.5 which was reproduced from the results of Ramachandran and King (7). It is interesting to relate the plots in Fig. 3.26 with the silicon transfer curves shown in Fig. 3.27 where the amounts of Si transferred from the metal to the slag are plotted against time, the negative value indicating the transfer from the slag to the metal. This silicon transfer rate curves show that the rates of silica reduction for the slow second stage of desulphurization from about 30 minutes of reaction time are nearly similar for each experiment, thus a similar rate of silica reduction may result in the similar rate of desulphurization for the second slow stage. This may be considered to indicate that the sulphur transfer for the slow second stage is controlled predominantly by the silica reduction reaction. However in view of the difficulty to follow accurately the slow silica reduction within the short reaction time of an hour the above conclusion may need more evidence to confirm. To determine whether a relationship exists between sulphur transfer and silica reduction the ratio of sulphur in the slag to sulphur in the metal has been plotted against the ratio of silicon in the metal to silica in the slag in Fig. 3.28 for the present experiments and for data obtained from previous workers. For the later stage of the desulphurization process these all show nearly parallel straight lines indicating that there is a strong relationship between silicon and sulphur transfer. However as the slope of this line indicates a 1 : 1 ratio of (% S)/[% S] to [% Si] / (% SiO_2) this would suggest that the equilibrium is more complex than might be expected.

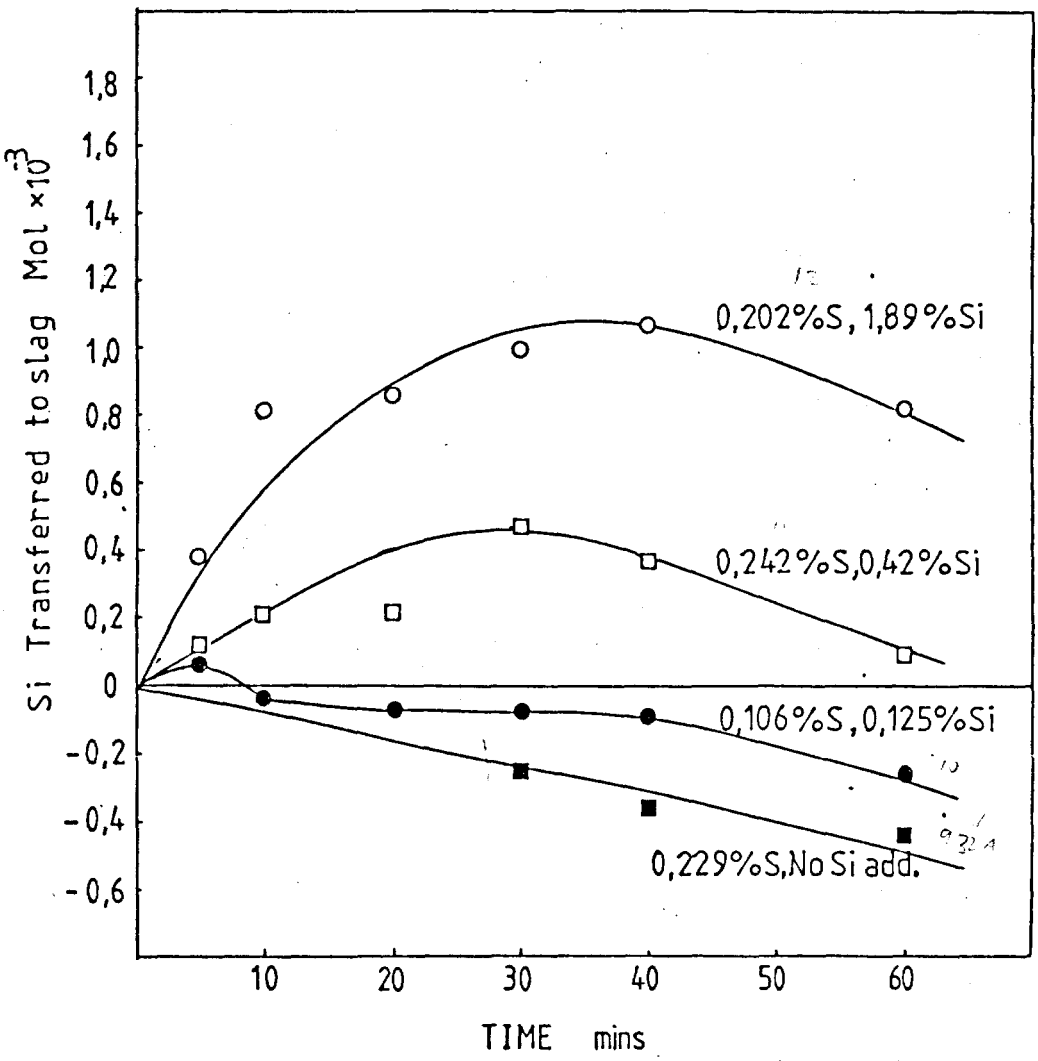

FIG. 3.27. SILICON TRANSFER FOR THE SAME EXPERIMENTS AS FIG. 3.26.

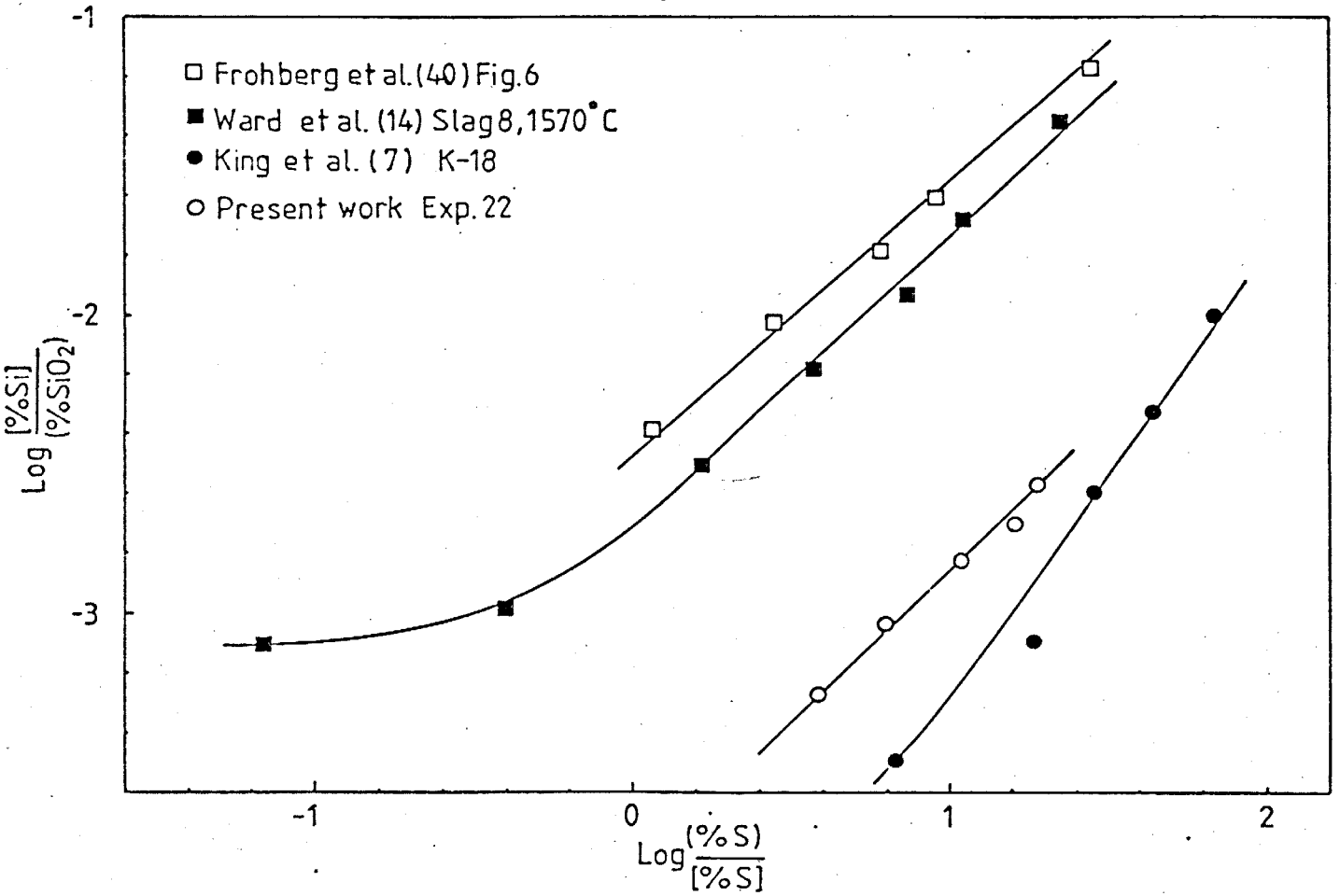

FIG. 3.28. LOG [% Si] / (SiO_2) vs LOG (% S) / [% S] PLOTS FOR THE PRESENT WORK AND FOR DATA CALCULATED FROM PREVIOUS WORKERS (7) (14) (40).

3.7. EFFECTS OF MnO AND FeO ADDITION

From the preceding discussion of the effect of silica reduction on desulphurization rate it is to be expected that the addition of easily reducible oxides such as MnO and FeO to the slag would decrease the desulphurization rate. Grant et al.(5) observed the effect of manganese and its oxide on desulphurization by blast furnace type slags; they found that the addition of manganese and manganous oxide to the reaction melts during the later stage of desulphurization caused an almost immediate sulphur reversion into the metal, an observation which is well in line with the above prediction. However, their results do not show the effect of MnO addition on the desulphurization during the initial fast reaction period.

In the present experiments the effects of MnO and FeO on the initial desulphurization rate were studied by adding various amounts of the oxides to the initial slag and following the changes in sulphur, manganese and iron contents in the slag from the beginning of the reaction. For one experiment(Exp. 50) MnO additions were made twice at different reaction times during desulphurization. The experimental conditions employed for the present study and the results are summarised in table F.

The effect of MnO additions on sulphur transfer rates is shown in Fig.3.29, plotted as the change in sulphur content of the slag with time for Exps. 43, 39, and 40 carried out using a 0.256 % S metal and SL 456 slags to which were added 2, 4, and 8 wt.% of MnO respectively; the rate curve for Exp.1 without MnO addition is included for comparison. As seen from the rate curves in Fig. 3.29.

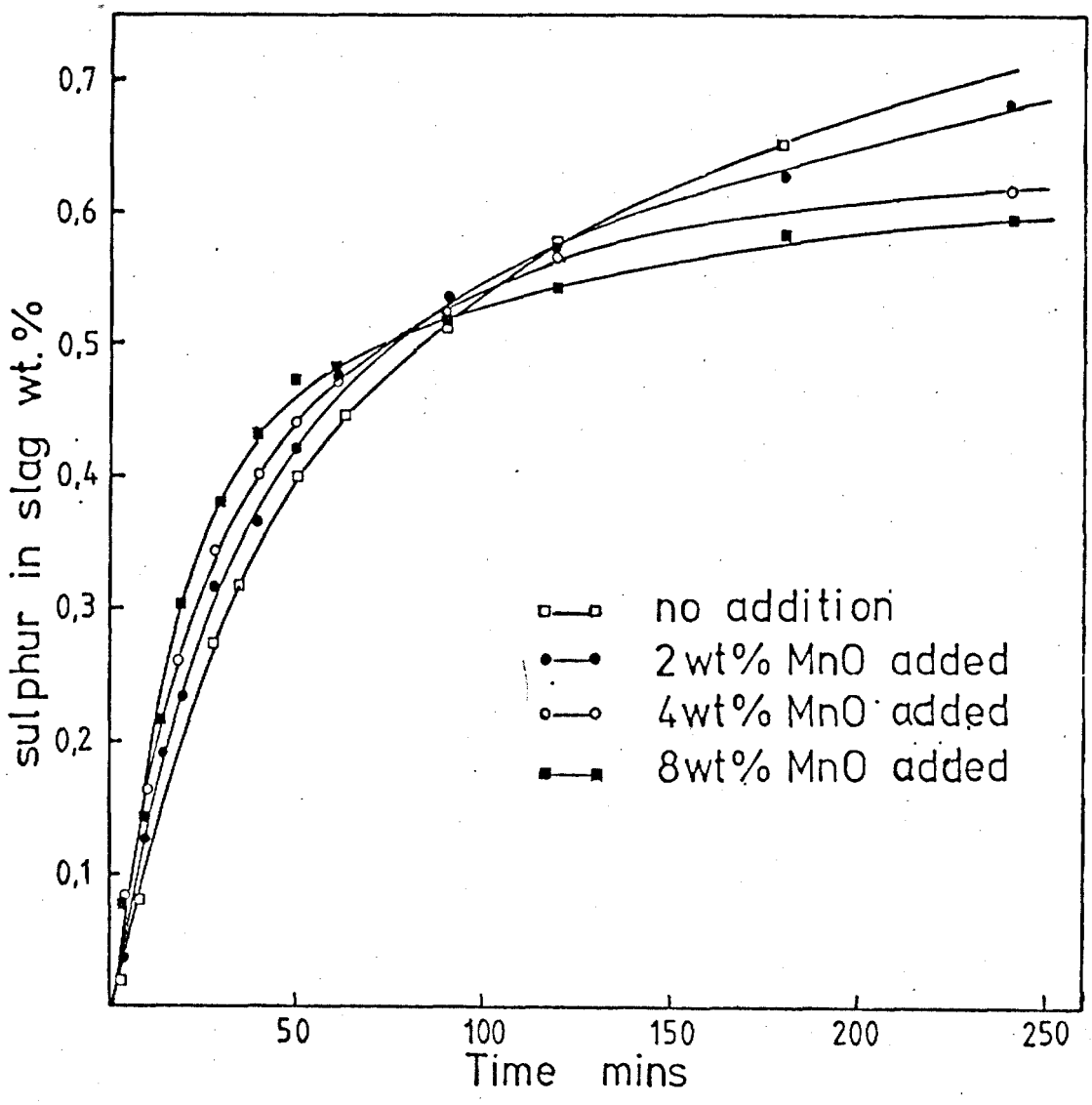

FIG. 3.29. EFFECT OF MnO ADDITIONS ON SULPHUR TRANSFER RATE.

SLAG : 45 % SiO_2, 6 % MgO, 49 % CaO

METAL : 0.251 % S, C - SATURATED IRON

EXPS. 1, 39, 40, AND 43. (TABLE 13).

TABLE F

Exp.No.	Slag	Initial [% S]	Oxide addition	Rate coeff., Km, g cm^{-2} min^{-1}	Result
1	SL 456	0.242	No addition	0.0017	table 13, 1
43	SL 456	0.251	2 wt.% MnO	0.0020	table 13
39	SL 456	0.251	4 wt.% MnO	0.0024	table 13
40	SL 456	0.251	8 wt.% MnO	0.0025	table 13
41	SL 456	0.614	4 wt.% MnO	0.0029	table 14
42	SL 456	0.614 + 4 % Mn	No addition	0.0029	table 14
48	SL 456	0.507	0.5 % MnO	0.0020	table 15
47	SL 456	0.507	1 % MnO	0.0021	table 15
49	SL 456	0.507	2 % MnO	0.0020	table 15
50	SL 456	0.229	1st. 1.2g MnO 2nd. 1.2g MnO		table 16
9	SL 476	0.456	No addition	0.0011	table 2
7	SL 476	0.256	2 wt.% FeO	0.0027	table 17
8	SL 476	0.456	2 wt.% FeO	0.0016	table 17
14	SL 556	0.456	No addition	0.0003	table 3
17	SL 556	0.456	2 wt.% FeO	0.0005	table 17

MnO additions increase the fast initial desulphurization rate proportionally with the amount of MnO added, but after the fast period of desulphurization the rate slows down more rapidly with a

higher MnO addition, giving a much lower sulphur partition ratio at the end of the experiment. The effect of MnO during the initial period is represented by the rate coefficients in table F which were evaluated from the plots of Ln ($[\%\ S]_t - [\%\ S]_e$ / $[\%\ S]_o - [\%\ S]_e$) against time as shown in Fig 3.30. Fig.3.30 indicates more clearly the effect of MnO on slowing down the rate during the later slow stage, an observation which is in agreement with the predictions of previous workers. The effect of MnO in increasing the desulphurization rate during the initial period observed above is quite contrary to the effect expected from the reduction of the oxide in the slag.

Part of the reason for this contradictory behaviour may be found from consideration of the rate curves of MnO reduction in Fig. 3.31, where the rate curves are compared with those for the experiments carried out by Pomfret and Grieveson(50) with the same experimental conditions as the present study except using sulphur free carbon saturated iron. As seen in Fig.3.31, the presence of sulphur increases the rate of transfer of manganese from slag to metal during the first five minutes of reaction and this increase in rate is proportional to the amount of sulphur in the slag. After five minutes the total manganese in the slag remains constant or increases slightly with a high sulphur level in the metal and this persists for the duration of the fast desulphurization period (40 - 50 minutes). However, in the absence of sulphur the fast rate of manganese transfer continues for about 50 minutes. After 50 minutes of the fast desulphurization period the total manganese in the slag falls at about the same rate as that observed in a sulphur free system. However, the amount of manganese in the slag is at

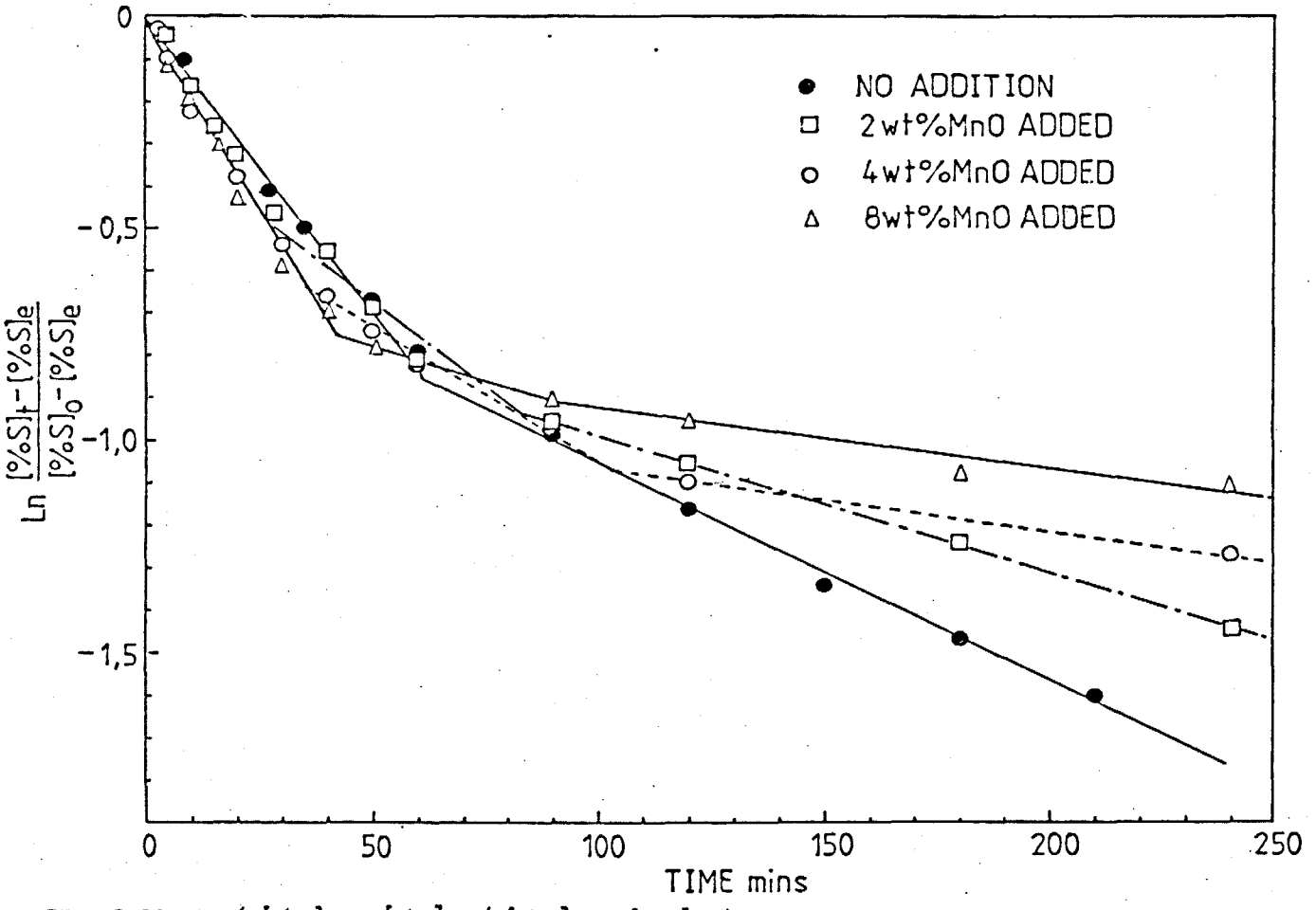

FIG. 3.30. Ln ($[\%\,S]_t - [\%\,S]_e$ / $[\%\,S]_o - [\%\,S]_e$) vs TIME PLOTS FOR THE SAME EXPERIMENTS AS FIG. 3.29.

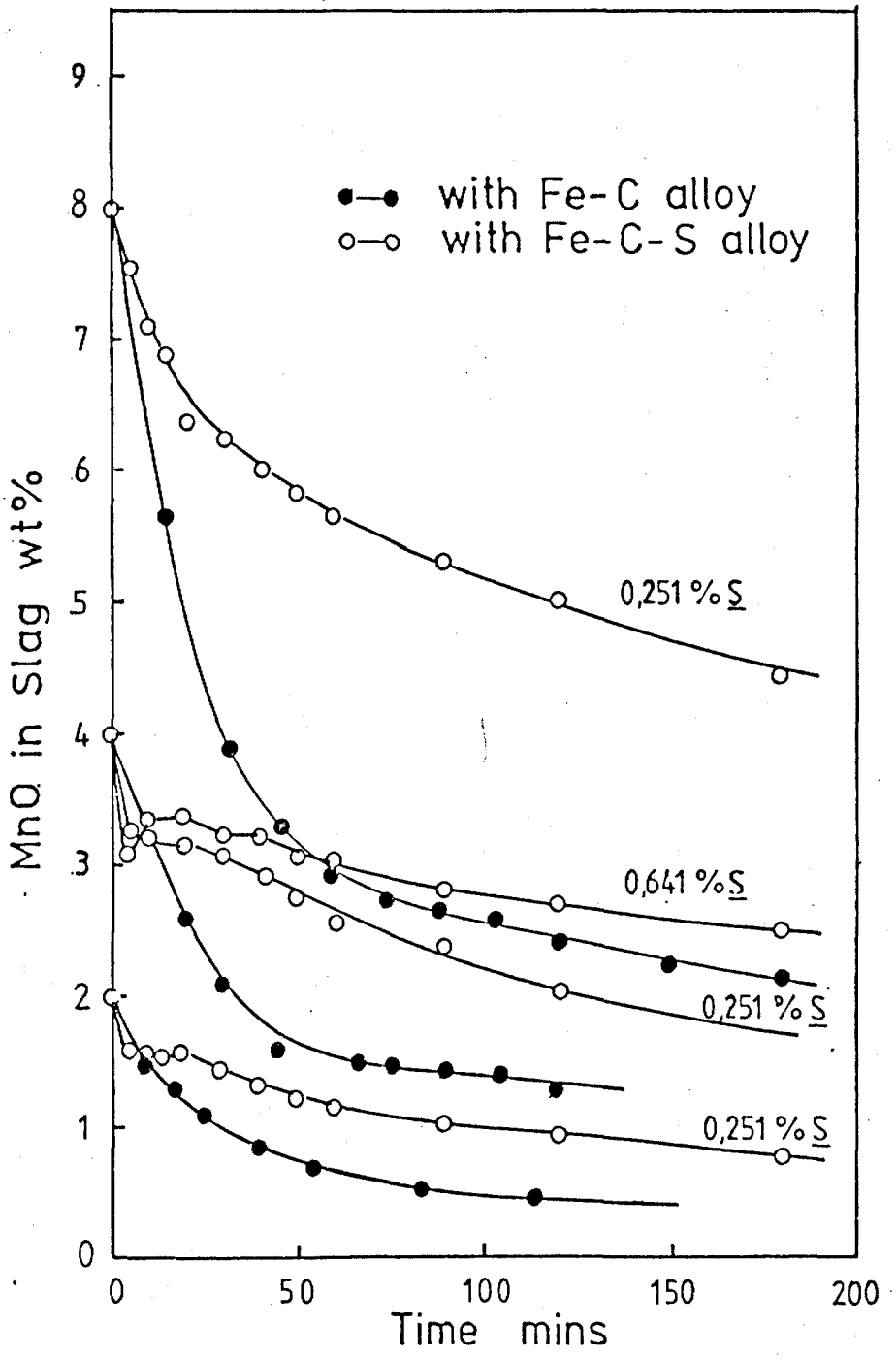

FIG. 3. 31. COMPARISON OF MnO REDUCTION RATES FOR VARIOUS SULPHUR ALLOYS WITH THAT OF SULPHUR FREE ALLOY (SULPHUR FREE DATA FROM R.J.PONFRET AND P.GRIEVESON (50))
EXPS. 39, 40, 43, AND 41. (TABLES 13, 14)

a level where we could expect a fast rate of transfer in a sulphur free system. This indicates that much of the manganese in the slag must now be associated with sulphur not oxygen. Thus, it is proposed that manganese transfers to the metal by reduction of MnO and then transfers back to the slag in association with sulphur as indicated in equations 3.45 and 3.46.

$$(MnO) + [C] = [Mn] + CO_{(g)} \qquad (3.45)$$

$$[Mn] + [S] = (MnS) \qquad (3.46)$$

The slag manganese level remains high because the overall reaction, $(MnO) + [C] + [S] = (MnS) + CO_{(g)}$, is achieved by no net manganese transfer to the metal while the driving force for manganese reduction is reduced.

The above recycling of manganese with sulphur seems to partially explain the effect of MnO addition in increasing the desulphurization during the initial period, but such an explanation can not be applied to the fact that during the first five minutes of reaction the desulphurization rate is increased when the rate of MnO reduction also increases. This puzzling effect of MnO can be explained by the effect of MnO addition on the sulphide capacity. From the data of Abraham and Richardson(55) on the sulphide capacity measurements for binary silicate melts it is apparent that at any chosen basicity the value of sulphide capacity of the manganese and ferrous silicates is much higher than that for the lime silicates. Therefore MnO addition to the present slag must increase the sulphide capacity. Thus for the initial period of desulphurization while the driving force for sulphur transfer from metal to slag, i.e. $[a_S] / (a_S)$ ratio,

is at a high level the effect of the increased sulphide capacity imposed by MnO addition on desulphurization may surpass the unfavourable effect of increased oxidation potential of the reaction system by MnO addition, thus enhancing the sulphur transfer rate. However when the driving force becomes smaller as desulphurization proceeds the unfavourable oxidizing effect of MnO on desulphurization begins to exceed the effect of the increased sulphide capacity, thus slowing down the sulphur transfer rate proportionally to the amount of MnO added during the later stage of the reaction as shown in Fig.3.29. This effect can be substantiated by considering Exp.50, which was carried out by adding 1.2g of MnO to slag at 21 minutes and another 1.2g of MnO at 123 minutes during desulphurization as shown in Fig. 3.32. The arrow mark in Fig.3.32 indicates the time of each addition of MnO. It is clearly seen that the first addition of MnO during the fast initial period when the driving force for sulphur transfer to slag is still relatively high, (% S) / [% S] = 1.6, does show a slight immediate increase of the rate, but the second addition when the driving force is small, (% S) / [% S] = 6.3, shows an immediate sulphur reversion similar to that observed by Grant et al.(5).

However, the fact that the presence of sulphur increases the MnO reduction rate in the first five minutes of reaction indicates that the MnO reduction may be assisted by the CO bubbling produced from desulphurization. In a recent study into the kinetics of the initial stage of reduction of MnO from silicate slags by carbon in molten iron by Pomfret and Grieveson(50), they suggested that the fast stage takes place by an exchange mechanism : (MnO) + [Fe] = (FeO) + [Mn], and the rate of this reaction is controlled by mass transport in the slag phase which is influenced by the rate of

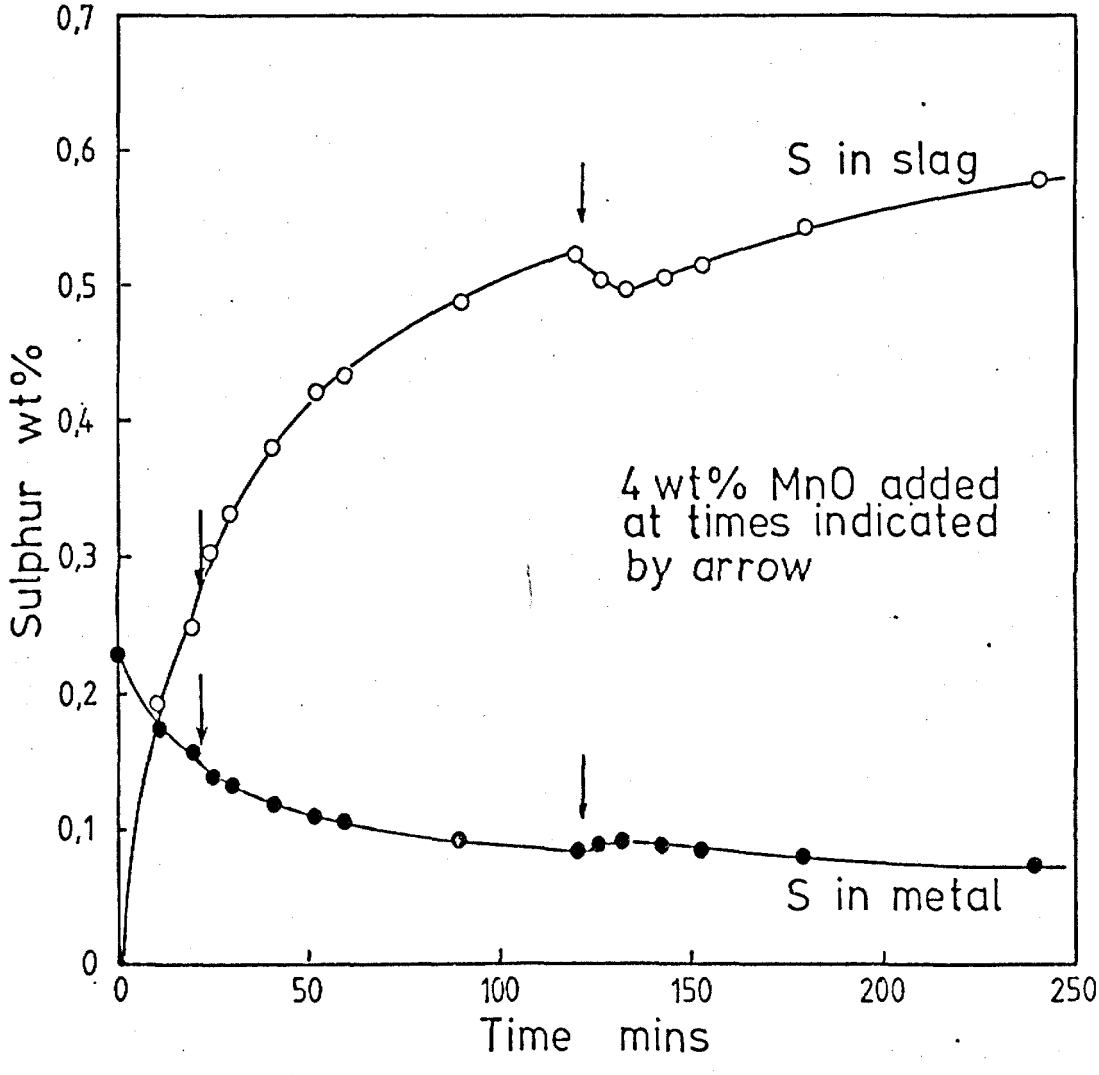

FIG. 3.32. EFFECT OF MnO ADDITIONS AT DIFFERENT TIMES ON SULPHUR TRANSFER.

EXP. 50 (TABLE 16)

evolution of CO bubbles produced by the concurrent reduction of the iron oxide in the slag. Thus it can be proposed that the CO bubbling produced by the desulphurization reaction provides a stirring effect to the reaction melts, enhancing the mass transport of MnO in the slag to the slag-metal interface and giving a faster reduction rate in the first five minutes of reaction. It is also possible to consider that CO bubbles associated with MnO reduction could eliminate the CO gas nucleation problem for desulphurization, thus enhancing the sulphur transfer rate. However such an effect of CO bubbling on desulphurization rate is not apparent, because the effect of MnO in increasing sulphide capacity is more evident ; the fact that most of the manganese remaining at a constant level in the slag after the first five minutes of rapid reduction is considered to be held with sulphur indicates strong evidence for the effect of MnO on the sulphide capacity during the fast desulphurization period.

The similar effect of oxide addition on the desulphurization can also be substantiated by sulphur transfer experiments using a FeO addition. Exps. 7 and 8 were carried out using SL 476 slag with 2 % FeO initially added and Exp. 17 was also carried out using SL 556 slag with a 2 % FeO addition. The results are shown in Fig. 3.33, plotted as change in sulphur content of metal and FeO content of slag with time for Exps. 8 and 17 compared with Exps. 9 and 14 without the FeO addition. As seen from the desulphurization curves of Fig.3.33, the reaction rates during the initial fast period are increased for both SL 476 and SL 556 slags with an addition of FeO, but later during the slow stage there is no apparent effect of FeO in slowing down the rate similar to that observed with MnO (shown

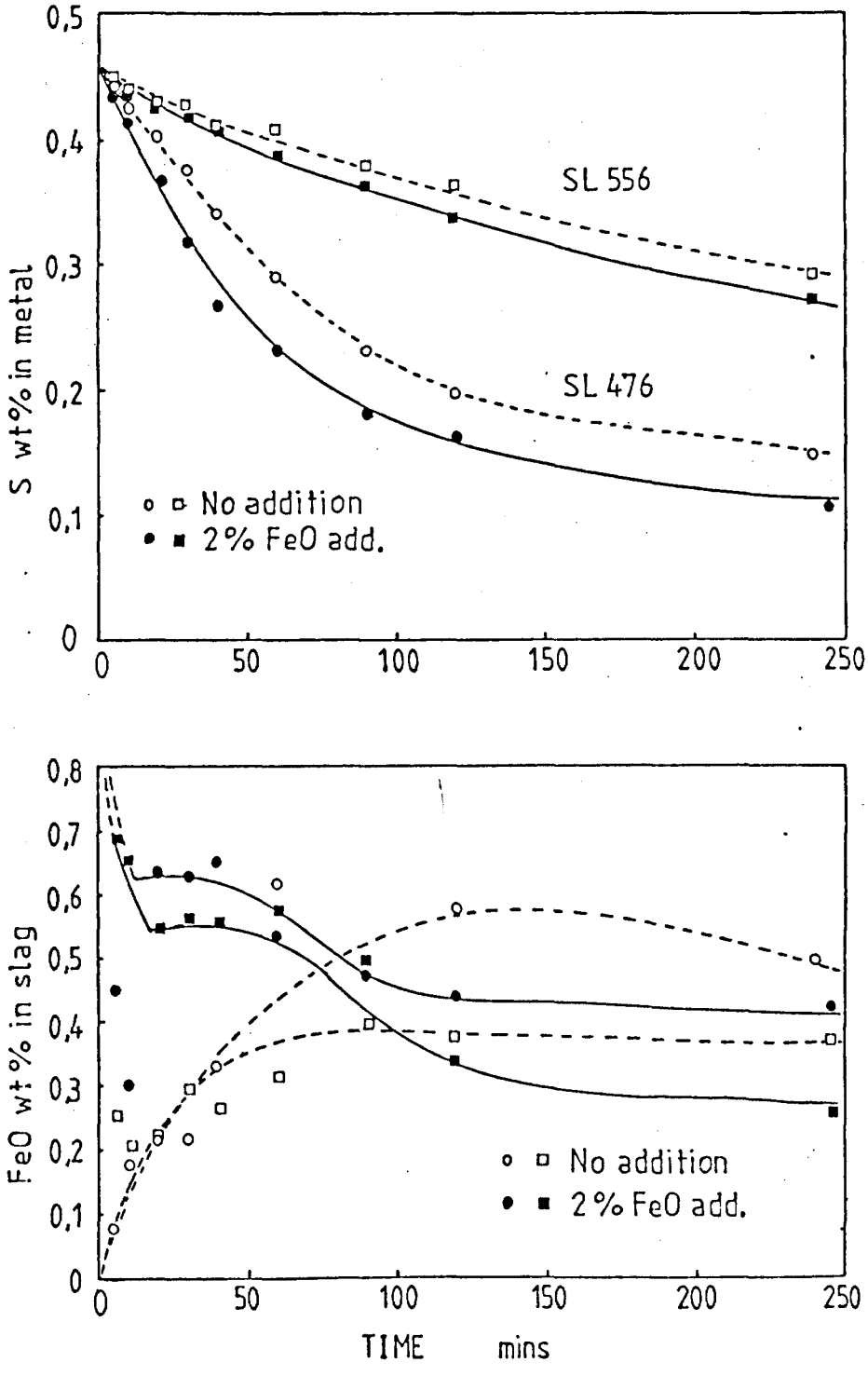

FIG. 3.33. SULPHUR AND IRON TRANSFERS FOR THE EXPERIMENTS WITH AND WITHOUT FeO ADDITIONS.

EXPS. 8, 9, 17, AND 14 (TABLES 17, 2, 3)

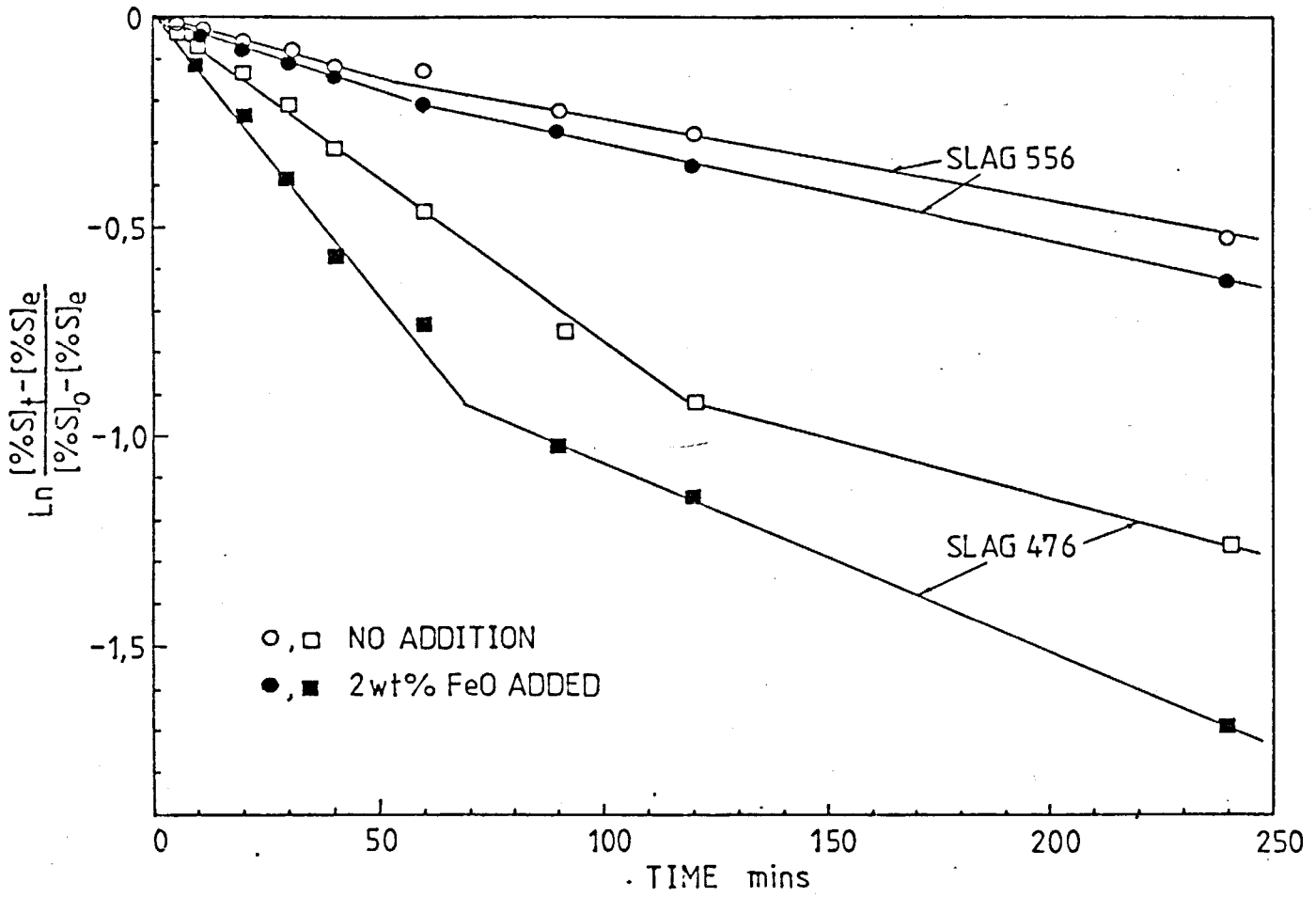

FIG. 3.34. Ln ($[\%S]_t - [\%S]_e$ / $[\%S]_o - [\%S]_e$) vs TIME PLOTS FOR THE SAME EXPERIMENTS AS FIG. 3.32.

in Figs.3.29 and 3.30). This is more clearly seen in Fig.3.34. This effect can be explained by reference to the iron transfer curves in Fig.3.33 ; the 2 % FeO initially added to the slag had been reduced to less than 0.7 % before the first sample was taken at 5 minutes of reaction time, then persisting at an almost constant level during the fast desulphurization period (50 - 60 minutes) and decreases to a lower level than for the experiments without FeO addition during the later slow stage of desulphurization. Thus for the later stage the effect of an initial FeO addition completely disappears. Even though the observed results are not considered to show exactly the effect of 2 % FeO addition due to the fast reduction to a low level at the beginning of the reaction, the strong effect of FeO on sulphide capacity could account for the increase in desulphurization rate during the initial period. It is interesting to note that the iron content in the slag changes in the exactly same way as the MnO in the above experiments ; after being reduced rapidly a relatively high level of iron in the slag remains constant for the duration of fast desulphurization period, then starts falling down to a low level. The higher persisting level of iron compared with the maximum level for the experiment without FeO addition is considered to result from the faster sulphur transfer due to the increased sulphide capacity by FeO addition. The lower level of iron in the slag for the experiment with FeO addition than without FeO during the later stage of reaction is considered to result from more rapid reduction for the longer period of reaction because the higher level of iron oxide content in the slag exerts a bigger driving force for reduction and the ceiling level of iron oxide which seems to be related

to a value of (% S) / [% S] ratio is achieved earlier with FeO addition.

It is also interesting to compare the silicon content of the final metal after the experiment shown in table G ; in spite of the fact that the oxidation state of the reaction system with FeO addition must retard silica reduction the silicon content of the final metal for the experiment with FeO addition is higher than that for the experiment without any FeO addition.

TABLE G

Exp.No.	Slag	Initial [% S]	Oxide addition	Final [% Si]	Reaction time Min.
6	SL 476	0.252	0	0.13	240
7	SL 476	0.252	2 % FeO	0.17	240
9	SL 476	0.456	0	0.09	240
8	SL 476	0.456	2 % FeO	0.14	240
14	SL 556	0.456	0	0.26	240
17	SL 556	0.456	2 % FeO	0.44	360
1	SL 456	0.242	0	0.24	270
43	SL 456	0.251	2 % MnO	0.07	240
39	SL 456	0.251	4 % MnO	0.07	240
40	SL 456	0.251	8 % MnO	0.08	240

This apparent anomaly can be explained by the fact that because reduction of iron oxide for the experiment with FeO addition starts earlier, silica reduction from the slag can take place from the start

of decrease in oxygen potential for a longer period, thus resulting in a higher silicon content of the final metal. This explanation is more clearly supported by the very small silicon content of the final metal for the experiment with MnO addition ; the very small amount of silicon reduced from the slag indicates that during the whole period of reaction under high oxygen potential due to the relatively high level of MnO in the slag silica reduction is suppressed.

Thus it can be deduced that when the oxygen potential is lowered sufficiently silica reduction takes place effectively and affects the desulphurization. In Fig.3.34 for the experiments with SI476 slag the break points from the fast stage to the slow stage of desulphurization appear at the almost the same time as the iron oxide level commences to fall. The overall indication is that the slow second stage of desulphurization is controlled by silica reduction from the slag similar to the observation with silicon transfer in Fig.3.27 and 3.26.

It can be concluded that the additions of MnO and FeO enhance the desulphurization rate during the initial fast period of sulphur transfer due to the effect of the oxides on the sulphide capacity of the slags in spite of the unfavourable oxidizing effect on desulphurization. However during the later slow stage the rate is controlled by the oxygen potential of the reaction system due to the high level of MnO in the slag for the experiment with MnO addition and by silica reduction for the experiment with FeO addition.

It is difficult to establish the effect of oxidizing with MnO and FeO additions against the expected effect of CO bubbling associated with the reduction of the oxides in favouring desulphurization

by elimination of the nucleation problem of CO gas because of the strong effect of the both oxides on sulphide capacity of slag. For this observation it is considered to be preferable to use an oxide which is easily reducible but does not affect the sulphide capacity.

It is interesting to consider the reaction equilibria for sulphur and manganese transfers with the present data as some experiments were carried out for more than four days. According to Turkdogan(53) the sulphur-manganese reaction may be represented by

$$CaO(S) + \underline{Mn}(1\ \%) + \underline{S}\ (1\ \%) = CaS(S) + MnO(S) \qquad (3.47)$$

This reaction can be considered to be a combination of the following two reactions :

$$MnO(S) + C\ (gr) = \underline{Mn}\ (1\ \%) + CO\ (g) \qquad (3.48)$$

$$CaO(S) + \underline{S}\ (1\ \%) + C\ (gr) = CaS(S) + CO\ (g) \qquad (3.49)$$

The activities of reactants are relative to the standard states indicated by symbols in parentheses (S - solid, gr - graphite, g - gas at 1 atm, and 1 % - weight percent in metal).

The equilibrium constant for the reduction of MnO, Eq. 3.48, is

$$K_{Mn} = \frac{[\%\ Mn]\ .\gamma'_{Mn}}{a_{MnO}}\ .\ \frac{P_{CO}}{a_C} \qquad (3.50)$$

An estimated value of $\gamma'_{Mn} = 0.8$ may be used for graphite-saturated melts. The total number of moles of the constituent oxides per 100g of the slag SL 456 is about 1.7. Therefore, the activity of MnO, a_{MnO}, may be represented in terms of the weight percent of MnO and its activity coefficient, γ_{MnO} :

$$a_{MnO} = \frac{(\%\ MnO)}{71\ X\ 1.7}\ .\gamma_{MnO} \qquad (3.51)$$

For unit activity of carbon, Eqs. 3.50 and 3.51 give

$$K_{Mn} = 96.6 \frac{[\% \text{ Mn}]}{(\% \text{ MnO})} \cdot \frac{P_{CO}}{\gamma_{MnO}} \qquad (3.52)$$

The temperature dependence of the equilibrium constant, K_{Mn}, is

$$\text{Log } K_{Mn} = -\frac{15{,}090}{T} + 10{,}970 \qquad (3.53)$$

The equilibrium constant for the sulphur reaction, Eq. 3.49, is

$$K_S = \frac{a_{CaS}}{a_{CaO} \cdot [\% \text{ S}] \cdot \gamma'_S} \cdot \frac{P_{CO}}{a_C} \qquad (3.54)$$

As in the previous formulation the activities of CaS and CaO relative to pure solids may be presented in terms of the weight percentages of CaS and CaO and their activity coefficients, so that

$$\frac{a_{CaS}}{a_{CaO}} = \frac{56}{32} \cdot \frac{(\% \text{ S})}{(\% \text{ CaO})} \cdot \frac{\gamma_{CaS}}{\gamma_{CaO}} \qquad (3.55)$$

In graphite-saturated iron the activity coefficient of sulphur, γ'_S, is 7 ; inserting this and Eq. 3.55 in Eq.3.54 gives

$$K_S = 0.25 \frac{(\% \text{ S})}{[\% \text{ S}]} \cdot \frac{\gamma_{CaS} \cdot P_{CO}}{\gamma_{CaO} (\% \text{ CaO})} \qquad (3.56)$$

The temperature dependence of the equilibrium constant, K_s, is

$$\text{Log } K_S = -\frac{6010}{T} + 5.935 \qquad (3.57)$$

Thus, from Eqs. 3.52 and 3.56 the equilibrium constant for sulphur and manganese transfer reaction, Eq. 3.47 is represented by

$$K_{MS} = \frac{K_S}{K_{Mn}} = 25.9 \times 10^{-4} \cdot \frac{(\% \text{ S})}{[\% \text{ S}]} \cdot \frac{\gamma_{CaS}}{\gamma_{CaO}} \cdot \frac{\gamma_{MnO}}{(\% \text{ CaO})} \cdot \frac{(\% \text{ MnO})}{[\% \text{ Mn}]} \qquad (3.58)$$

Thus,

$$\frac{(\%\ S)}{[\%\ S]} = 386 \left(\frac{K_S}{K_M} \cdot \frac{\gamma_{CaO}}{\gamma_{CaS}} \cdot \frac{(\%\ CaO)}{\gamma_{MnO}} \right) \frac{[\%\ Mn]}{(\%\ MnO)} \qquad (3.59)$$

The value of γ_{MnO} for SL 456 slag, $\gamma_{MnO} = 0.72$, is evaluated from a curve in the paper of Turkdogan(53), plotted as CaO / SiO_2 ratio vs γ_{MnO} taken from data of Abraham et al.(56) for the activity coefficient of MnO in $CaO - Al_2O_3 - SiO_2 - MnO$ slags at 1500 and 1600° C. The activity coefficient ratio, $\gamma_{CaO} / \gamma_{CaS} = 13.3 \times 10^{-4}$ is derived for the slag SL 456 from the gas - slag equilibrium measurements of Sharma and Richardson(57). Inserting these values in Eq. 3.59 and combining Eqs. 3.59, 3.53, and 3.57 gives

$$\text{Log} \frac{(\%\ S)}{[\%\ S]} = \frac{9080}{T} - 5.182 + \text{Log}\ (\%\ CaO) + \text{Log} \frac{[\%\ Mn]}{(\%\ MnO)} \qquad (3.60)$$

In Fig. 3.35 this equilibrium relationship of the sulphur - manganese transfer reaction for the SL 456 slag at 1460° C is compared with data for the present experiments with MnO additions and for an experiment with manganese addition to metal. As seen in Fig. 3.35 the sulphur-manganese reaction in the experiments with MnO additions is close to equilibrium after the fast initial reaction period. The similar trend was reported(53) for practical blast furnace data.

In order to compare the effect of Mn addition to metal on the sulphur-manganese transfer rate with that of MnO additions to slag Exp. 42 was carried out by using a metal, prepared directly in the reaction crucible with addition of 4 % manganese and covered with

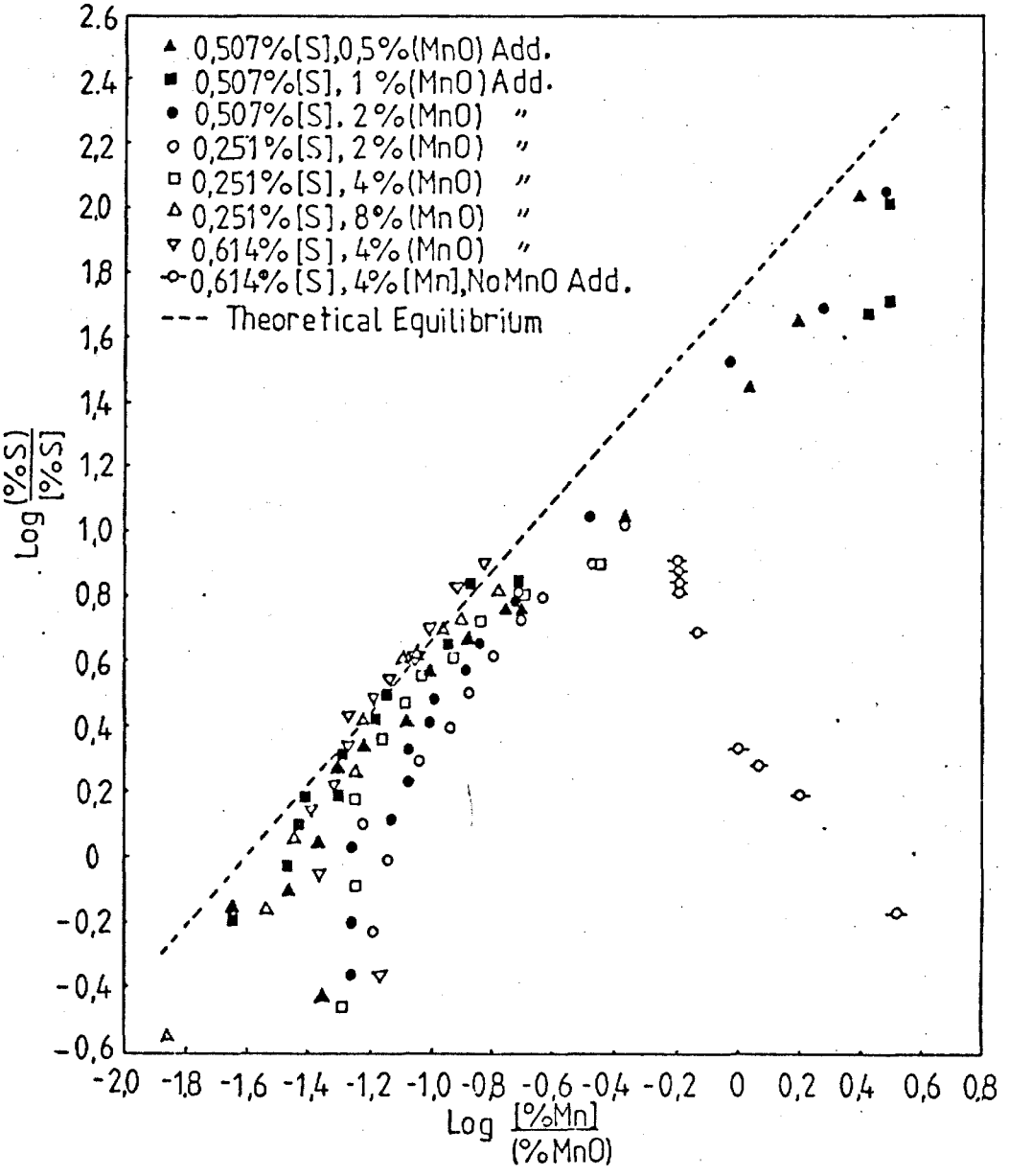

FIG. 3.35. SULPHUR AND MANGANESE DISTRIBUTION RATIOS FOR EXPERIMENTS WITH MnO ADDITIONS AND FOR AN EXPERIMENT WITH Mn ADDITION, COMPARED WITH EQUILIBRIUM RELATIONS FOR 1460 °C.

EXPS. 39 - 43 AND 47 - 49. (TABLES 13, 14, 15)

30g of SL 456 slag without MnO addition. The result is shown in Fig. 3.36, plotted as change in sulphur content of metal with time. As previously mentioned, Mn addition to metal increases the desulphurization rate even though Mn decreases the activity coefficient of sulphur in metal. But it is interesting to compare the effect of Mn addition to metal with that of MnO addition to slag ; during the fast initial period the desulphurization rates for both experiments are not much different. This is more clearly seen in Fig. 3.37, plotted as Ln ($[\% S]_t - [\% S]_e$ / $[\% S]_o - [\% S]_e$) vs time ; $[\% S]_e$ for the experiment with Mn addition was calculated, taking into account the effect of Mn in decreasing the activity coefficient of sulphur in the metal. The sulphur-manganese transfer for the experiment with 4 % Mn addition is seen in the right side of Fig. 3.35 ; the ratio of [% Mn] / (% MnO) decreases rapidly as sulphur transfers from metal to slag and remains almost constant value until the end of 4 hours of the experiment while the ratio of (% S) / [% S] is approaching equilibrium. Even though the experiment was continued only up to 4 hours, it is to be expected that at a later stage the ratio of [% Mn] / (% MnO) will be increased by reduction of MnO following the equilibrium as the sulphur distribution ratio, (% S) / [% S] approaches its equilibrium.

It is interesting to note from Fig. 3.35 that after the fast initial period of reaction the sulphur-manganese reaction reaches partial equilibrium and the (% S) / [% S] and [% Mn] / (% MnO) ratios are increasing slowly at apparent equilibrium during the long period of reaction time (106 - 119 hours). In order to consider silicon reaction together with the above reaction if the silicon content of

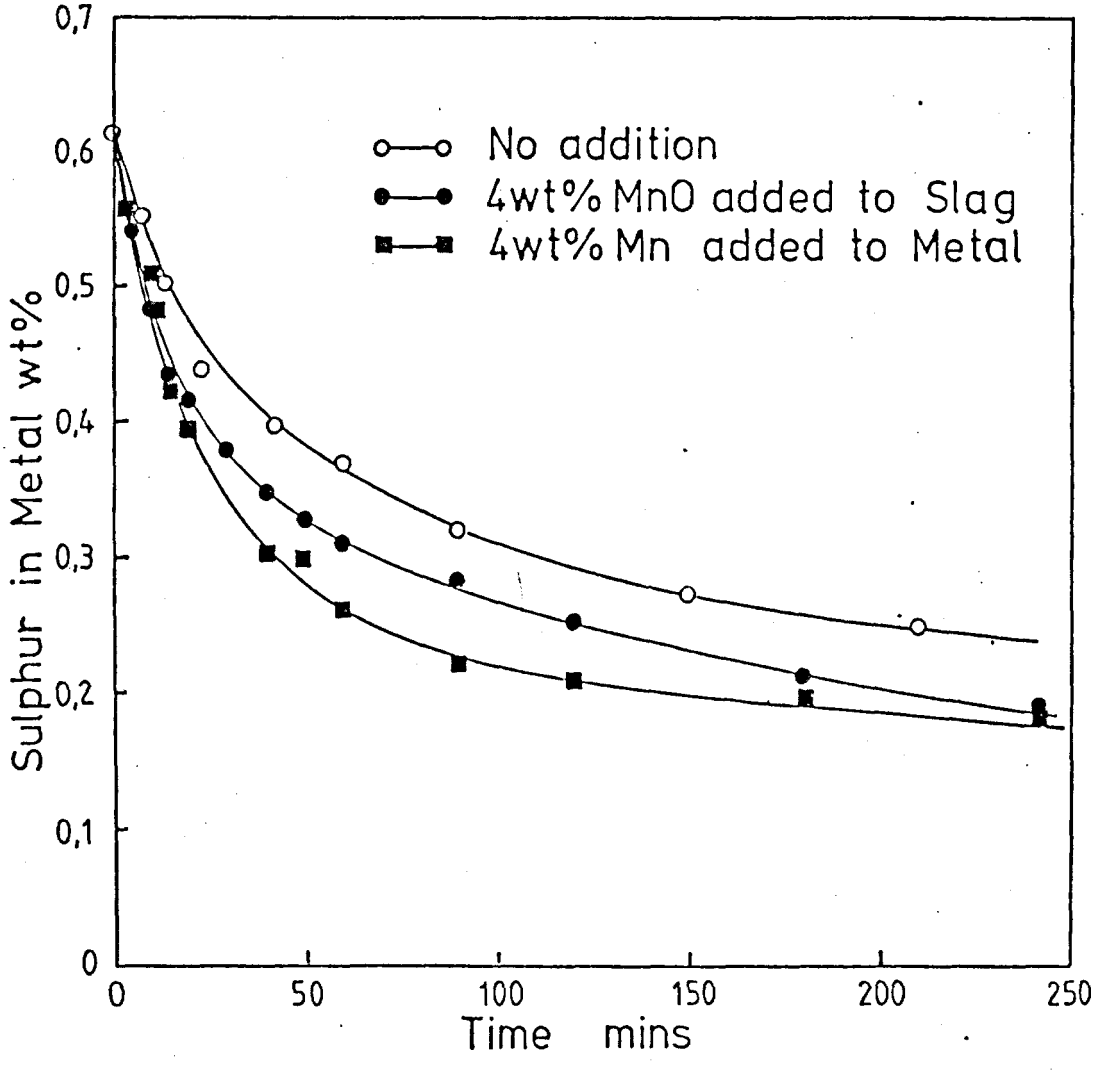

FIG. 3. 36. THE EFFECTS OF Mn AND MnO ADDITION ON DESULPHURIZATION RATE.

EXPS. 4, 41, AND 42 (TABLES 1, 14)

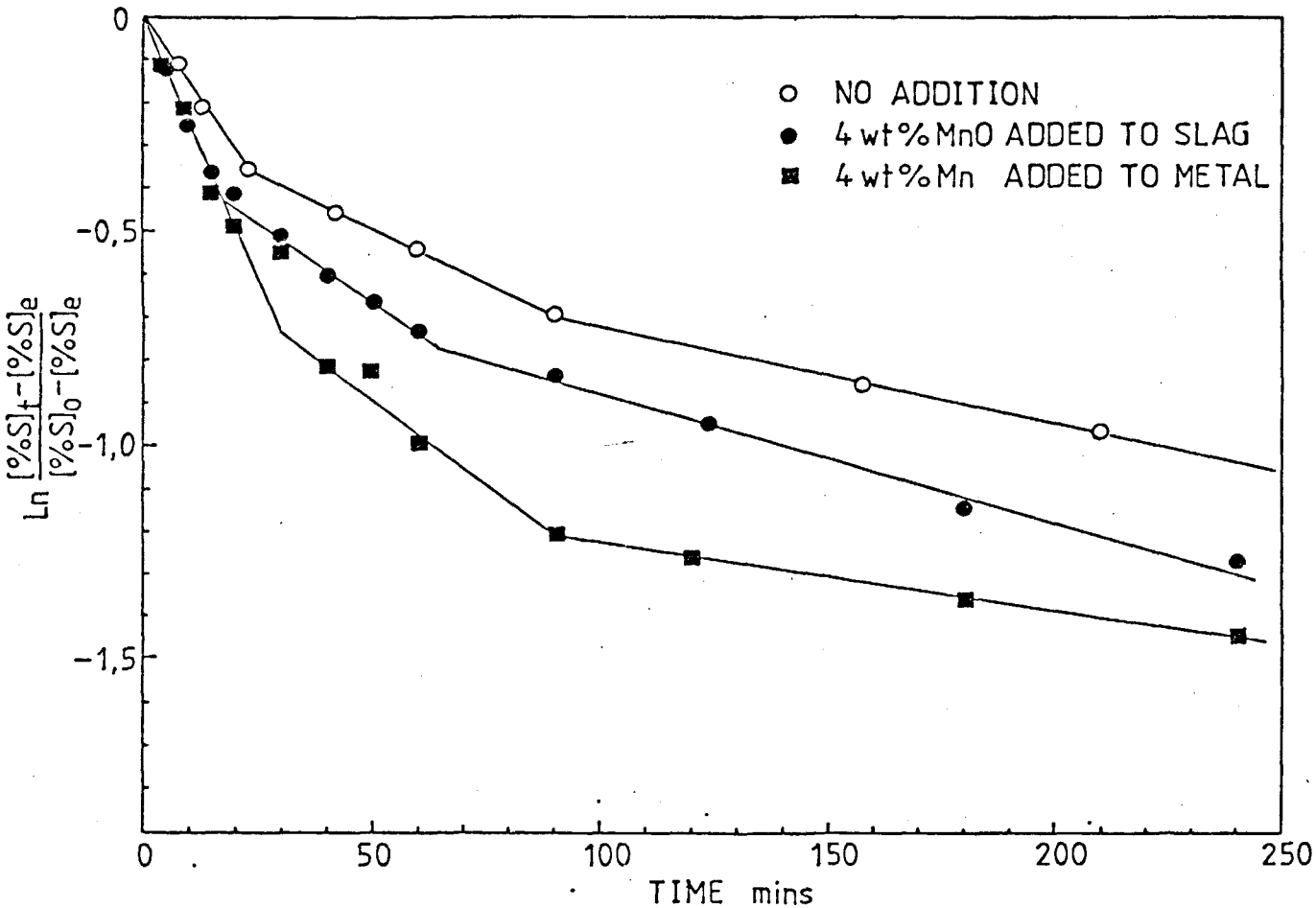

FIG. 3.37. Ln ($[\%\ S]_t - [\%\ S]_e$ / $[\%\ S]_o - [\%\ S]_e$) vs TIME PLOTS FOR THE SAME EXPERIMENTS AS FIG. 3.36.

the metal is examined according to reaction time, the silicon content after 4 hours reaction is about 0.07 % as mentioned above whilst after the long period of about 4 days the silicon content was increased up to 0.9 % (see table 13 and 15). This indicates that there was virtually no silica reduction during the fast sulphur-manganese reaction to reach partial equilibrium and after this period silica reduction proceeds slowly for the long period to build up to the high level as silica reduction is a very slow reaction. However the sulphur-manganese reaction is much faster than silica reduction. Thus the (% S) / [% S] and [% Mn] / (% MnO) ratios keep changing for the long period at the equilibrium predicted for the sulphur manganese reaction, the variation being controlled by the slow silica reduction. It is to be expected that when the silica reduction reaches equilibrium the sulphur-manganese partition ratios will be fixed eventually at the final thermodynamic equilibrium value for the sulphur-manganese-silicon reaction.

3.8. EFFECT OF AMBIENT PRESSURE

Because the desulphurization reaction involves CO evolution as a concurrent reaction, the reaction rate may be expected to be influenced by a change in the ambient pressure ; if CO evolution is the rate controlling step for the desulphurization, the rate is expected to increase with a decrease in the ambient pressure. However, no previous work on the effect of ambient pressure on the desulphurization rate has been reported.

The present experiments were carried out by using ambient pressures of 1, 1/2, and 1/4 atm. of carbon monoxide. Constant pressures were maintained using a cartesian manostat to vent the evolved gas.

The desulphurization reaction could not be followed by sampling during the reaction because of the requirement to keep the pressure constant, thus in individual experiments the reaction was stopped after a predetermined time and the slag and metal analysed. 35 g of metal and 10 g of SL 456 slag were used with a 1.91 cm in dia. crucible.

The experimental conditions and results are listed in table H.

TABLE H

Exp.No.	Metal composition		Ambient pressure	Rate coeff., K_M,	Results
	wt.% S	wt.% Si	P_{CO} ; atm.	g cm^{-2} $min.^{-1}$	
32A	0.229	0	1	0.0025	table 9
32B	0.229	0	1/2	0.0032	table 9
32C	0.229	0	1/4	0.0040	table 9
33	0.106	0.125	1	0.0071	table 10
35	0.106	0.125	1/2	0.0102	table 10
36	0.106	0.125	1/4	0.0114	table 10
34	0.242	0.42	1	0.0077	table 11
37	0.242	0.42	1/2	0.0112	table 11
38	0.242	0.42	1/4	0.0139	table 11
24	0.202	1.89	1	0.0078	table 12
28	0.202	1.89	1/2	0.0162	table 12
29	0.202	1.89	1/4	0.0198	table 12

The effect of ambient pressure on the rate of desulphurization and silica reduction is shown in Fig. 3.38, plotted as the change in sulphur and silicon contents of metal with time for Exps. 32A, B,

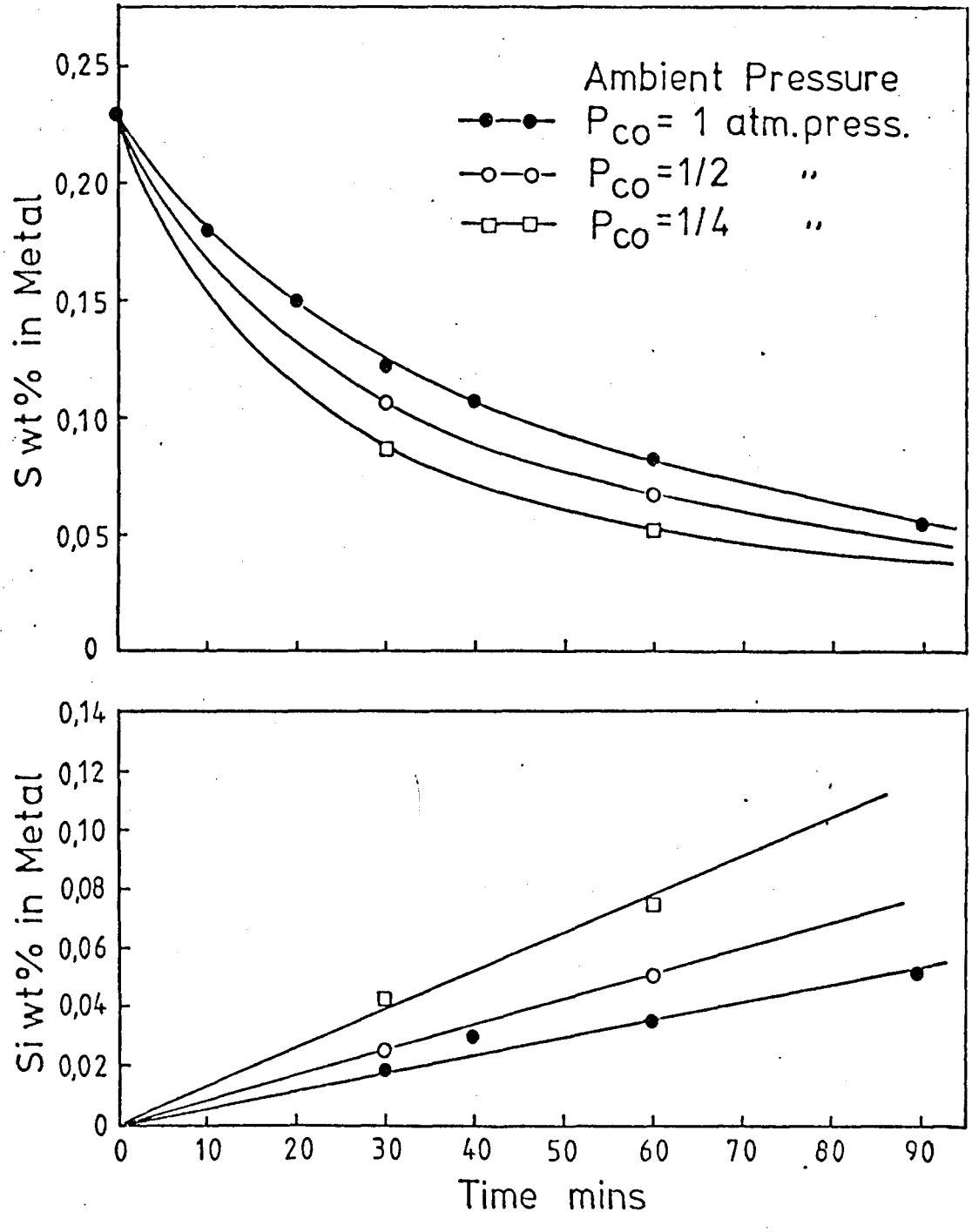

FIG. 3.38. EFFECT OF AMBIENT PRESSURE ON RATES OF SULPHUR TRANSFER FROM METAL TO SLAG AND SILICON TRANSFER FROM SLAG TO METAL FOR EXPERIMENTS USING SILICON Si FREE METAL.
INITIAL METAL : 0.229 % S, No Si ADDED,
SLAG : 45 % SiO_2, 6 % MgO, 49 % CaO,
CRUCIBLE SIZE : 1.91 cm dia. METAL 35 g, SLAG 10 g.
EXPS. 32A, 32B, 32C. (TABLE 9)

and C using silicon free metal. It is clear from the rate curves that both rates of desulphurization and silica reduction are increased by reducing the ambient pressure, but later for the slow stage of desulphurization the effect of ambient pressure on the desulphurization rate seems to become insignificant whilst the rate of silica reduction is almost linearly increased with time with a higher rate under a lower pressure.

This is more clearly seen in Fig. 3.39, the rate curves of desulphurization and silica reduction for the experiments using a metal containing 0.125 % Si initially, and Fig. 3.40, plotted as Ln $([\% S]_t - [\% S]_e / [\% S]_o - [\% S]_e)$ against time for experiments using different sulphur and silicon contents of metal ; during the initial period of about twenty minutes, the desulphurization rate increases with a decrease of ambient pressure even though the silica reduction rate increases at the same time, but after this period decreasing the ambient pressure causes the desulphurization rate to slow down whilst the silica reduction rate continues to be enhanced by decrease in the ambient pressure. This indicates that during the fast initial period decrease in the pressure eases the difficulty in CO evolution for both desulphurization and silica reduction, enhancing both rates of the reactions and the effect of decreasing the pressure in enhancing the CO evolution for desulphurization surpasses the harmful effect of increased silica reduction on the desulphurization rate. Thus, it can be concluded that during the fast initial period the desulphurization rate is controlled by CO evolution reaction rather than the concurrent silica reduction.

However, during the slow second stage the desulphurization

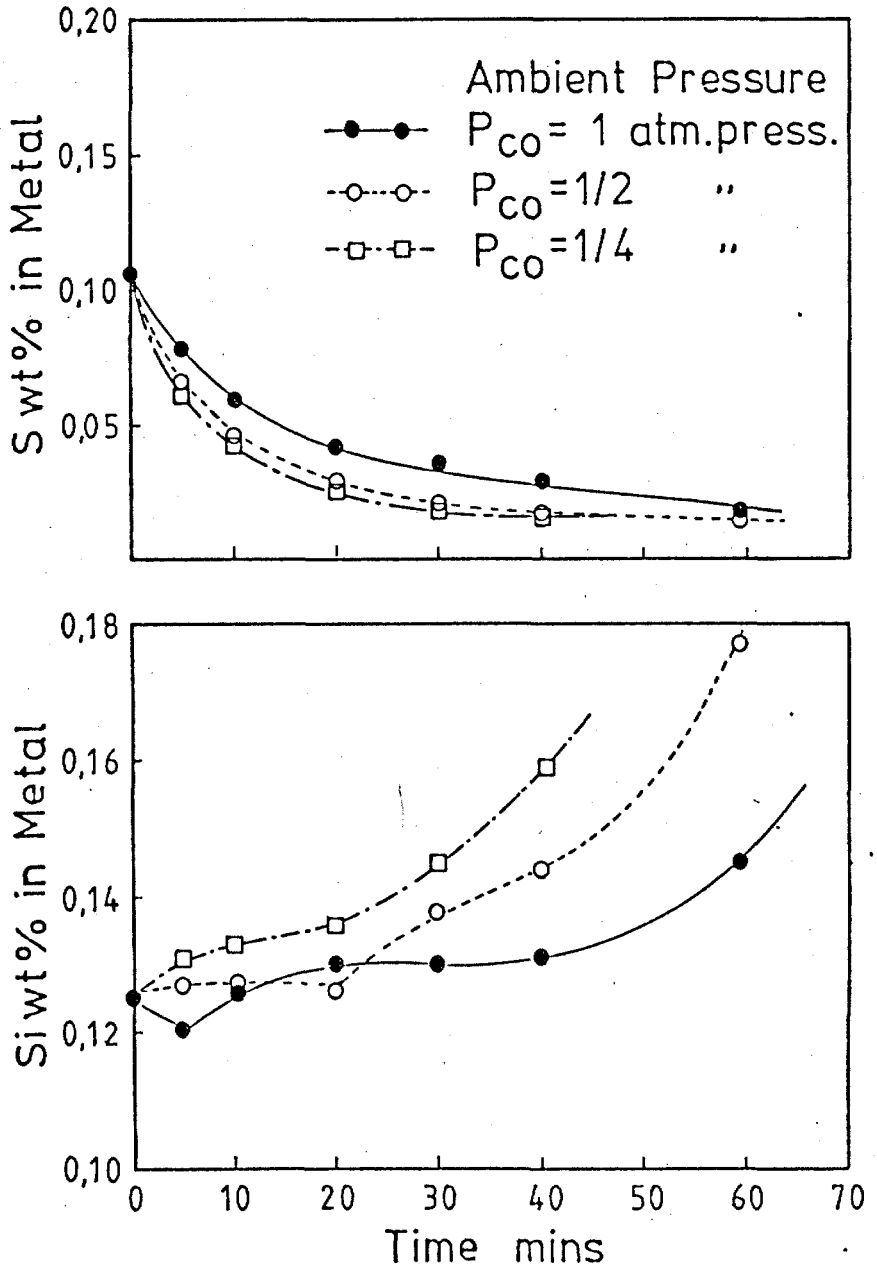

FIG. 3.39. EFFECT OF AMBIENT PRESSURE ON RATES OF SULPHUR TRANSFER FROM METAL TO SLAG AND SILICON TRANSFER FROM SLAG TO METAL FOR EXPERIMENTS USING METAL CONTAINING SILICON.
INITIAL METAL : 0.106 % S, 0.125 % Si,
SLAG : 45 % SiO_2, 6 % MgO, 49 % CaO,
CRUCIBLE SIZE : 1.91 cm dia. METAL 35 g, SLAG 10 g,
EXPS. 33, 35, 36. (TABLE 10)

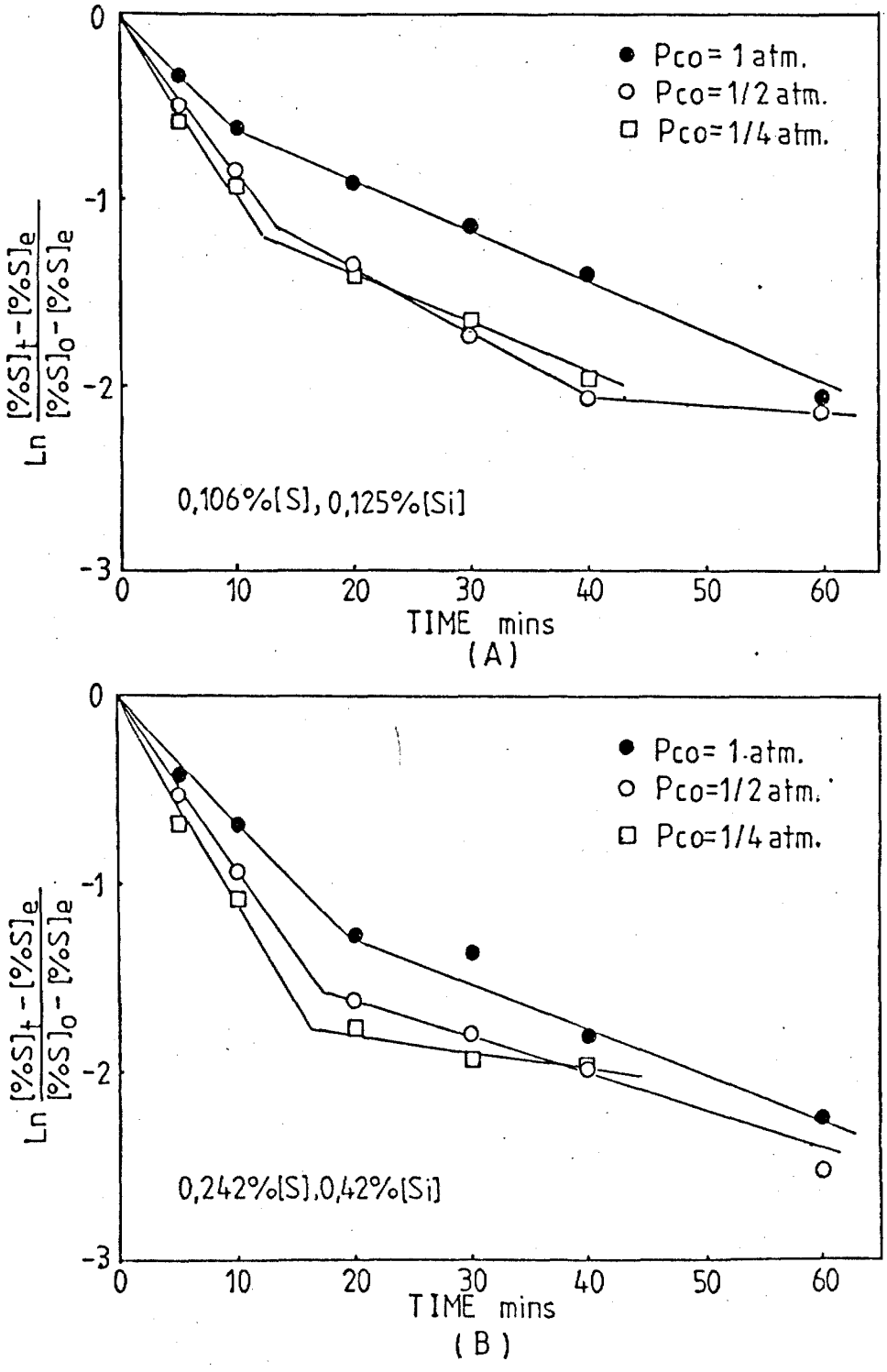

FIG. 3.40. Ln ($[\%S]_t - [\%S]_e$ / $[\%S]_o - [\%S]_e$) vs TIME PLOTS FOR EXPERIMENTS USING DIFFERENT S AND Si CONTENTS OF METAL.

(A). EXPS. 33, 35, 36. (TABLE 10)

(B). EXPS. 34, 37, 38. (TABLE 11)

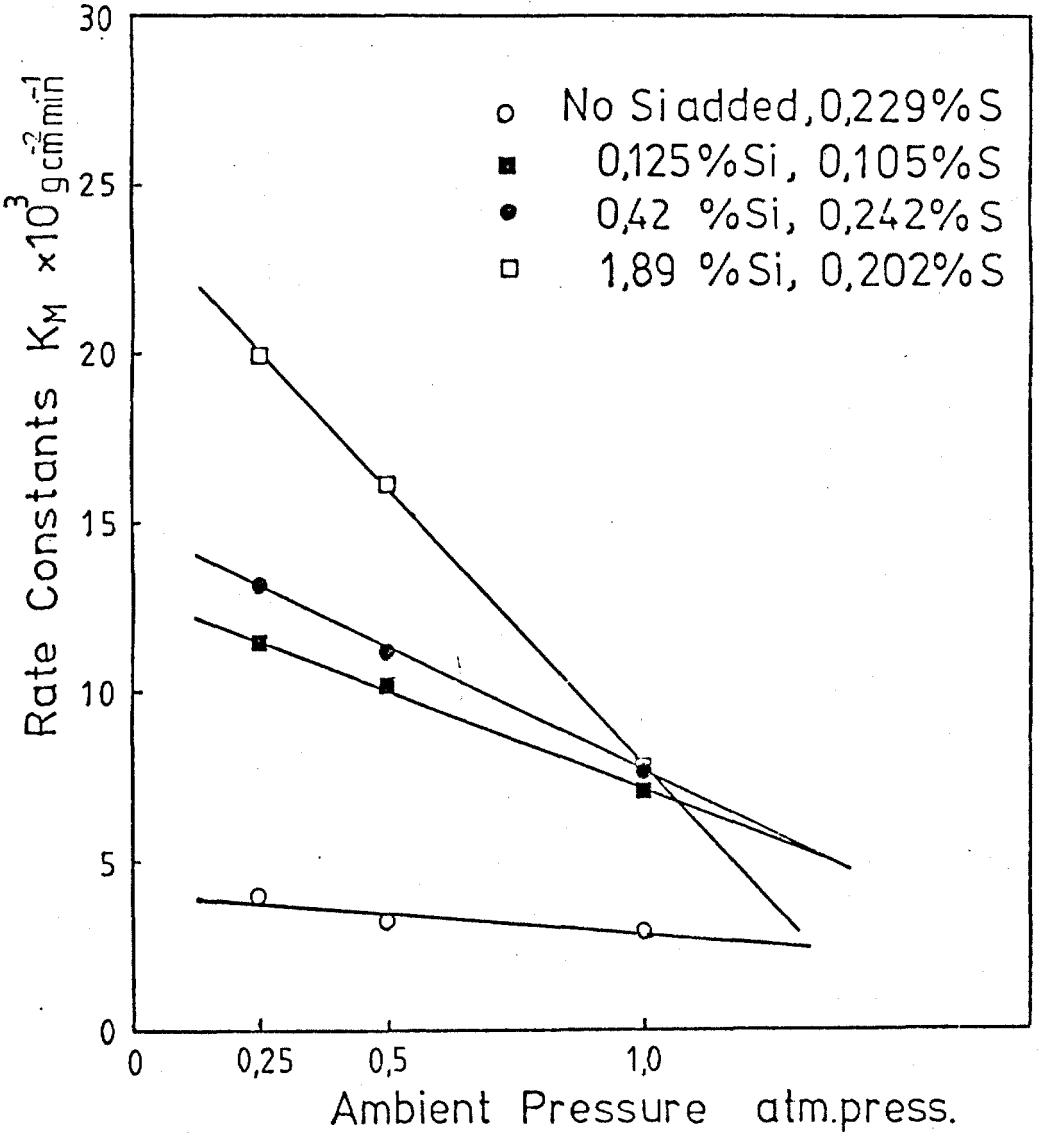

FIG. 3.41. RELATION BETWEEN MASS TRANSFER RATE COEFFICIENT OF SULPHUR FROM METAL TO SLAG, Km, AND AMBIENT PRESSURE FOR DIFFERENT METAL COMPOSITIONS.

EXPS. 24, 28, 29, 32(A,B,C), 33 - 38. (TABLES 9 - 12)

rate is slowed down by the enhanced silica reduction, indicating that the slow second stage of the desulphurization is controlled by the silica reduction.

The effects of ambient pressure for different metal compositions are summarised in Fig. 3.41, plotted as the change in the rate coefficient with ambient pressure. The rate constant seems to increase linearly with the decrease in the ambient pressure within the range of pressure under consideration. For an alloy of higher silicon content the rate is increased more by the same decrease in the ambient pressure.

3.9. GENERAL DISCUSSION

3.9.1. MASS TRANSPORT CONTROL

As mentioned in the preceding literature review, from time to time a number of investigators reported that the rate of sulphur transfer from metal to slag is controlled by either diffusion of sulphur in the metal to the slag-metal interface or at the slag side of the interface. If the reaction is diffusion controlled, it would normally be expected that the rate is influenced by the viscosity of the melts and enhanced by agitation which reduces or eliminates diffusion gradients within both the slag and the metal and increases the area of the slag-metal interface. Thus, most of the investigators who suggested mass transport control for the reaction interpreted their observations on the reaction rate in terms of the effect of viscosity of the melts on desulphurization leading to a diffusion control mechanism.

(1) DIFFUSION CONTROL OF SULPHUR IN METAL

Travin et al.(58) reported that the order of the overall reaction was temperature dependent and increased from unity at about 1400 °C to second order at 1700 °C. The effect of temperature on the order of the reaction was expressed as $- d[\%\,S] / dt = K\,[\%\,S]^{(1+B)}$ where K was the rate constant and B was a 'turbulance factor' which increased from zero to unity as the temperature was raised. It was regarded as a correction to the increase in the reaction rate to allow for the decrease in the viscosity of the slag and the increased turbulence of the metal caused by CO evolution as the temperature increased. They also reported that a thick concentration gradient of sulphur in the metal side of the slag-metal interface was observed in their experiment with radioactive S^{35} (9). With the above observations they suggested that the rate of sulphur transfer is controlled by diffusion of sulphur in the metal.

Fulton and Chipman(16) reported that the rate of sulphur transfer could be explained well in terms of the diffusion of sulphur in the metal side of the interface on the basis of the boundary layer diffusion theory by showing a reasonable thickness of effective diffusion layer.

However, the present experiments with different slag compositions show strong evidence for the fact that the rate constant of sulphur transfer is entirely dependent on the sulphide capacity of slag, not on the sulphur content of metal under a given temperature and pressure. This is confirmed by a number of previous investigations (3)(4)(7)(12)(14).

Furthermore, the observed change in the desulphurization rate

due to the variation of the slag composition does not follow the diffusion rate equation derived on the basis of the boundary layer diffusion theory. In fact the effective boundary layer thickness calculated from the present rate data with the diffusion equation does show a value of reasonable order of magnitude, but this kind of information can not be considered to constitute proof of diffusion control in view of the above apparent contradictory observations.

Sulphide capacity of the slag increases with temperature. Thus the effect of the temperature in increasing the rate can be explained by the increased sulphide capacity of slag. Thus it can be concluded that the sulphur transfer reaction is not controlled by diffusion of sulphur in the metal.

(2) DIFFUSION CONTROL OF SULPHUR IN SLAG

In most processes, the slag has a higher viscosity than the metal at the working temperature, thus it can be considered to be the properties of the slag which are more important in the diffusion problem of sulphur. Recently Hatano(8) also reported a change in the order of the sulphur transfer reaction according to the viscosity of slag; the order is almost unity for a viscous basic slag whilst for slags with low viscosity, to which are added about 4 - 10 % Na_2O or CaF_2, the order increases to 1.26 - 1.37. He examined the concentration profile of sulphur in the vicinity of the interface by using the same radioisotope S^{35} as Travin. However, he found the presence of a thick boundary layer for diffusion in the slag phase and the effect of CO bubbles accompanying desulphurization on the state of the interface by examining sections of the quenched system

during the reaction. He considered that the stirring effect of CO bubbling might decrease the diffusion boundary layer and the extent of such a stirring effect depends on the viscosity of slag. Thus, he suggested that desulphurization is controlled by diffusion of sulphur in the slag.

It is generally accepted that when a sulphur atom enters the slag it becomes a negatively charged ion and to preserve electroneutrality either an oxygen ion must be transferred simultaneously in the reverse direction or a metal atom such as Fe accompanies the sulphur atom across the interface and donates electrons to the sulphur. In the discussion on the paper of King et al. Darken(59) made a suggestion that one should look to the diffusion layer in the slag at the slag-metal interface as a limiting condition because of the very low iron content of the slags in the experiment of King et al., thus implying that the slow step for desulphurization reaction could be the diffusion of oxygen ions across the boundary layer in the slag side of the interface. However King et al.(7)(32) demonstrated that the diffusion of oxygen ions could not account for the observed rate of CO evolution associated with sulphur transfer in the experiment with a simple lime-alumina binary slag on the basis of the boundary layer diffusion theory. The ionic size of sulphur is larger than that of oxygen and it is more probable that the diffusion of sulphur ions in the slag away from the interface may be rate controlling. However, the present experiments with different melt geometry show that the rate is increased as the slag depth increases and the diameter of crucible decreases keeping melt depth constant. The effect of slag depth was confirmed by Fulton and Chipman(16).

However, changes in melt geometry, specifically melt depth, should not affect either the diffusivity of sulphur or the effective boundary layer thickness for sulphur diffusion. Thus, the observed effect of melt geometry in the present experiment can not be explained by a diffusion controlled process.

In fact the fluidity and sulphide capacity of slags both increase due to the addition of metal oxide up to a certain limit. Richardson(60) explained the change in viscosity of binary silicate from the point of view of silica structure. The fundamental building unit in silica and all silicates is the silicate tetrahedron consisting of four nearly close-packed oxygen atoms or ions, surrounding a small silicon atom. In molten silica these tetrahedra sharing each corner of oxygen are tightly linked in all directions, thus the melt has a very high viscosity. But when a metal oxide such as lime or magnesia is added to molten silica the oxygen atoms from the added oxide join into the silicate tetrahedra so that a shared corner is freed at every point where an oxygen is added as it can be represented by $\vdots Si - O - Si \vdots + CaO = \vdots Si - O' + O' - Si \vdots + Ca^{2+}$. Each oxygen atom at such breaks carries a negative charge, and the cations Ca^{2+} or Mg^{2+} are localized near the break, being accomodated in holes in the network. As such oxides are added in increasing concentrations, the silica network is increasingly broken down, and the viscosity falls correspondingly. Finally the stage is reached at which no corners are shared. Further additions of oxide results in a melt containing SiO_4^{4-} groups and free oxygen ions (O^{2-}) together with the equivalent numbers of cations. It must not be supposed, however, that there are no oxygen ions in slags with more

silica than corresponds to the stoichiometric composition $2MO \cdot SiO_2$, e.g. Ca_2SiO_4. At any instant there will be a proportion depending on the thermal dissociation of the silicate groups, as might be represented by $2 (\vdots Si - O') = \vdots Si - O - Si \vdots + O^{2-}$, and one free oxygen ion can be produced. Thus, even in highly silicious melts the occasional oxygen ion can exist which is unattached to either one or two silicon atoms.

Thus as the metal oxide is added to the silicate and the temperature increases, apart from the change in viscosity of slag, the sulphide capacity is also considerably increased due to the increase of activity of free oxygen ions.

In view of the above consideration of the effect of metal oxide addition to silicate slag on the viscosity and sulphide capacity, the observed increase in the sulphur transfer rate with more fluid basic slag can not be explained solely by the decrease of viscosity in terms of a diffusion process, but by the increase of sulphide capacity and possibly by the reduced problem for CO gas evolution due to the decreased viscosity. In fact the ease of CO evolution in a less viscous slag was well demonstrated by Hatano's experiment(8), examining CO bubbles in sections of the quenched system during the reaction.

The effect of agitation in increasing the desulphurization rate is frequently quoted as a practical evidence for diffusion control of the reaction; for example, sulphur transfer is rapid in the steel making process where the bath is stirred either by oxygen injection or by the carbon boil and when the metal is quiet, as during the reducing slag stage of the electric arc process, the reaction rate

can be increased by induced agitation of the bath with electromagnetic stirrers. This increase in the rate is explained by the effect of enhanced diffusion of sulphur due to the increase in the slag-metal interface and the decrease or elimination of the diffusion gradient by the agitation. However, the effect of agitation in increasing the interface can also contribute to the interfacial chemical reaction.

In some experiments of laboratory scale with normal blast-furnace type metal and slag, the rate was not altered substantially by mechanical agitation(1)(5). In the experiment of Fulton and Chipman(16) the reaction rate was virtually unchanged by agitation up to 35 r.p.m., but when the agitation was increased drastically up to 500 r.p.m., the rate was increased significantly. Under this drastic agitation, droplets of metal may be entrained into the slag. Thus, the increase in the rate appears primarily to be based on the increase in the reaction interfacial area.

Apart from the above discussions, the argument on diffusion control may be further elucidated by consideration of the solubility of sulphur in the slag. According to the data on the solubility of calcium sulphide in lime-silica melts at 1500 °C, measured by Sharma and Richardson(57), the solubility of calcium sulphide in mole fractions range from 0.05 to 0.12, as the mole fractions of silica change from 0.4 to 0.52. From their data the solubility of calcium sulphide in the present SL 456 slag is assumed to be about $N_{CaS} = 0.08$, which is equivalent to 10 % CaS. Thus the solubility of sulphur in the SL 456 slag is about 4.4 % at 1500 °C.

If the desulphurization is controlled by diffusion of sulphur

in the slag, then all chemical reactions must be considered to be at equilibrium. The equilibrium partition ratio at the slag-metal interface for the SL 456 slag is Ls = (% S) / [% S] = 78 at 1460° C. Then, the sulphur concentration in metal, [% S], at equilibrium with the maximum solubility of slag, i.e. 4.4 % (S), is not more than about 0.056 % [S]. Therefore, until the sulphur concentration in the metal is reduced from the initial sulphur content, i.e. 0.2 - 0.6 % [S], to this level of 0.056 %, the slag at the interface must be saturated with sulphur. Therefore from the Fick's first law,

$\frac{d(\%\ S)}{dt} = D \frac{dC_s}{dx}$, as the concentration C_s does not change, the flux of sulphur diffusion in the slag must be constant for a long time. However, the rate of sulphur transfer observed in the present experiments does change during this reaction time, a fact which is confirmed by all previous investigations. Therefore the proposed diffusion of sulphur in the slag can not be the rate controlling step in the desulphurization process.

In addition to this consideration, the effect of ambient pressure and silicon additions on the reaction rate observed in the present experiments can not be correlated with this diffusion control mechanism.

In view of the abundant experimental evidence; the effect of melt geometry, Si additions and ambient pressure on the rate and considerations of sulphur solubility in the slag, it can be concluded that sulphur transfer is not controlled by diffusion of sulphur in either slag or metal, but by some chemical reaction process.

3.9.2. CHEMICAL REACTION CONTROL

As discussed in the preceding section 3.5 , the sulphur

transfer reaction must be explained by electrochemical reactions. Thus, it can be considered that there are two major anodic reactions supplying electrons for cathodic reaction of sulphur ionization, i.e. CO evolution, $C + (O^{2-}) = CO + 2e$, and ionization of metal atoms such as Fe, Si, Mn, and Al. In the case of silicate slags, another important cathodic reaction of silica reduction, competing for electrons with sulphur, must be considered. These reactions are all inter-related to keep electroneutrality and their relative rates are determined by the potential current relationships.

In the very initial stage of sulphur transfer reaction because of the difficulty of the CO evolution reaction, the relatively easier anodic reaction such as the ionization of iron is expected to take place to provide electrons for sulphur, helping the delayed supply of electrons from the anodic reaction of CO evolution. In the presence of Si or Al which is more easily ionized than iron, the anodic reaction of such an atom will take place more actively, replacing the necessity of sluggish CO evolution, and more rapid desulphurization is to be expected.

The above consideration is substantiated by examination on the iron transfer rate accompanying the sulphur transfer. As seen in Fig.3.16 the sulphur transfer rate appears to be the same as the iron transfer on a molar basis for acid slags during the initial period, but such a trend is not so clear for the basic slag except at the very beginning of the reaction especially with low sulphur contents. This apparent difference between acid and basic slags can be explained by the properties of slag affecting the anodic reaction of CO evolution; as a basic slag is less viscous and has a higher activity of oxygen

ions than an acid slag, the anodic reaction of CO evolution is expected to be much easier in the basic slag. Thus, it more effectively takes part in sulphur transfer, and the dependence of sulphur transfer on the anodic reaction of iron transfer is considerably reduced after the CO evolution is initiated. In acid slags with higher viscosity and low activity of oxygen ions the problem of CO evolution to supply electrons to sulphur is greater than in basic slags, and sulphur transfer heavily depends on the anodic reaction of iron transfer, thus a strong relationship between the rate of sulphur transfer and that of iron transfer appears in the initial period. Similar observations were reported by Derge et al.(4), who proposed that the sulphur crosses the interface in chemical combination with iron. This idea was strongly opposed by King et al.(7) (32) who observed that the iron transfer was not equivalent to the sulphur transfer in the initial stages and the rate of sulphur transfer was equivalent to the total of CO evolution rate and other concurrent anodic reactions such as iron and silicon transfer on a basis of electrochemical equivalents. However, it is worth while to note that in the experiments of King et al.(7), the melts were stirred with a graphite rod and they did not use a viscous slag with high silica concentration (e.g. the most acidic slag was 44 % SiO_2, 16 % Al_2O_3, 40 % CaO). In contrast, Derge et al.(4) used a very high silica slag (e.g. 55 % SiO_2, 15 % Al_2O_3, 30 % CaO) and did not stir the melts. For the conditions of King et al's experiments the problem of CO evolution might be greatly reduced due to the stirring and low viscosity of slag, thus the strong relationship of sulphur and iron transfer in the initial stage such as in the work of Derge

et al.(4) and the present investigation may still be compatible.

It is interesting to note an observation of Kozakevitch(61), who states that in many cases of sulphur transfer, almost no carbon monoxide bubbles appear at the slag metal interface in the early stage as observed by X-ray fluoroscopy. In fact he noted that little obvious chemical reaction took place at the interface initially if the slag is not very basic and the sudden decrease in interfacial tension is related to the diffusion of $Fe^{2+} \cdot S^{2-}$ units (or couples) through the interface. This idea is similar to the original suggestion of Derge et al.(4).

Furthermore, Kozakevitch(61) observed that in the exceptional cases when the pig iron was saturated with sulphur and the relative quantities of the metal and slag were such that the transfer of sulphur made the slag rich enough in $Fe^{2+} \cdot S^{2-}$, a violent boil started after a while in the mass of the slag and on the graphite walls of the crucible rather than at the slag-metal interface, and in some cases emulsification of the metal occurred due to this violent stirring. He considered that the reactions FeS + CaO and FeO + C (SiC or CaC_2) took place in the mass of the slag and on the graphite crucible.

Thus,it may be reasonable to consider that in acid slags the anodic reaction of iron transfer plays a major role in sulphur transfer in the initial stages, but for basic slags with low viscosity and high activity of oxygen ion the anodic reaction of CO evolution and iron transfer, take part simultaneously in sulphur transfer during the initial period.

In view of the above considerations, it is interesting to compare the change in sulphur content of the slag initially in the

experiments with SL 476 slag and SL 556 slag, and different initial sulphur contents in metal. In Exps. 6 and 9 with slag 476 (see table 2 at appendix) the sulphur transfer rate is identical for the different initial sulphur contents up to the first 10 minutes of reaction. The similar trend appears in Exps. 15 and 14 (see table 3). If this is really true, then from the reaction

$$[\,Fe] + [\,S\,] = (\,Fe^{2+}) + (\,S^{2-}),$$

as the rate of sulphur transfer is independent of the sulphur content of metal, the only possible rate controlling factor of the reaction rate is iron concentration. However, as carbon saturated iron was used in the experiments, the effect of variation of iron concentration could not be observed. Furthermore diffusion of sulphur can not be the important step for the reaction rate as fully discussed above. Contrary to the above results, the rate of sulphur transfer for the SL 456 basic slag in the first five minutes appears to be proportional to the sulphur content of metal (see table 1). Thus it is not clear what is controlling this very initial reaction of iron accompanying the sulphur transfer. But it seems reasonable to invoke that a $(\,S - O\,)''$ complex is important. It is extremely difficult to examine the reaction accurately at the very early stages where the highest rate is exhibited. Apart from the above observations it is very interesting to note that when the rate of sulphur transfer in terms of the change in sulphur content in the slag is compared with the changing mode of iron transfer, the break points appear to be approximately coincident for the rate curves of sulphur and iron transfer in most of the present experiments as shown in Fig. 3.42. Instead of drawing a smooth curve as generally shown in a reaction

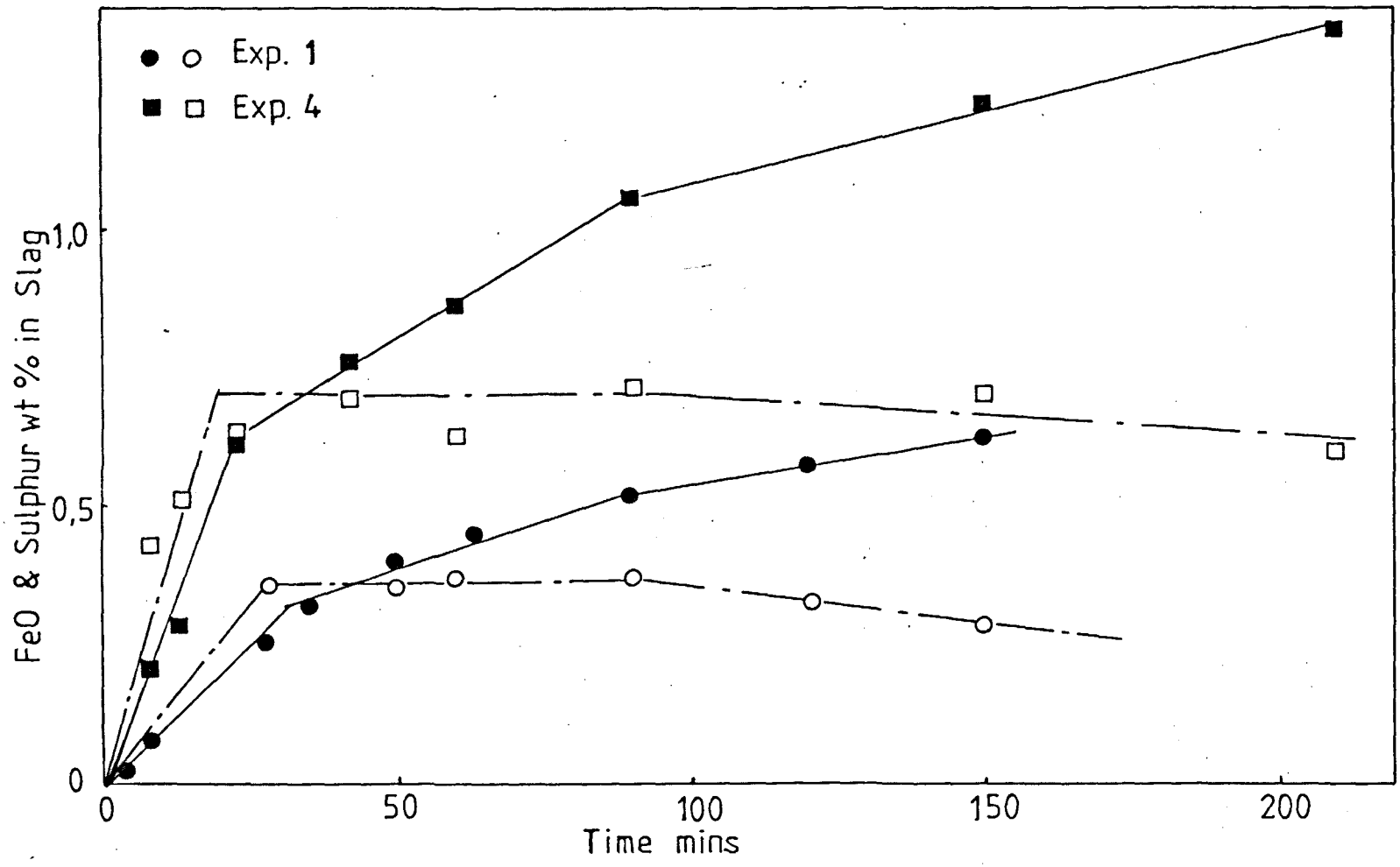

FIG. 3.44. THE RATES OF SULPHUR AND IRON TRANSFER FROM METAL TO SLAG

EXPS. 1, 4. (TABLE 1)

rate plot, a reasonable straight line can be drawn to show changes in the reaction stage.

The reaction for sulphur transfer appears to be divided into three stages; the initial fast stage, a second medium rate stage, and the third slowest stage. For iron transfer the reaction stages also can be divided into the first fast stage of increasing concentration, the second stage of constant iron slag concentration, and the third stage with decreasing concentration. All the break points between the stages for sulphur and iron transfer are coincident.

During the first stage, a rapid increase of iron transfer accompanies the fastest sulphur transfer. As discussed above, this implies that for the basic slag (SL 456) the anodic reaction of iron transfer plays an important role together with CO evolution. In view of the relation of iron transfer with sulphur on a molar basis it appears that at the beginning of this stage the iron transfer contributes to the major part of sulphur transfer but later the extent of iron reaction contribution decreases as the anodic reaction of CO evolution starts to take part in the reaction increasingly. Thus, during the second stage the CO evolution seems to play the major part in the reaction whilst the iron transfer with sulphur is at a steady state with iron reduction. However, for the third stage of reaction the sulphur transfer seems to be controlled by silica reduction occurring effectively after partial equilibrium for the iron and sulphur reactions has been established as discussed in the preceding sections.

In most of the plots according to the rate equation on the basis of the change in sulphur content of metal the first break point

observed between the initial and second stage does not appear clearly due to the logarithmic plots of the rate equation. But some plots for high initial sulphur content, e.g. Exps.4 with 0.6 % S, show the first and second break points and these points are coincident with the break points on the rate curve in Fig. 3.42. As discussed in the preceding section, according to the plot of the rate equation it appeared that the reaction seemed to proceed in two stages; the first fast stage controlled by CO evolution and the second stage controlled by silica reduction. However, it appears better to consider the reaction stages with direct comparison of the changes in the transfer rate curve referring to concurrent reaction rates.

Silicon in the metal appears to act in exactly the same way as iron in the sulphur reaction as shown in Fig. 3.24. and 3.27; at the first fastest stage silicon transfers to the slag as an anodic reaction to supply electrons for sulphur transfer. During the second stage the transferred silicon remains constant, and for the final slowest stage silicon is reduced back to metal. As a result of the silicon role in the reaction, the desulphurization rate is significantly enhanced due to the easier ionization of silicon, compared with iron. This is substantiated by the low slag iron level observed in the silicon alloyed systems. During the final slowest stage similar rates of silica reduction for a given slag composition appear to be related to the similar slow rate of sulphur transfer and the equivalent slopes of the plots according to the rate equation as shown in Fig. 3.26. This indicates that the final slowest stage is controlled entirely by the silica reduction.

The observed effects of ambient pressure also support the above reaction mechanism; reducing the ambient pressure increases both the

sulphur transfer and silica reduction in the fast period due to the decreased problem of CO evolution, but later the continuous increase of silica reduction appears to retard the sulphur transfer.

The silica reduction role during the final slowest stage is also clearly demonstrated by the fact that in the experiment with MnO additions, after the initial fast reaction periods the sulphur and manganese partition ratios between metal and slag change slowly, keeping the sulphur-manganese partial equilibrium, due to the silica reduction proceeding slowly toward the sulphur-manganese-silicon equilibrium as shown in Fig. 3.35.

Therefore it is considered to be reasonable to draw the conclusion that sulphur transfer reaction takes place in three distinct stages; the initial fastest stage controlled by the sulphur transfer process with simultaneous anodic reactions such as iron transfer (in the presence of Si or Mn, transfer of these metallic atoms) and CO evolution. The second medium rate stage is controlled by the CO evolution, related to the steady state iron or silicon reduction and sulphur transfer reactions, and the final slowest stage controlled by silica reduction from the silicate slag. The reaction mechanism during the initial stage appears to depend on the properties of slag; for acid slags with high viscosity and low oxygen ion activity the reaction is controlled predominantly by the anodic reactions of metallic atoms transfer to slag such as iron or silicon transfer due to carbon monoxide nucleation problem whilst for basic slags with low viscosity and high oxygen ion activity, CO evolution is equally important.

CHAPTER 4

CONCLUSION

CHAPTER 4

CONCLUSION

From the observed results of sulphur transfer experiments under varying experimental conditions such as sulphur content of metal, slag composition, melt geometry, Si addition, MnO and FeO addition, and ambient pressure the following conclusions can be made;

(1) In view of the effects of melt geometry, silicon additions to the metal, and ambient pressure on the rate of sulphur transfer from metal to slag and the solubility of sulphide in the slag at the slag - metal interface, the desulphurization is not controlled by either diffusion of sulphur in metal, or that in slag, but by an electrochemical reaction.

(2) For a given metal composition, temperature and pressure the desulphurization rate depends entirely on the properties of slag such as sulphide capacity and viscosity; the slag with higher sulphide capacity and lower viscosity gives a higher desulphurization rate.

(3) The rate constant of desulphurization is affected by melt geometry such as slag depth and graphite crucible diameter; a higher slag depth or a smaller diameter of crucible for a constant melt depth increases the reaction rate. This effect of melt geometry can be explained by a 'local cell' reaction.

(4) Desulphurization takes place in three reaction stages controlled by different reaction mechanisms; the initial fastest stage is dependent upon anodic reactions of iron transfer and CO evolution, the second medium rate stage is controlled by CO

evolution, and the final slowest stage controlled by silica reduction from silicate slag with partial equilibrium for all simultaneous reactions established. The reaction mechanism during the initial stage is dependent on the properties of slag; for acid slags with high viscosity and low oxygen ion activity, the anodic reaction of iron transfer seems to predominate whilst for basic slags with low viscosity and high oxygen ion activity the anodic reaction of CO evolution plays a significant role.

(5) The additions of MnO and FeO into the initial slag increase the desulphurization for an initial period due to the increased sulphide capacity. But after the fast period, a higher MnO addition slows down the rate more rapidly, giving a lower sulphur partition ratio due to the high oxygen potential remaining for the later period. The immediate sulphur reversion was confirmed by addition of MnO during only the later slowest stage.

(6) Silicon additions to metal increase significantly the desulphurization rate for an initial fast period up to a certain limit of addition by decreasing the necessity of the sluggish CO evolution for desulphurization, but during the final slowest stage the rate seems to be independent of the silicon content of the metal and controlled by a similar silica reduction rate for a given silicate slag.

(7) The rates of desulphurization and silica reduction are both increased during a fast reaction period by decreasing the ambient pressure, but for the slowest stage the desulphurization rate is slowed down as the rate of silica reduction continues to increase.

REFERENCES

1. G.G.Hatch and J.Chipman : Trans. A.I.M.E., (1949) 185 , 274
2. E.W.Filer and L.S.Darken : Trans. A.I.M.E., (1952) 194 , 253
3. L.C.Chang and K.M.Goldman : Trans. A.I.M.E., (1948) 176 , 309
4. G.Derge, W.O.Philbrook, and K.M.Goldman : Trans. A.I.M.E., (1950) 188 , 1111
5. N.J.Grant, U.Kalling, and J.Chipman : Trans. A.I.M.E., (1951) 191 , 666
6. E.T.Turkdogan, R.A.Hancock, and J.Pearson : J.I.S.I., (1955) 179 , 338
7. S.Ramachandran, T.B.King, and N.J.Grant : Trans. A.I.M.E., (1956) 206 , 1549
8. M.Hatano : Tetsu-to-Hagane (1969) 55 , S 704
9. O.V.Travin and L.A.Shvartsman : 'Peaceful Use of Atomic Energy' Conf. Acd. Sci. US.S.R., Div, Techn. Sci (1956) 27
10. F.D.Richardson : in discussion of the paper of P.T.Carter, Discussions of Faraday Soc. (1948) 4 , 341
11. W.F.Holbrook and T.L.Joseph : Trans. A.I.M.E., (1936) 120 , 99
12. T.Saito and Y.Kawai : Sci. Repts. Tohoku Univ. (1953) Ser. A5. No.5. 460
13. Y.Kawai : Sci. Repts. Tohoku Univ. (1957) Ser. A9. 520
14. R.G.Ward and K.A.Salmon : J.I.S.I., (1960) 196 , 393
15. L.S.Darken : 'The physical Chemistry of Steel Making' M.I.T. Press and John-Willey, New York (1958) 106
16. J.C.Fulton and J.Chipman : ibid. (1958) 113
17. A.Nilas and M.G.Frohberg : Arch. Eisenhuttenws, (1970) 41 , 951
18. K.Ogino and A.Adachi : Tech. Rept. Osaka Univ. (1965) 15 , 31
19. K.M.Goldman, G.Derge, and W.O.Philbrook : Trans. A.I.M.E., (1956) 200 , 534

20. M.G.Frohberg, A.Nilas, and B.Schuh : Arch. Eisenhuttenws. (1969) 40 , 191

21. T.Saito and Y.Kawai : J.Japan, Inst. Metals (1955) 19 , 170

22. N.J.Grant, U.Kalling, and J.Chipman : Trans. A.I.M.E., (1951) 191 , 672

23. E.T.Turkdogan : J.I.S.I., (1955) 179 , 147

24. E.T.Turkdogan and J.Pearson : ibid. (1954) 176 , 59

25. E.T.Turkdogan and P.Grieveson : Trans. A.I.M.E., (1962) 224 , 316

26. R.G.Ward and K.A.Salmon : J.I.S.I., (1963) 201 , 222

27. M.Ohtani and N.A.Gocken : 'Physical Chemistry of Process Metallurgy' New York. Interscience (1961) 1213

28. T.Rosenquist : Discussion of Paper by G.Derge et al. Ref. (4)

29. C.Wagner : 'The Physical Chemistry of Steel Making' (1958) M.I.T. Press and John Wiley. New York, p.237

30. F.D.Richardson and J.C.Billington : Bull. Inst. Mining. Met. (1956) 593 , 273

31. C.J.B.Fincham and F.D.Richardson : Proc. Roy. Soc., (1954) A223 , 40

32. T.B.King and S.Ramachandran : 'The Physical Chemistry of Steel Making' M.I.T. Press and John Wiley New York (1958) p.125

33. S.Ramachandran, T.B.King, and N.J.Grant : Proc. A.I.M.E., Blast Fnc., Conference (1955)

34. T.B.King : in H.D.Merchant ed. 'Recent Research on Cast Iron' Gordon & Breach Pub. New York, (1964)

35. F.D.Richardson : Howe Memorial Lecture Met. Soc. A.I.M.E., (1964) Feb.

36. F.D.Richardson : 'Physical Chemistry of Melts in Metallurgy' (1974) Academic Press, London p.506 - 511

37. De Hemptinne et al. : 'Physical Chemistry of Process Metallurgy' ed. C. St. Pierre (1961) New York, Interscience, Part 1, p.65

38. W.K.Lu : Int. Conf. Sci. Tech. of Iron and Steel. (1970) Sept. Tokyo, Part 1, p.524 - 526

39. M.G.Frohberg, M.L.Kapoor and A.Nilas : Arch. Eisenhuttenws, (1971) 41 (1) 5 - 10

40. C.J.B.Fincham and F.D.Richardson : J.I.S.I., (1952) Sept. 53

41. R.F.Jones, P.Gale, P.Hopkins, and L.N.Powell : ibid. (1966) May, 505

42. A.I.Vogel : 'Quantitative Inorganic Analysis' Green and Co., London (1945) p.368

43. R.J.Pomfret and P.Grieveson, 1. CHEM. E. SYMPOSIUM (1975) No. 43, Paper 27

44. C.Bodsworth and H.B.Bell : 'Physical Chemistry of Iron and Steel Manufacture' Longman (1972) p.177

45. C.J.B.Fincham and F.D.Richardson : J.I.S.I., (1954) 178 , 4

46. H.R.Kalyanram, T.G.Macfarlane, and H.B.Bell : ibid., (1960) 195 , 58

47. K.P.Abraham, M.W.Davies, and F.D.Richardson : ibid., (1960) 196 , 309

48. F.D.Richardson : 'Physical Chemistry of Melts in Metallurgy' Academic Press. (1974) p.294 - 296

49. C.Bodsworth and H.B.Bell : 'Physical Chemistry of Iron and Steel Manufacture' Longman (1972) p.113

50. R.J.Pomfret and P.Grieveson : to be Published in Iron Making and Steel Making

51. K.Uphadya. Ph.D Thesis, Dept. Metallurgy Univ. of Strathclyde (1977)

52. S.Ban-Ya and J.Chipman. Trans. Met. Soc. A.I.M.E., (1969) 245 , 142

53. E.T.Turkdogan, Met. Trans. B. (1978) 9B , 163

54. R.H.Rein and J.Chipman : Trans. T.M.S. A.I.M.E., (1965) 233 , 415

55. K.P.Abraham and F.D.Richardson : J.I.S.I., (1960) 196 , 313

56. K.P.Abraham, M.W.Davies, and F.D.Richardson : J.I.S.I., (1960) 196 , 82

57. R.A.Sharma and F.D.Richardson : J.I.S.I., (1962) 200 , 373

58. O.V.Travin and L.A.Shvartsman : Sessiya Akad. Nauk, (1955), p.48 ; Zhur. Fizi. Khimu, (1955) 29 , 2031

59. L.S.Darken : In discussion of the paper of King et al., 'Physical Chemistry of Steel Making', (1958), New York, John Wiley, p.133

60. F.D.Richardson : ibid. p.55

61. P.Kozakevitch : ibid. p.89

ACKNOWLEDGEMENTS

I would like to express sincere gratitute to my supervisor, Professor P. Grieveson for his invaluable discussion, help and encouragement during the whole period of this project.

Sincere appreciation is also due to Dr. R.J.Pomfret for his great help in discussion and experimental works.

I am also grateful to the British Council for the financial support.

Finally I wish to thank my dear wife, Eun-Ja, for her unfailing patience and understanding during this research and especially for typing this thesis.

APPENDIX

TABLE 1 continued

Experiment No		1			3		
Exp. Designation		SL 456 - 24 S			SL 456 - 34 S		
Initial S % in Metal		0.242			0.342		
Temperature °C		1469			1462		
Slag Sample wt. & Analysis (wt. %)		(S)	Sample wt. (g)	(FeO)	(S)	Sample wt. (g)	(FeO)
Time	0	0	0	0	0	0	0
(Min)	5	4 Min. 0.018	0.60		6 Min. 0.059	1.00	
	10	8 Min. 0.076	0.23	0.18			
	15						
	20						
	30	28 Min. 0.270	0.75	0.35	26 Min. 0.402	0.62	0.39
	40	35 Min. 0.316	0.83				
	50	0.398	0.67	0.36	46 Min. 0.546	0.75	0.52
	60	63 Min. 0.447	0.79	0.38			
	90	0.514	1.24	0.38	86 Min. 0.664	0.95	0.64
	120	0.572	0.48	0.33			
	150	0.622	0.75	0.29	146 Min. 0.773	0.87	0.54
	180	0.650	0.65	0.26			
	210	0.699	0.60	0.21	206 Min. 0.865	0.73	
	240						
	270	0.749	0.50	0.19	266 Min 0.901	0.85	0.53
	386				0.946	0.85	0.41
	501				0.995	0.50	0.27
Rate Coefficient Km, g cm^{-2} Min^{-1}		0.0017			0.0019		
Initial C % in Metal		4.2			4.2		
Final C % in Metal		5.0			5.0		
Initial Si % in Metal		Not Added			Not Added		
Final Si % in Metal		0.25			0.23		
Final S % in Metal (Analysis)		0.041			0.067		
Final S % in Metal (Calculated)		0.041			0.067		

Metal ; 100 g, Slag ; 30 g, Crucible dia. ; 3.18 cm

TABLE 1

46			4		
SL 456 - 50 S			SL 456 - 61 S		
0.507			0.614		
1462			1462		
(S)	Sample wt.(g)	(FeO)	(S)	Sample wt.(g)	(FeO)
0	0	0	0	0	0
0.113	0.66	0.16			
0.226	1.01	0.20	8 Min. 0.204	0.80	0.43
0.308	0.39	0.32	13 Min. 0.381	0.90	0.51
0.378	0.54	0.41	23 Min. 0.610	0.80	0.62
0.469	0.70	0.39			
0.574	0.96	0.44	42 Min. 0.756	1.11	0.69
0.734	0.47	0.56			
0.764	0.39	0.54	0.864	0.93	0.64
0.929	0.56	0.59	1.058	0.70	0.71
1.029	0.41	0.51			
			1.235	0.91	0.69
1.293	0.36	0.46	1.345	1.09	0.60
			1.464	0.58	0.65
			330 Min. 1.548	0.50	0.52
0.0018			0.0018		
4.0			3.8		
4.7			5.0		
Not Added			Not Added		
0.05			0.12		
0.166			0.129		
0.167			0.127		

TABLE 2 continued

Experiment No		6			9		
Exp. Designation		SL 476 - 25 S			SL 476 - 45 S		
Initial S % in Metal		0.252			0.456		
Temperature °C		1460			1465		
Slag Sample wt. & Analysis (wt. %)		(S)	Sample wt.(g)	(FeO)	(S)	Sample wt.(g)	(FeO)
Time	0	0	0	0	0	0	0
(Min)	5	0.048	1.25	0.08	0.048	0.83	0.08
	10	0.103	1.01	0.16	0.103	0.71	0.19
	20	0.123	0.88	0.10	0.186	1.10	0.22
	30	0.222	0.96	0.25	0.289	0.97	0.22
	40	0.251	0.70	0.19	0.420	0.48	0.34
	60	0.373	0.68	0.26	0.616	1.10	0.62
	90	0.517	0.47	0.44	0.856	0.79	0.49
	120	0.586	0.73	0.43	0.985	0.81	0.58
	240	0.726	0.77	0.40	1.195	0.77	0.50
Rate Coefficient Km, g cm^{-2} Min^{-1}		0.0010			0.0011		
Initial C % in Metal		4.3			4.0		
Final C % in Metal		5.0			5.0		
Initial Si % in Metal		Not Added			Not Added		
Final Si % in Metal		0.13			0.09		
Final S % in Metal (Analysis)		0.058			0.133		
Final S % in Metal (Calculated)		0.060			0.143		

Metal ; 100 g, Slag ; 30 g, Crucible dia ; 3.18 cm.

TABLE 2

Experiment No		10		
Exp. Designation		SL 476 - 25 S		
Initial S % in Metal		0.252		
Temperature °C		1463		
Slag Sample wt. & Analysis (wt. %)		(S)	Sample wt.(g)	(FeO)
Time	0	0	0	0
(Min)	5	0.057	0.70	0.02
	10	0.063	0.56	0.23
	20	0.112	0.84	0.24
	30	0.217	0.57	0.29
	40	0.262	0.61	0.33
	60	0.346	0.77	0.25
	90	0.444	0.84	0.38
	120	0.549	0.57	0.64
	240	0.685	0.71	0.43
Rate Coefficient Km, g cm^{-2} Min^{-1}		0.0010		
Initial C % in Metal		4.3		
Final C % in Metal		5.0		
Initial Si % in Metal		Not Added		
Final Si % in Metal		0.13		
Final S % in Metal (Analysis)		0.060		
Final S % in Metal (Calculated)		0.065		

TABLE 3

Experiment No		15			14		
Exp. Designation		SL 556 - 25 S			SL 556 - 45 S		
Initial S % in Metal		0.252			0.456		
Temperature °C		1463			1465		
Slag Sample wt. & Analysis (wt. %)		(S)	Sample wt.(g)	(FeO)	(S)	Sample wt.(g)	(FeO)
Time	0	0	0	0	0	0	0
(Min)	5	0.022	0.37	0.08	0.027	0.67	0.24
	10	0.050	0.63	0.20	0.044	0.68	0.21
	20	0.061	0.34	0.32	0.093	0.80	0.22
	30	0.086	0.47	0.37	0.102	0.80	0.30
	40	0.120	0.41	0.33	0.164	0.55	0.26
	60	0.149	0.50	0.37	0.169	0.66	0.31
	90	0.199	0.34	0.40	0.288	0.51	0.39
	120	0.246	0.42	0.35	0.351	0.47	0.37
	240	0.394	0.35	0.31	0.616	0.48	0.37
Rate Coefficient Km, g cm^{-2} Min^{-1}		0.0004			0.0003		
Initial C % in Metal		4.3			4.0		
Final C % in Metal		5.0			5.0		
Initial Si % in Metal		Not Added			Not Added		
Final Si % in Metal		0.34			0.26		
Final S % in Metal (Analysis)		0.141			0.293		
Final S % in Metal (Calculated)		0.143			0.296		

Metal ; 100 g, Slag ; 30 g, Crucible dia. ; 3.18 cm.

TABLE 4

Experiment No		2			13		
Exp. Designation		SL 646 - 24 S			SL 646 - 45 S		
Initial S % in Metal		0.242			0.456		
Temperature °C		1465			1469		
Slag Sample wt. & Analysis (wt. %)		(S)	Sample wt.(g)	(FeO)	(S)	Sample wt.(g)	(FeO)
Time	0	0	0	0	0	0	0
(Min)	10				0.033	1.70	0.20
	20				0.046	1.59	0.27
	30				0.064	0.64	0.38
	40				0.078	0.84	0.47
	60	0.049	1.91	0.27	0.106	0.69	0.61
	90				0.152	0.83	0.81
	120	0.100	1.66	0.47	0.182	0.68	0.91
	240	0.199	2.08	0.41	0.299	0.93	0.85
	420	0.242	1.58		0.406	0.59	0.85
	660	0.272	1.65	0.41			
	1380	0.345	1.83	0.38			
	1500	0.355	1.15	0.45			
	1860	0.376	0.96	0.30			
	2070	0.391	0.50	0.23			
Rate Coefficient Km, g cm^{-2} Min^{-1}		0.00014			0.00014		
Initial C % in Metal		4.2			4.0		
Final C % in Metal		4.6			4.7		
Initial Si % in Metal		Not Added			Not Added		
Final Si % in Metal		1.51			0.37		
Final S % in Metal (Analysis)		0.118			0.336		
Final S % in Metal (Calculated)		0.146			0.355		

Metal ; 100 g, Slag ; 30 g, Crucible dia.; 3.18 cm.

TABLE 5 continued

Experiment No		55			56		
Initial S % in Metal		0.491			0.491		
Slag Weight (g)		30			60		
Metal Weight (g)		100			100		
Temperature °C		1464			1465		
Slag Sample wt. & Analysis (wt. %)		(S)	Sample wt.(g)	(FeO)	(S)	Sample wt.(g)	(FeO)
Time	0	0	0	0	0	0	0
(Min)	5	0.061	0.58	0.49	0.080	1.73	0.17
	10	0.157	0.53	0.73	0.178	2.29	0.33
	15	0.211	0.58		0.228	0.46	
	20	0.271	0.56		0.271	0.60	0.27
	30	0.401	0.54	0.67	0.330	0.57	0.34
	40	0.505	0.63	0.69	0.436	0.77	0.32
	60	0.689	0.35	0.63	0.540	0.65	0.34
	90	0.794	0.60	0.53	0.619	0.69	0.37
	120	0.904	0.67	0.40	0.663	0.62	0.30
	240	1.21	0.62	0.23	0.742	0.60	0.17
Rate Coefficient Km, g cm^{-2} Min^{-1}		0.0011			0.0024		
Initial Si % in Metal		Not Added			Not Added		
Final Si % in Metal		0.08			0.18		
Final S % in Metal (Analysis)		0.170			0.080		
Final S % in Metal (Calculated)		0.167			0.084		

Slag ; 47 % SiO_2, 6 % MgO, 47 % CaC, Crucible dia. ; 3.18 cm.

TABLE 5

57			58		
0.491			0.491		
30			60		
50			100		
1464			1465		
(S)	Sample wt. (g)	(FeO)	(S)	Sample wt. (g)	(FeO)
0	0	0	0	0	0
0.048	1.15	0.06	0.084	1.22	0.15
0.114	0.45	0.22	0.166	0.59	0.16
0.135	0.53	0.15	0.211	0.78	0.16
0.262	0.43	0.28	0.263	0.49	0.23
0.328	0.45	0.22	0.325	0.60	0.33
0.416	0.42	0.27	0.421	0.57	0.29
0.503	0.38	0.33	0.521	0.51	0.36
0.551	0.48	0.39	0.620	0.49	
0.631	0.50	0.34	0.647	0.49	0.26
0.704	0.42	0.17	0.723	0.47	0.31
0.0010			0.0024		
Not Added			Not Added		
0.10			0.18		
0.110			0.081		
0.109			0.084		

TABLE 6

Experiment No		61				32 A				1		
Slag Weight (g)		2.5				10				30		
Metal Weight (g)		8.75				35				100		
Initial S % in Metal		0.229				0.229				0.242		
Crucible Diameter (mm)		9.5 (3/8 in.)				19.1 (3/4 in.)				31.8 (1 1/4 in.)		
Temperature °C		1464				1466				1469		
(Slag), Metal wt. %		(S)	[S]	Si	(FeO)	(S)	[S]	Si	(FeO)	(S)	[S]	(FeO)
Time	0	0	0.229	0	0	0	0.229	0	0	0	0.242	0
(Min)	5	0.109	0.198		0.06					4M 0.018	0.237	
	10	0.152	0.186		0.10	0.172	0.180		0.18	8M 0.076	0.220	0.18
	15	0.241	0.160		0.12							
	20	0.322	0.137	0.01	0.20	0.278	0.150		0.23	28M 0.270	0.163	0.35
	30	0.368	0.124	0.02	0.14	0.376	0.122	0.02	0.32			
	40					0.424	0.108	0.03	0.26	35M 0.316	0.150	
	50	0.434	0.105	0.03	0.16					0.398	0.128	0.36
	60					0.508	0.084	0.04	0.24	53M 0.447	0.114	0.38
	90	0.569	0.067	0.09	0.18	0.603	0.057	0.05	0.24	0.514	0.097	0.38
Rate Coefficient Km, g cm^{-2} Min^{-1}		0.0031				0.0024				0.0017		

Slag ; 45 % SiO_2, 6 % MgO, 49 % CaO.

TABLE 7 continued

Experiment No		11			12		
Slag Designation		SL 476			SL 476		
Initial S % in Metal		0.256			0.450		
Initial Si % in Metal		2.10			1.91		
Temperature °C		1469			1468		
Slag Sample wt. & Analysis (wt. %)		(S)	Sample wt.(g)	(FeO)	(S)	Sample wt.(g)	(FeO)
Time	0	0	0	0	0	0	0
(Min)	5	0.076	0.92	0.11	0.202	1.32	0.15
	10	0.296	0.87		0.501	0.48	0.23
	20	25 Min. 0.549	0.62	0.14	0.889	0.82	0.25
	30	0.611	0.89	0.11	1.137	0.99	0.23
	40	0.747	0.85	0.11	1.217	0.75	0.16
	60	0.805	0.68	0.27	1.405	0.56	0.19
	90	0.836	0.61	0.23	1.451	0.69	0.24
	120	0.847	0.92	0.20	1.485	0.67	0.22
	240	0.861	1.13	0.20	1.504	0.71	0.27
Rate Coefficient Km, g cm^{-2} Min^{-1}		0.0050			0.0048		
Initial C % in Metal		4.1			3.6		
Final C % in Metal		4.5			4.7		
Final Si % in Metal		2.13			1.93		
Final S % in Metal (Analysis)		0.015			0.031		
Final S % in Metal (Calculated)		0.015			0.031		

Metal ; 100 g, Slag ; 30 g, Crucible dia. ; 3.18 cm.

TABLE 7

Experiment No		16		
Slag Designation		SL 556		
Initial S % in Metal		0.450		
Initial Si % in Metal		1.91		
Temperature °C		1465		
Slag Sample wt. & Analysis (wt. %)		(S)	Sample wt.(g)	(FeO)
Time	0	0	0	0
(Min)	5	0.035	0.63	0.19
	10	0.124	0.64	0.18
	20	0.340	0.35	0.18
	30	0.426	0.37	0.16
	40	0.494	0.47	0.20
	60	0.609	0.42	0.30
	90	0.763	0.50	0.30
	120	0.792	0.38	0.36
	240	0.971	0.35	0.49
Rate Coefficient Km, g cm^{-2} Min^{-1}		0.0014		
Initial C % in Metal		3.6		
Final C % in Metal		4.5		
Final Si % in Metal		1.6		
Final S % in Metal (Analysis)		0.156		
Final S % in Metal (Calculated)		0.170		

TABLE 8 continued

Experiment No		31			25		
Slag Designation		SL 456			SL 456		
Initial S % in Metal		0.230			0.242		
Initial Si % in Metal		0.06			0.42		
Temperature °C		1466			1467		
Slag Sample wt. & Analysis (wt. %)		(S)	Sample wt.(g)	(FeO)	(S)	Sample wt.(g)	(FeO)
Time	0	0	0	0	0	0	0
(Min)	5	0.086	1.32	0.16	0.156	2.60	0.26
	10	0.166	1.20	0.13	0.235	1.21	0.14
	20	0.338	0.92	0.13	0.494	1.40	0.11
	25						
	30	0.411	0.73	0.21	0.553	0.65	0.08
	40	0.488	1.19	0.18	0.615	0.74	0.09
	60	0.542	0.92	0.22	0.705	0.70	0.08
	90				0.768	0.54	0.13
	120				0.785	0.71	0.10
	240				0.795	0.70	0.10
Rate Coefficient Km, g cm^{-2} Min^{-1}		0.0032			0.0047		
Final Si % in Metal		0.09			0.41		
Final S % in Metal (Analysis)		0.081			0.037		
Final S % in Metal (Calculated)		0.081			0.035		

Metal ; 100 g, Slag ; 30 g, Crucible dia. ; 3.18 cm.

TABLE 8

26			27		
SL 456			SL 456		
0.226			0.184		
0.98			2.40		
1468			1469		
(S)	Sample wt.(g)	(FeO)	(S)	Sample wt.(g)	(FeO)
0	0	0	0	0	0
0.085	0.74	0.03	0.088	0.98	0.09
0.304	0.76	0.16	0.265	0.66	0.22
			0.417	0.53	0.10
0.551	0.69	0.30			
0.595	0.45	0.12	0.505	0.82	0.04
0.614	0.76	0.04	0.560	0.60	0.07
0.682	0.80	0.07	0.580	0.64	0.11
0.697	0.60	0.07	0.581	0.52	0.08
0.730	0.72	0.12	0.599	0.86	0.05
0.731	0.64	0.14	0.630	0.38	0.08
0.0059			0.0065		
1.04			2.48		
0.021			0.008		
0.018			0.006		

TABLE 9 continued

Experiment No		22				32 A			
Ambient Pressure (Atm.)		1				1			
Initial S % in Metal		0.237				0.229			
Temperature °C		1466				1466			
(Slag), Metal wt. %		(S)	[S]	(FeO)	[Si]	(S)	[S]	(FeO)	[Si]
Time	0	0	0.237	0	0	0	0.229	0	0
(Min)	5	0.093	(0.210) 0.210	0.10					
	10	0.185	(0.192) 0.184	0.17		0.172	(0.180) 0.180	0.18	
	20	0.275	(0.157) 0.158	0.22		0.278	(0.151) 0.150	0.23	
	30	0.324	(0.142) 0.145	0.31		0.376	(0.122) 0.122	0.32	0.02
	40	0.430	(0.124) 0.114	0.27	0.03	0.424	0.108	0.26	0.03
	60	0.574	(0.077) 0.073	0.28	0.04	0.508	0.084	0.24	0.04
	90	0.633	(0.058) 0.056	0.23	0.07	0.603	0.057	0.24	0.05
	120	0.682	(0.045) 0.042	0.23	0.09				
	240	0.697	(0.036) 0.038	0.22	0.12				
Rate Coefficient Km, g cm^{-2} Min^{-1}		0.0024				0.0024			

1. Numbers in ( ) show analysed S wt. % in metal.
2. Metal ; 35 g, Slag ; 10 g, Crucible dia ; 1.91 cm.
3. Slag ; 45 % SiO_2, 6 % MgO, 49 % CaO.

TABLE 9

32 B				32 C			
1/2				1/4			
0.229							
1466				1466			
(S)	[S]	(FeO)	[Si]	(S)	[S]	(FeO)	[Si]
0	0.229	0	0	0	0.229	0	0
30 Min. 0.432	(0.109) 0.106	0.34	0.03	30 Min. 0.498	(0.090) 0.087	0.303	0.04
60 Min. 0.564	0.068	0.27	0.05	60 Min. 0.619	0.052	0.344	0.08
0.0032				0.0040			

TABLE 10

Experiment No		33				35				36			
Initial S % in Metal		0.106				0.106				0.106			
Initial Si % in Metal		0.125				0.125				0.125			
Ambient Pressure (Atm.)		1				1/2				1/4			
Temperature °C		1466				1469				1469			
(Slag), Metal wt. %		(S)	[S]	(FeO)	[Si]	(S)	[S]	(FeO)	[Si]	(S)	[S]	(FeO)	[Si]
Time	0	0	0.106	0	0.125	0	0.106	0	0.125	0	0.106	0	0.125
(Min)	5	0.095	(0.078) 0.078	0.05	0.120	0.138	(0.065) 0.066	0.04	0.127	0.156	(0.056) 0.061	0.10	0.131
	10	0.162	(0.062) 0.059	0.07	0.126	0.206	(0.048) 0.047	0.06	0.127	0.219	(0.038) 0.043	0.19	0.133
	20	0.221	(0.046) 0.042	0.09	0.130	0.268	(0.027) 0.029	0.06	0.126	0.276	(0.025) 0.027	0.12	0.136
	30	0.241	0.037	0.07	0.130	0.298	0.020	0.07	0.138	0.295	0.021	0.13	0.145
	40	0.266	0.030	0.09	0.131	0.317	0.015	0.09	0.143	0.315	0.016	0.10	0.159
	60	0.309	0.017	0.10	0.145	0.319	0.015	0.13	0.177				
Rate Coefficient Km, g cm^{-2} Min^{-1}		0.0071				0.0102				0.0114			

1. Numbers in ( ) show analysed S wt. % in metal.
2. Metal ; 35 g, Slag ; 10 g, Crucible dia. ; 1.91 cm.
3. Slag ; 45 % SiO_2, 6 % MgO, 49 % CaO.

TABLE 11 continued

Experiment No		34				
Initial S % in Metal		0.242				
Initial Si % in Metal		0.42				
Ambient Pressure (Atm.)		1				
Temperature °C		1466				
(Slag), Metal wt. %		(S)	[S]	(FeO)	[Si]	[C]
Time	0	0	0.242	0	0.42	4.2
(Min)	5	0.275	(0.152) 0.163	0.30	0.41	4.6
	10	0.408	(0.115) 0.126	0.23	0.40	4.7
	20	21 Min 0.590	(0.071) 0.073	0.40	0.40	4.8
	30	0.611	0.068	0.21	0.38	4.8
	40	0.686	0.046	0.19	0.39	4.8
	60	0.731	(0.032) 0.033	0.20	0.41	4.9
Rate Coefficient Km, g cm^{-2} Min^{-1}		0.0077				

1. Numbers in ( ) show analysed S wt. % in metal.
2. Metal ; 35 g, Slag ; 10 g, Crucible dia. ; 1.91 cm.
3. Slag ; 45 % SiO_2, 6 % MgO, 49 % CaO.

TABLE 11

37					38				
0.242					0.242				
0.42					0.42				
1/2					1/4				
1469					1469				
(S)	[S]	(FeO)	[Si]	[C]	(S)	[S]	(FeO)	[Si]	[C]
0	0.242	0	0.42	4.2	0	0.242	0	0.42	4.2
0.332	(0.140) 0.147	0.27	0.41	4.6	5.6 Min 0.415	(0.123) 0.123	0.24	0.39	4.7
0.505	(0.103) 0.098	0.23	0.40	4.8	0.555	(0.083) 0.083	0.22	0.39	4.8
0.668	(0.055) 0.051	0.19	0.40	4.9	0.694	(0.039) 0.044	0.24	0.38	5.0
0.696	0.044	0.21	0.38	5.0	0.721	0.036	0.18	0.40	5.0
0.719	0.037	0.19	0.42	4.9	0.725	0.035	0.13	0.42	5.0
0.769	(0.024) 0.022	0.18	0.43	4.8					
0.0112					0.0132				

TABLE 12

Experiment No		24				28				29			
Initial S % in Metal		0.202				0.202				0.202			
Initial Si % in Metal		1.89				1.89				1.89			
Ambient Pressure (Atm.)		1				1/2				1/4			
Temperature °C		1468				1470				1470			
(Slag), Metal wt. %		(S)	[S]	(FeO)	[Si]	(S)	[S]	(FeO)	[Si]	(S)	[S]	(FeO)	[Si]
Time	0	0	0.202	0	1.89	0	0.202	0	1.89	0	0.202	0	1.89
	5	0.186	(0.150) 0.148	0.05	1.86	7 Min 0.423	(0.079) 0.081	0.08	1.86	6 Min 0.440	(0.078) 0.076	0.07	1.87
	10	0.353	(0.100) 0.101	0.06	1.83	11 Min 0.548	(0.049) 0.046	0.04	1.84	11 Min 0.587	(0.035) 0.034	0.04	1.85
	20	0.509	(0.053) 0.057	0.06	1.82	21 Min 0.617	(0.019) 0.026	0.08	1.84	21 Min 0.629	(0.023) 0.022	0.05	1.85
	30	0.572	0.039	0.07	1.81	0.658	(0.013) 0.014	0.05	1.89	0.661	0.013	0.05	1.88
	40	0.619	0.025	0.09	1.81	0.674	0.010	0.06	1.90	0.688	0.006	0.16	1.90
	60	0.640	0.019	0.09	1.83	0.669	0.011	0.06	1.90				
	90	0.657	0.014	0.08	1.83								
	120	0.667	0.012	0.10	1.83								
	240	0.680	(0.013) 0.008	0.10	1.84								
Rate Coefficient Km, g cm^{-2} Min^{-1}		0.0078				0.0162				0.0198			

1. Numbers in ( ) show analysed S wt. % in metal.
2. Metal ; 35 g, Slag ; 10 g, Crucible dia. ; 1.91 cm.
3. Slag ; 45 % SiO_2, 6 % MgO, 49 % CaO.

TABLE 13 continued

Experiment No		1			43			
Initial S % in Metal		0.242			0.251			
MnO Added into Initial Slag %		0			2			
Temperature °C		1469			1463			
Slag Sample wt. & Analysis (wt. %)		(S)	Sample wt.(g)	(FeO)	(S)	Sample wt.(g)	(FeO)	(MnO)
Time	0	0	0	0	0	0	0	2
(Min)	5	4 Min 0.018	0.60		0.036	0.79	0.02	1.59
	10	8 Min 0.074	0.23	0.18	0.125	0.52	0.27	1.56
	15				0.190	0.59	0.32	1.51
	20				0.234	0.55	0.41	1.58
	30	28 Min 0.270	0.75	0.35	0.317	0.54	0.45	1.42
	40	35 Min 0.316	0.83		0.364	0.44	0.57	1.31
	50	0.398	0.67	0.36	0.421	0.51	0.47	1.23
	60	63 Min 0.447	0.79	0.38	0.480	0.31		1.15
	90	0.514	1.24	0.38	0.537	0.54	0.34	1.04
	120	0.572	0.48	0.33	0.572	0.61	0.32	0.95
	180	0.650	0.75	0.26	0.627	0.36	0.23	0.77
	240	270 Min 0.749	0.50	0.19	0.682	0.56	0.20	0.65
Rate Coefficient Km, g cm^{-2} Min^{-1}		0.0017			0.0020			
Final Si % in Metal		0.24			0.07			
Initial Si in Metal		Not Added			Not Added			
Final S % in Metal (Calculated)		0.041			0.066			

1. Slag ; 45 % SiO_2, 6 % MgO, 49 % CaO.

2. Metal ; 100 g, Slag ; 30 g, Crucible dia. ; 3.18 cm.

TABLE 13

39				40			
0.251				0.251			
4				8			
1459				1460			
(S)	Sample wt.(g)	(FeO)	(MnO)	(S)	Sample wt.(g)	(FeO)	(MnO)
0	0	0	4	0	0	0	8
0.080	0.54	0.16	3.25	0.065	1.15	0.26	7.55
0.165	0.72	0.18	3.18	0.143	0.70	0.59	7.10
				0.217	0.71	0.78	6.90
0.262	0.43	0.50	3.18	0.301	0.53	0.92	6.35
0.345	0.48	0.54	3.08	0.379	0.51	1.04	6.25
0.402	0.44	0.55	2.91	0.430	0.48		6.00
0.440	0.43	0.45	2.78	0.472	0.48	0.82	5.83
0.474	0.43	0.36	2.55	0.481	0.40	0.54	5.65
0.524	0.45	0.32	2.37	0.523	0.58	0.65	5.30
0.568	0.46	0.23	2.01	0.541	0.56	0.60	5.00
				0.586	0.62	0.44	4.45
0.617	0.39	0.11	1.45	0.597	0.58	0.39	4.00
0.0024				0.0025			
0.07				0.08			
Not Added				Not Added			
0.078				0.089			

TABLE 14 continued

Experiment No		4			41			
Initial S % in Metal		0.614			0.614			
MnO Added into Initial Slag wt. %		0			4			
Temperature °C		1462			1462			
Slag Sample wt. & Analysis (wt. %)		(S)	Sample wt.(g)	(FeO)	(S)	Sample wt.(g)	(FeO)	(MnO)
Time	0	0	0	0	0	0	0	4
(Min)	5				0.236	0.35	0.39	3.10
	10	8 Min 0.204	0.81	0.43	0.438	0.60	0.72	3.36
	15	13 Min 0.381	0.90	0.51	0.608	0.47	0.96	3.39
	20	23 Min 0.610	0.80	0.62	0.676	0.34	0.96	3.28
	30				0.801	0.72	1.02	3.23
	40	42 Min 0.756	1.11	0.69	0.922	0.61	1.02	3.23
	50				0.990	0.40	0.99	3.07
	60	0.864	0.93	0.64	1.062	0.40	1.11	3.01
	90	1.052	0.70	0.71	1.166	0.48	0.75	2.82
	120	150 Min 1.235	0.91	0.69	1.277	0.42	0.64	2.72
	180	210 Min 1.345	1.09	0.60	1.438	0.49	0.64	2.49
	240	270 Min 1.464	0.58	0.65	1.526	0.49	0.50	2.32
	330	1.548	0.50	0.52				
Rate Coefficient Km, g cm^{-2} Min^{-1}		0.0018			0.0029			
Final Si % in Metal		0.12			0.03			
Initial Si % in Metal		Not Added			Not Added			
Final S % in Metal (Calculated)		0.194			0.191			

1. Slag ; 45 % SiO_2, 6 % MgO, 49 % CaO.
2. Metal ; 100 g, Slag ; 30 g, Crucible dia. ; 3.18 cm.

TABLE 14

42				39			
0.614 % S + 4 % Mn				0.251			
0				4			
1465				1459			
(S)	Sample wt.(g)	(FeO)	(MnO)	(S)	Sample wt.(g)	(FeO)	(MnO)
0	0	0	0	0	0	0	4
0.191	0.74	0.12	0.49	0.080	0.54	0.16	3.25
0.348	0.66	0.18	1.11	0.165	0.72	0.18	3.18
0.658	0.47	0.17	2.19				
0.753	0.65	0.19	2.88	0.262	0.43	0.50	3.18
0.815	0.73	0.17	3.22	0.345	0.48	0.54	3.08
1.101	0.32	0.26	4.19	0.402	0.44	0.55	2.91
1.109	0.32	0.19	4.16	0.440	0.43	0.45	2.78
1.250	0.30	0.13	4.19	0.474	0.43	0.36	2.55
1.405	0.28	0.24	4.52	0.524	0.45	0.32	2.37
1.441	0.33	0.17	4.61	0.568	0.46	0.23	2.01
1.493	0.45	0.13	4.61				
1.542	0.42	0.20	4.61	0.617	0.39	0.11	1.45
			4.61				
0.0029				0.0024			
0.18				0.07			
Not Added				Not Added			
0.186				0.078			

TABLE 15 continued

Experiment No		46			48			
Initial S % in Metal		0.507			0.507			
MnO Added into Initial Slag wt. %		0			0.5			
Temperature °C		1462			1462			
Slag Sample wt. & Analysis (wt. %)		(S)	Sample wt.(g)	(FeO)	(S)	Sample wt.(g)	(FeO)	(MnO)
Time	0	0	0	0	0	0	0	0.5
(MiN)	5	0.113	0.66	0.16	0.166	0.56	0.16	0.42
	10	0.226	1.01	0.20	0.276	0.50	0.14	0.46
	15	0.308	0.39	0.32	0.319	0.57	0.36	0.44
	20	0.378	0.54	0.41	0.421	0.52	0.47	0.42
	30	0.469	0.70	0.39	0.531	0.67	0.53	0.41
	40	0.574	0.96	0.44	0.627	1.01	0.54	0.41
	50	0.734	0.47	0.56	0.678	0.93	0.54	0.40
	60	0.764	0.39	0.54	0.759	0.40	0.43	0.37
	90	0.929	0.56	0.59	0.929	0.37	0.56	0.34
	120	1.029	0.41	0.51	1.03	0.27		0.31
	180				1.13	0.48	0.33	0.27
	240	1.293	0.36	0.46	210 Min. 1.14	0.38		0.26
					420 Min. 1.42	0.48	0.22	0.16
					1625 Min. 1.73	0.50	0.15	0.08
					2112 Min. 1.79	0.52	0.13	0.06
					3080 Min. 1.83	0.72	0.13	0.06
					6350 Min. 1.84		0.11	0.04
Rate Coefficient Km, g cm^{-2} Min^{-1}		0.0018			0.0020			
Final Si % in Metal		0.05			0.9			
Initial Si % in Metal		Not Added			Not Added			
Final S % in Metal (Analysis)		0.166			0.017			

1. Slag ; 45 % SiO_2, 6 % MgO, 49 % CaO.
2. Metal ; 100 g, Slag ; 30 g, Crucible dia. ; 3.18 cm.

TABLE 15

47				49			
0.507				0.507			
1				2			
1462				1462			
(S)	Sample wt.(g)	(FeO)	(MnO)	(S)	Sample wt.(g)	(FeO)	(MnO)
0	0	0	1	0	0	0	2
0.134	0.58	0.19	1	0.192	0.61	0.29	1.61
0.268	0.61	0.36	0.91	0.269	0.58	0.49	1.61
0.373	0.76	0.49	0.87	0.368	0.47	0.57	1.61
0.468	0.46	0.54	0.86	0.472	0.32	0.68	1.50
0.534	0.45	0.62	0.85	0.555	0.65	0.70	1.46
0.652	0.53	0.69	0.81	0.667	0.36	0.69	1.45
0.766	0.61	0.68	0.77	0.757	0.47	0.74	1.39
0.853	0.35	0.60	0.75	0.784	0.67	0.73	1.37
0.961	0.44	0.55	0.65	0.925	0.48	0.69	1.25
1.02	0.48	0.48	0.65	1.01	0.40	0.57	1.21
1.21	0.38	0.42	0.61	1.13	0.35	0.39	1.05
1.22	0.48	0.35	0.51	1.18	0.54	0.41	1.01
4190 Min. 1.81	1.68	0.11	0.07	450 Min. 1.42	0.86	0.23	0.77
5630 Min. 1.82	1.08	0.10	0.07	1620 Min. 1.74	0.43	0.12	0.34
7020 Min. 1.85	1.10	0.10	0.06	3120 Min. 1.81	0.35	0.10	0.19
				7155 Min. 1.93		0.06	0.12
0.0021				0.0020			
0.91				0.91			
Not Added				Not Added			
0.017				0.017			

TABLE 16

Experiment No		50			
Initial S % in Metal		0.229			
MnO Added		1st. Add. 1.2 g MnO at 22 Min. 2nd. Add. 1.2 g MnO at 123 Min.			
Temperature °C		1462			
Slag Sample wt. & Analysis (wt. %)		(S)	Sample wt.(g)	(MnO)	(FeO)
Time	0	0	0	0	0
(Min)	11	0.191	0.78		0.24
	20	0.248	0.93		0.27
	25	0.304	0.92	3.75	0.42
	30	0.332	1.08	3.48	0.64
	41	0.380	0.81	3.13	0.69
	52	0.420	0.36	2.95	0.56
	60	0.432	0.42	2.75	0.60
	90	0.488	0.51	2.53	0.58
	121	0.523	0.50	2.32	0.52
	128	0.504	0.39	6.30	0.70
	133	0.496	0.47	5.88	0.75
	143	0.507	0.47	5.65	0.74
	153	0.514	0.45	5.58	0.70
	180	0.543	0.63	5.10	0.61
	240	0.579	0.57	4.25	0.50
	360	0.693	0.73	3.68	0.37
Final Si % in Metal		0.018			
Final S % in Metal (Calculated)		0.048			

1. Metal ; 100 g, Slag ; 30 g, Crucible dia. ; 3.18 cm.
2. Slag ; 45 % SiO_2, 6 % MgO, 49 % CaO.

TABLE 17

Experiment No		7			8			17		
Exp. Designation		476 FeO 2 - 25 S			476 FeO 2 - 45 S			556 FeO 2 - 45 S		
Initial S % in Metal		0.252 %			0.456			0.456		
Temperature °C		1465			1464			1464		
Slag Sample wt. (g) & Analysis (%)		(S)	Sample wt.(g)	(FeO)	(S)	Sample wt.(g)	(FeO)	(S)	Sample wt.(g)	(FeO)
Time	0	0	0	2 % Add	0	0	2 % Add	0	0	2 % Add
(Min)	5	0.092	0.57	0.68	0.077	0.77	0.45	0.022	0.89	0.68
	10	0.130	0.99	0.31	0.151	1.81	0.30	0.064	0.39	0.65
	20	0.299	0.80	0.42	0.321	0.49	0.63	0.101	0.38	0.54
	30	0.375	0.87	0.51	0.502	0.51	0.63	0.140	0.42	0.56
	40	0.412	0.75	0.36	0.687	0.78	0.65	0.183	0.38	0.55
	60	0.503	0.84	0.39	0.824	0.45	0.52	0.254	0.39	0.57
	90	0.568	0.53	0.44	1.030	1.06	0.47	0.335	0.42	0.49
	120	0.637	0.73	0.52	1.100	0.56	0.44	0.424	0.34	0.34
	240	0.732	0.74	0.24	1.349	0.84	0.42	0.672	0.38	0.25
	360							0.843	0.36	0.32
Rate Coefficient Km, g cm^{-2} Min^{-1}		0.0027			0.0016					
Initial C % in Metal		4.3			4.0			4.0		
Final C % in Metal		5.1			5.1			4.9		
Initial Si % in Metal		Not Added			Not Added			Not Added		
Final Si % in Metal		0.17			0.14			0.44		
Final S % in Metal (Analysis)		0.05			0.10			0.23		
Final S % in Metal (Calculated)		0.05			0.10			0.23		

Metal ; 100 g, Slag ; 30 g, Crucible dia. ; 3.18 cm.

TABLE 18

Experiment No		60	
Slag Composition		80 % CaF_2, 20 % CaO	
Initial S % in Metal		0.493 %	
Slag Weight (g)		10	
Metal Weight (g)		35	
Temperature ^{o}C		1464	
(Slag), Metal wt. %		[S]	(FeO)
Time	0	0.493	0
(Min)	3	0.043	0.18
	5	0.026	0.10
	8	0.025	0.08
	12	0.024	0.05
	17	0.021	0.06
Rate Coefficient Km, g cm^{-2} Min^{-1}		0.10	

Crucible dia. ; 1.91 cm.